

การศึกษากลุ่มโมเลกุลในสารละลายโดยวิธีทางทฤษฎี: กรดเบนโซอิกและฟีนอล
ในสารละลายเบนซีน

นางสาวเสริมศิริ ไชยวงศ์วัฒนะ

วิทยานิพนธ์นี้เป็นส่วนหนึ่งของการศึกษาตามหลักสูตรปริญญาวิทยาศาสตรดุษฎีบัณฑิต
สาขาวิชาเคมี
มหาวิทยาลัยเทคโนโลยีสุรนารี
ปีการศึกษา 2551

**THEORETICAL STUDIES OF MOLECULAR
CLUSTERS IN SOLUTIONS: BENZOIC ACID AND
PHENOL IN BENZENE SOLUTIONS**

Sermsiri Chaiwongwattana

**A Thesis Submitted in Partial Fulfillment of the Requirements
for the Degree of Doctor of Philosophy in Chemistry**

Suranaree University of Technology

Academic Year 2008

**THEORETICAL STUDIES OF MOLECULAR CLUSTERS
IN SOLUTIONS: BENZOIC ACID AND PHENOL
IN BENZENE SOLUTIONS**

Suranaree University of Technology has approved this thesis submitted in partial fulfillment of the requirements for the Degree of Doctor of Philosophy.

Thesis Examining Committee

(Assoc. Prof. Dr. Malee Tangsathikulchai)

Chairperson

(Prof. Dr. Kritsana Sagarik)

Member (Thesis Advisor)

(Prof. Dr. Supot Hannongbua)

Member

(Assoc. Prof. Dr. Anan Tongraar)

Member

(Asst. Prof. Dr. Visit Vao-Soongnern)

Member

(Prof. Dr. Pairote Sattayatham)

Vice Rector for Academic Affairs

(Assoc. Prof. Dr. Prapan Manyum)

Dean of Institute of Science

เสริมศิริ ไชยวงศ์วัฒน์ : การศึกษากลุ่มโมเลกุลในสารละลายโดยวิธีทางทฤษฎี: กรดเบนโซอิกและฟีนอลในสารละลายเบนซีน (THEORETICAL STUDIES OF MOLECULAR CLUSTERS IN SOLUTIONS: BENZOIC ACID AND PHENOL IN BENZENE SOLUTIONS) อาจารย์ที่ปรึกษา : ศาสตราจารย์ ดร. กฤษณะ ศาคริก, 143 หน้า.

วิทยานิพนธ์เรื่องนี้ศึกษาผลของความสัมพันธ์ระหว่างพันธะไฮโดรเจน (H-bond) และอันตรกิริยา $\pi-\pi$ ต่อโครงสร้างและเสถียรภาพของกลุ่มโมเลกุลตัวถูกละลายในสารละลายที่ไม่ใช่น้ำ โดยใช้แบบจำลองเป็นกลุ่มโมเลกุลกรดเบนโซอิกและกลุ่มโมเลกุลฟีนอลในสารละลายเบนซีน และวิธีทางทฤษฎี การจำลองโมเลกุลพลวัต (Molecular Dynamics (MD) Simulations) ของกรดเบนโซอิก ไคเมอร์และสารประกอบที่เกิดจากการรวมตัวของกรดเบนโซอิกและน้ำ (BA-H₂O) แสดงว่าอันตรกิริยาระหว่างตัวถูกละลายกับตัวทำละลายและอันตรกิริยาระหว่างตัวทำละลายกับตัวทำละลายในระบบโมเลกุลนี้ค่อนข้างอ่อน และชั้นซอลเวชันรอบกลุ่มโมเลกุลตัวถูกละลายไม่แข็งแรง และสามารถเคลื่อนไหวได้ โดยเฉพาะอย่างยิ่งที่อุณหภูมิห้อง ยิ่งไปกว่านั้น พลังงานความร้อนและลักษณะโครงสร้างชั้นซอลเวชันมีบทบาทสำคัญอย่างมากในการกำหนดโครงสร้างและเสถียรภาพของกลุ่มโมเลกุลกรดเบนโซอิก ผลการการจำลองโมเลกุลพลวัตแสดงว่า สารประกอบกรดเบนโซอิกกับน้ำที่ไม่เสถียรในสถานะแก๊สกลับมีช่วงชีวิตยาวในสารละลายเบนซีน เนื่องจากโครงสร้างและอันตรกิริยาที่อ่อนและสลับซับซ้อน ทั้งที่เป็นอันตรกิริยาระหว่างตัวถูกละลายกับตัวทำละลายและระหว่างตัวทำละลายกับตัวทำละลาย ซึ่งในกรณีนี้ประกอบด้วยอันตรกิริยาระหว่างพันธะ C-H... π , O-H... π และ $\pi-\pi$ ส่งผลต่อโครงสร้างและเสถียรภาพของกลุ่มโมเลกุลที่มีพันธะไฮโดรเจน

ผลการจำลองโมเลกุลพลวัตพบการแลกเปลี่ยนพันธะไฮโดรเจนสองชนิดในสารประกอบกรดเบนโซอิกกับน้ำ ได้แก่การแลกเปลี่ยนพันธะไฮโดรเจนชนิดที่ตัวให้โปรตอนยังคงอยู่ในโมเลกุลเดิม และการแลกเปลี่ยนพันธะไฮโดรเจนชนิดที่ตัวให้โปรตอนเปลี่ยนเป็นตัวรับโปรตอน ซึ่งการแลกเปลี่ยนพันธะไฮโดรเจนทั้งสองชนิด สังเกตได้ก็ต่อเมื่อนำพฤติกรรมเชิงพลวัตของตัวทำละลายมาพิจารณาในแบบจำลองเท่านั้น ทั้งนี้ การแลกเปลี่ยนพันธะไฮโดรเจนดังกล่าว ไม่สามารถตรวจสอบได้จากคำนวณโดยวิธีกลศาสตร์โมเลกุล หรือวิธีการหาโครงสร้างที่เหมาะสมโดยวิธีแอบอินิซิโอ (*ab initio*)

สำหรับกลุ่มโมเลกุลฟีนอลแบบจำลองเทสพาร์ทิเคิล (Test particle model; T-model) และการจำลองโมเลกุลพลวัตแสดงว่ามีโมเลกุลเบนซีนอย่างน้อยสามโมเลกุลที่กลุ่ม O-H และโมเลกุลฟีนอลสามารถเป็นได้ทั้งตัวให้โปรตอนและตัวรับโปรตอน ภูมิภาคพลังงานศักย์เฉลี่ยสุทธิและภูมิภาคพลังงานศักย์เฉลี่ย ซึ่งคำนวณได้จากการจำลองโมเลกุลพลวัต แสดงขนาดและรูปร่างของ

พลังงานศักย์ที่มีค่าค่อนข้างสูง ทั้งนี้ ขนาดและรูปร่างของภูมิภาคพลังงานศักย์เฉลี่ยสุทธิ ถูกกำหนดโดยค่าอันตรกิริยาเฉลี่ยระหว่างตัวทำละลายกับตัวทำละลาย การที่ภูมิภาคพลังงานศักย์เฉลี่ยสุทธิของการแลกเปลี่ยนตัวทำละลายที่กลุ่ม O-H มีค่าสูง แสดงต่อไปว่าโมเลกุลเบนซีนที่กลุ่ม O-H สามารถสร้างกรงตัวทำละลายจำกัดเฉพาะ (local solvent cage) ที่ค่อนข้างแข็งแรงรอบตัวถูกละลาย

แผนภาพการแลกเปลี่ยนพันธะไฮโดรเจนแสดงว่า โมเลกุลเบนซีนที่กลุ่ม O-H ของโมเลกุลฟีนอล สามารถแลกเปลี่ยนได้โดยการเคลื่อนที่ของนิวเคลียสชนิดแอมพลิจูดใหญ่ (large amplitude nuclear motion) และกระบวนการแลกเปลี่ยนตัวทำละลายที่กลุ่ม O-H เป็นแบบการสับเปลี่ยนรวม (associative-interchange) ทั้งนี้ ช่วงชีวิตของสารประกอบโมเลกุลฟีนอลและเบนซีนที่ได้จากการคำนวณมีค่าใกล้เคียงกับที่ได้จากการทดลอง 2D-IR เนื่องจากอันตรกิริยาระหว่างโมเลกุลที่ค่อนข้างอ่อนและการกระเพื่อมของพลังงานความร้อนที่ 298 เคลวิน พันธะไฮโดรเจนในกลุ่มโมเลกุลฟีนอลไคเมอรัลไม่เสถียรและแยกออกในระหว่างการจำลองโมเลกุลพลวัต ส่วนพันธะไฮโดรเจนแบบไซคลิกในกลุ่มโมเลกุลฟีนอลไคเมอรัลเพียงเปิดออกบางส่วนเท่านั้นในสารละลายเบนซีน การที่พันธะไฮโดรเจน O-H...O ในกลุ่มโมเลกุลฟีนอลไคเมอรัลค่อนข้างเสถียร เนื่องจากโมเลกุลฟีนอลทั้งสามอยู่ใกล้ชิดกัน จึงเป็นการยากที่โมเลกุลเบนซีนจะแทรกเข้าไปได้ ซึ่งต่างจากกรณีของโมเลกุลฟีนอลไคเมอรัล จึงสรุปได้ว่าการแข่งขันกันระหว่างอันตรกิริยาระหว่างตัวถูกละลายกับตัวทำละลายและอันตรกิริยาระหว่างตัวทำละลายกับตัวทำละลายดังกล่าว สามารถศึกษาได้ก็ต่อเมื่อมีโมเลกุลตัวทำละลายอยู่ในแบบจำลองเท่านั้น

SERMSIRI CHAIWONGWATTANA : THEORETICAL STUDIES OF
MOLECULAR CLUSTERS IN SOLUTIONS: BENZOIC ACID AND
PHENOL IN BENZENE SOLUTIONS. THESIS ADVISOR : PROF.
KRITSANA SAGARIK, Ph.D. 143 PP.

BENZOIC ACID DIMER/PHENOL CLUSTERS/BENZENE SOLUTIONS/T-
MODEL/ MOLECULAR DYNAMICS SIMULATIONS

The interplay between H-bond and π - π interactions in non-aqueous environment was theoretically studied using clusters of benzoic acid (BA) and phenol (PhOH) in benzene (Benz) solutions as model systems. MD simulations on (BA)₂ and the BA-H₂O m : n complexes, m and n = 1 - 2, showed that, since the solute-solvent and solvent-solvent interactions are moderate in the BA systems, the solvation shells around the solute clusters are weak and mobile, especially at room temperature. This allows the thermal energy and the structure of the solvation shells to play important roles in determining the structures and stability of the BA clusters. It was also illustrated that, due to the solvent effects, some microhydrates not particularly associated in the gas phase appeared with long lifetime in the course of MD simulations.

The MD results showed two types of the H-bond exchange in the BA systems namely, the mutual and non-mutual ones. Both H-bond exchanges were detected since the dynamic behaviors were taken into account in the present theoretical model. For the PhOH systems, (PhOH)_n, n = 1 - 3, based on the T-model potentials, MD simulations showed at least three Benz molecules solvate at the O-H group, and

PhOH could act both as proton donor and acceptor towards Benz molecules. The average potential energy landscapes and cross section plots obtained from MD simulations indicated that the size and shape of the average potential energy wells are determined nearly exclusively by the average solvent-solvent interactions. Since the average potential energy barriers to solvent exchanges at the O-H group are quite high, Benz molecules at the O-H group could form part of quite strong local solvent cage.

Investigation on the H-bond exchange diagrams revealed that, Benz molecules at the O-H group of PhOH could exchange through large-amplitude nuclear motions and the solvent exchanges seem to favor the associative-interchange scheme. The lifetimes of the PhOH-Benz complex were approximated and in reasonable agreement with 2D-IR vibrational echo experiment. It appeared that, due to weak interaction and the thermal energy fluctuation at 298 K, the O-H...O H-bond in $(\text{PhOH})_2$ was disrupted in MD simulations, whereas cyclic H-bonds in $(\text{PhOH})_3$ were only opened in $[(\text{PhOH})_3]_{\text{Benz}}$; the O-H...O H-bonds in $(\text{PhOH})_3$ are quite well protected by the three PhOH molecules, therefore not easily accessible by Benz molecules as in the case of $(\text{PhOH})_2$. This suggested that, the competition between solute-solute and solute-solvent interactions could be studied only when explicit solvent molecules are taken into account in the model calculations.

School of Chemistry

Academic Year 2008

Student's Signature_____

Advisor's Signature_____

ACKNOWLEDGEMENTS

I would like to take this opportunity to express my deeply grateful thank to my thesis advisor, Prof. Dr. Kritsana Sagarik for his guidance, valuable suggestions and encouragement during the period of my study.

I would also like to acknowledge the financial support from the Thailand Research Fund (TRF) through the Royal Golden Jubilee (RGJ) Ph.D. program (Grant No. PHD/0071/2547). Special thanks should go to the School of Chemistry and the School of Mathematics, Institute of Science, Suranaree University of Technology (SUT), as well as the National Electronics and Computer Technology Center (NECTEC) and the National Nanotechnology Center (NANOTEC), for providing computer facilities.

I am thankful to all the lectures at the School of Chemistry, Suranaree University of Technology for their useful comments. I would like to particularly thank to Assoc. Prof. Dr. Anan Tongraar for his encouragement and help. Furthermore I would like to thank the thesis examining committee for their valuable suggestions and comments.

Thanks to all of my friends at the Computational Chemistry Research Laboratory (CCRL) group, Suranaree University of Technology for their friendship and assistance. In addition, I would like to express my sincere thanks to Prof. Dr. Fu Ming Tao at California State University, Fullerton, USA, and Prof. Dr. Thanh N.

Truong at University of Utah, USA, who provide me valuable advices and suggestions with respect to my work.

Finally, I would like to take this opportunity to express my deepest gratitude to my parents, grandmother and grandfather for their lot of love, understanding, and encouragement.

Sermsiri Chaiwongwattana

CONTENTS

	Page
ABSTRACT IN THAI.....	I
ABSTRACT IN ENGLISH	III
ACKNOWLEDGEMENTS.....	V
CONTENTS.....	VII
LIST OF TABLES.....	IX
LIST OF FIGURES	X
LIST OF ABBREVIATIONS.....	XIV
CHAPTER	
I INTRODUCTION.....	1
II RESEARCH METHODOLOGY	9
2.1 The T-model potentials	10
2.2 Equilibrium structures in the gas phase	13
2.3 MD simulations.....	14
2.3.1 [(BA) ₂] _{Benz} and [BA-H ₂ O] _{Benz}	14
2.3.2 [(PhOH) _n] _{Benz}	16
2.4 Computer softwares and facilities.....	21

CONTENTS (Continued)

	Page
III RESULTS AND DISCUSSION	22
3.1 (BA) ₂ and BA-H ₂ O complexes	22
3.1.1 Structures and energetic in the gas phase.	22
3.1.2 MD simulations of benzene solutions.....	29
3.2 PhOH-Benz complexes	46
3.2.1 Structures and energetic in the gas phase	46
3.2.2 MD simulations of benzene solutions.....	53
IV CONCLUSION	81
REFERENCES	86
APPENDICES	97
APPENDIX A THE T-MODEL PARAMETERS.....	98
APPENDIX B SUPPLEMENTARY RESULTS FOR MD SIMULATIONS OF [PhOH] _{Benz}	101
APPENDIX C SUPPLEMENTARY RESULTS FOR MD SIMULATIONS OF [(PhOH) ₂] _{Benz}	114
APPENDIX D LISTS OF PRESENTATIONS.....	127
APPENDIX E LISTS OF PUBLICATIONS.....	129
CURRICULUM VITAE	143

LIST OF TABLES

Table		Page
3.1	MD results on (BA) ₂ and BA-H ₂ O complexes in Benz solutions. The number of Benz molecules in [(BA) ₂] _{Benz} ^{T=298} , [1:1] _{Benz} ^{T=X} and [1:2] _{Benz} ^{T=X} are 124 and those in [2:1] _{Benz} ^{T=X} and [2:2] _{Benz} ^{T=X} are 122, X = 280 and 298 K...	35
3.2	Some average H-bond distances ($\langle R_{A-H..B} \rangle$) and angles ($\langle \theta_{A-H..B} \rangle$), as well as the H-bond lifetimes ($\langle t_{A-H..B} \rangle$), derived from MD simulations. Only solute clusters are shown in the table	36
3.3	Energetic results obtained from MD-[(PhOH) _n] _{Benz} ^{frozen} and MD-[(PhOH) _n] _{Benz} ^{free} , n = 1 – 3. Energies are in kJ mol ⁻¹	54
3.4	The highest probabilities at the labeled contours on the π -PD maps ($\langle P^{\pi-PD} \rangle_{\max}$), in Figure 3.9, together with the corresponding lowest average interaction energies ($\langle \Delta E_{Benz}^X \rangle_{\min}$) obtained from MD-[(PhOH) _n] _{Benz} ^{frozen}	56
3.5	The highest probabilities at the labeled contours on the π -PD maps ($\langle P^{\pi-PD} \rangle_{\max}$), in Figure 3.11, together with the corresponding lowest average interaction energies ($\langle \Delta E_{Benz}^X \rangle_{\min}$) obtained from MD-[(PhOH) _n] _{Benz} ^{frozen}	69

LIST OF FIGURES

Figure	Page
2.1 a) Second virial coefficients for Benz. b) Second virial cross-coefficients for Benz-H ₂ O complex.....	12
2.2 The conformations of BA and PhOH with running number.....	13
2.3 a) - b) Reference planes for PhOH and (PhOH) ₂ in Benz solutions	18
3.1 Structures of the CHP and SOT dimmers computed from the T-model potentials.....	23
3.2 The absolute and two local minimum energy geometries of the BA-H ₂ O 1 : 1 complexes computed from the T-model potentials	24
3.3 The absolute and two local minimum energy geometries of the BA-H ₂ O 1 : 2 complexes computed from the T-model potentials	25
3.4 The absolute and two local minimum energy geometries of the BA-H ₂ O 2 : 1 complexes computed from the T-model potentials	27
3.5 The absolute and two local minimum energy geometries of the BA-H ₂ O 2 : 2 complexes computed from the T-model potentials	28
3.6 Equilibrium structures and interaction energies of the PhOH-Benz 1 : 1 complexes in the gas phase, computed from the T-model potentials	49
3.7 Equilibrium structures and interaction energies of the PhOH-Benz 1 : 2 complexes in the gas phase, computed from the T-model potentials	50

LIST OF FIGURES (Continued)

Figure	Page
3.8 Equilibrium structures and interaction energies of the PhOH-Benz $m : n$ complexes in the gas phase, computed from the T-model potentials. a) – b) The PhOH-Benz 2 : 1 complexes. c) – e) The PhOH-Benz 2 : 2 complexes	51
3.9 Structural and energetic results obtained from MD-[PhOH] _{Benz} ^{frozen} . X-, Y- and Z-axes are in Å, energies in kJ mol ⁻¹ . a) – d) The π -PD, PB-PD and PB-BB-PD maps. e) – f) Average potential energy landscapes and the cross section plots computed from longitudinal and transverse profile lines. _____ PB-BB-PD cross section plot. - - - - - PB-PD cross section plot. - - - - - BB-PD cross section plot.....	59
3.10 Structural and dynamic results obtained from MD-[PhOH] _{Benz} ^{free} . a) – b) $g(R)$; characteristic distances given with $n(R)$ in parentheses. c) Example of H-bond exchange diagram. d) Fourier transformations of the O-H.. π H-bond and $\pi_{ph}..\pi$ distances. $\tau_{O-H..\pi}^{PhOH-Benz}$ = the lifetime of the PhOH-Benz complex computed from FFT of the O-H.. π H-bond distance. $\tau_{\pi_{ph}..\pi}^{PhOH-Benz}$ = the lifetime of the PhOH-Benz complex computed from FFT of the $\pi_{ph}..\pi$ distance	62

LIST OF FIGURES (Continued)

Figure	Page
3.11 Structural and energetic results obtained from MD- $[(\text{PhOH})_2]_{\text{Benz}}^{\text{frozen}}$. X, Y- and Z-axes are in Å, energies in kJ mol^{-1} . a) – d) The π -PD, PB-PD and PB-BB-PD maps. e) – f) Average potential energy landscapes and the cross section plot computed from longitudinal and transverse profile lines. _____ PB-BB-PD cross section plot. - - - - - PB-PD cross section plot. - - - - -BB-PD cross section plot. π -PD contour: min = 0.0 : max = 0.13: interval = 0.01. PB-PD contour: min = -30.0 : max = -1.0 : interval = 4.5. PB-BB-PD contour: min = -99.0 : max = -70.0: interval = 7.2	72
3.12 Structural and dynamic results obtained from MD- $[(\text{PhOH})_2]_{\text{Benz}}^{\text{free}}$. a) – c) $g(R)$; characteristic distances given with $n(R)$ in parentheses. d) Snapshots of the PhOH-Benz clusters in $[(\text{PhOH})_2]_{\text{Benz}}$. e) – f) example of H-bond exchange diagram	75
3.13 $g(R)$ obtained from MD- $[(\text{PhOH})_3]_{\text{Benz}}^{\text{free}}$, together with characteristic distances	80
B.1 The π -PD, PB-PD, BB-PD and PB-BB-PD maps with respect to reference plane II obtained from MD- $[\text{PhOH}]_{\text{Benz}}$	102

LIST OF FIGURES (Continued)

Figure	Page
B.2	The π -PD, PB-PD, BB-PD and PB-BB-PD maps with respect to reference plane III obtained from MD-[PhOH] _{Benz}
	106
B.3	The π -PD, PB-PD, BB-PD and PB-BB-PD maps with respect to reference plane I obtained from MD-[PhOH] _{Benz}
	110
C.1	The π -PD, PB-PD, BB-PD and PB-BB-PD maps with respect to reference plane II obtained from MD-[(PhOH) ₂] _{Benz}
	115
C.2	The π -PD, PB-PD, BB-PD and PB-BB-PD maps with respect to reference plane III obtained from MD-[(PhOH) ₂] _{Benz}
	119
C.3	The π -PD, PB-PD, BB-PD and PB-BB-PD maps with respect to reference plane I obtained from MD-[(PhOH) ₂] _{Benz}
	123

LIST OF ABBREVIATIONS

Å	=	Angström
D	=	Debye
K	=	Kelvin
M	=	molar
kJ mol^{-1}	=	kilo Joule per mole
H-bond	=	hydrogen bond
π -H-bond	=	π -Hydrogen bond
fs	=	femtosecond
ps	=	picosecond
L	=	simulation box length
BA	=	benzoic acid
Benz	=	benzene
CCl_4	=	carbon tetrachloride
H_2O	=	water
PhOH	=	phenol
Tyr	=	tyrosine
$\text{Gdm}^+\text{-FmO}^-$	=	guanidinium-formate complex
CHP	=	cyclic planar hydrogen bond
SOT	=	side-on type
T-model	=	test-particle model

LIST OF ABBREVIATIONS (Continued)

MC	=	Monte Carlo
MD	=	molecular dynamics
NVE-MD	=	microcanonical ensemble-MD simulations
B3LYP	=	Becke three-parameters hybrid functional combined with Lee-Yang-Parr correlation function
MP2	=	second-order Møller-Plesset
SCF	=	self-consistent field
CHelpG	=	charges from electrostatic potentials using a grid based method
[Benz] _{liquid}	=	liquid benzene
[Benz] _{crystal}	=	benzene molecule in crystal
(PhOH) _n	=	phenol cluster
(H ₂ O) _n	=	water cluster
BA-H ₂ O	=	benzoic acid–water complex
[(BA) _n] _{Benz}	=	benzoic acid cluster in benzene solution
PhOH-Benz	=	phenol– benzene complex
PhOH-H ₂ O	=	phenol–water complex
[(PhOH) _n] _{Benz}	=	phenol cluster in benzene solution
NMR	=	nuclear magnetic resonance
2D-IR	=	two-dimensional IR
ΔE	=	interaction energy

LIST OF ABBREVIATIONS (Continued)

$B(T)$	=	second-virial coefficient
$B_{12}(T)$	=	second-virial cross-coefficient
A-H..B	=	hydrogen-bond between the proton donor A and acceptor B
$\Delta E_{T\text{-model}}$	=	test particle model interaction energy
ΔE_{SCF}^1	=	first-order SCF interaction energy
ΔE^r	=	higher-order energy
g cm^{-3}	=	gram per cubic centimeter
$g(R)$	=	atom-atom pair correlation functions
$n(R)$	=	average running coordination numbers
I_a	=	associative-interchange scheme
FFT	=	fast Fourier transformations
SD	=	standard deviation
π	=	center of mass of Benz
π_{Ph}	=	center of mass of PhOH
$[1:1]_{\text{Benz}}$	=	BA-H ₂ O 1 : 1 complex in Benz solution
$[1:2]_{\text{Benz}}$	=	BA-H ₂ O 1 : 2 complex in Benz solution
$[2:1]_{\text{Benz}}$	=	BA-H ₂ O 2 : 1 complex in Benz solution
$[2:2]_{\text{Benz}}$	=	BA-H ₂ O 2 : 2 complex in Benz solution
PD	=	probability distribution
π -PD	=	solvent probability distribution

LIST OF ABBREVIATIONS (Continued)

PB-PD	=	solute-solvent interaction energy probability distribution
BB-PD	=	solvent-solvent interaction energy probability distribution
PB-BB-PD	=	combinations of the solute-solvent and solvent-solvent interaction energy probability distribution
$\langle R_{A-H..B} \rangle$	=	average H-bond distances between proton donor A and acceptor B
$\langle \theta_{A-H..B} \rangle$	=	average angles between the A-H bond and the line connecting atoms A and B
$\langle t_{A-H..B} \rangle$	=	percentage of simulation step during which H-bond donor A and acceptor B are coming close enough to engage in H-bond formation
$\langle E_{Benz}^{pot} \rangle$	=	average potential energy of Benz solution
$\langle E_{Benz}^{sol-sol} \rangle$	=	average solute-solute interaction energies in Benz solution
$\langle E_{Benz}^{solu-solv} \rangle$	=	average solute-solvent interaction energies in Benz solution
$\langle P^{\pi-PD} \rangle_{max}$	=	the highest probabilities at the labeled contours on the π -PD maps

LIST OF ABBREVIATIONS (Continued)

- $\langle \Delta E_{\text{Benz}}^{\text{PB-PD}} \rangle_{\text{min}}$ = the lowest-average interaction energies on the solute-solvent probability distributions in Benz solution
- $\langle \Delta E_{\text{Benz}}^{\text{BB-PD}} \rangle_{\text{min}}$ = the lowest-average interaction energies on the solvent-solvent probability distributions in Benz solution
- $\langle \Delta E_{\text{Benz}}^{\text{PB-BB-PD}} \rangle_{\text{min}}$ = the lowest-average interaction energies on the sum of solute-solvent and solvent-solvent probability distributions in Benz solution
- $\langle E_{\text{Benz}}^{\text{L}} \rangle$ = the average potential energy barriers to the diffusion of water molecules within and between the H-bond networks in Benz solution
- $\langle E_{\text{Benz}}^{\text{T}} \rangle$ = the average potential energy barriers to the diffusion of water molecules between the H-bond networks and the outside in Benz solution
- $\tau_{\text{O-H}.. \pi}^{\text{PhOH-Benz}}$ = lifetime of the PhOH-Benz complex computed from FFT of the O-H.. π H-bond distance.
- $\tau_{\pi_{\text{ph}}.. \pi}^{\text{PhOH-Benz}}$ = lifetime of the PhOH-Benz complex computed from FFT of the $\pi_{\text{ph}}.. \pi$ distance.

CHAPTER I

INTRODUCTION

Clusters of molecules formed from aromatic compounds have been of interest since they represent interactions between π -systems found in DNA and side chains of proteins (Van Holde, Johnson, and Ho, 1998). Various experimental and theoretical investigations have been performed in the past two decades to obtain basic information concerning with the driving forces responsible for the interactions in aromatic systems especially among biomolecules (Brutschy, 2000). As an example, the so-called “ π -hydrogen bond” (π -H-bond) has been put forward due to its importance in biological systems, e.g. the ability to stabilize α -helix in proteins (Knee, Khundkar, and Zewail, 1987; Perutz, 1993; Meyer, Castellano, and Diederich, 2003).

The presence of π -electrons enables clusters of aromatic compounds, generated in continuous or pulsed supersonic beams, to be examined effectively using modern spectroscopic techniques, such as resonance two photon ionization (Roth et al., 1998; Mikami, 1995; Lipert and Colson, 1988), disperse fluorescence (Jacoby et al., 1998), cluster ion dip spectroscopy (Sawamura, Fujii, Sato, Ebata, and Mikami, 1996; Ohashi, Inokuchi, and Nishi, 1996) and ionization-detected stimulated Raman spectroscopy (Hartland, Henson, Ventura, and Felker, 1992). Advancement in computational chemistry software packages and parallel computer technology (Young, 2001) has also allowed *ab initio* calculations that include the effects of

electron correlations to study larger clusters of aromatic compounds with higher accuracy (Sinnokrot and Sherrill, 2004). It has, therefore, become a general practice in the area of molecular association to apply structural models obtained from *ab initio* calculations for the fitting of spectroscopic observations (Rode et al., 2005). Since a large number of review articles on molecular associations have been published, only some important information relevant to the present thesis will be briefly summarized.

Clusters of benzene ((Benz)_n) have been considered as prototypes for the π - π and C-H.. π interactions. They have been extensively studied by theoretical and experimental methods (Ricci et al., 2001; Magro et al., 2005; Sun and Bernstein, 1996; Kearley, Johnson, and Tomkinson, 2006; Chelli et al., 2000; Bartell and Dulles, 1995; Grover, Walters, and Hui, 1987). Theoretical methods (Sinnokrot and Sherrill, 2004; Sinnokrot, Valeev, and Sherrill, 2002) suggested at least four equilibrium structures of benzene dimer ((Benz)₂) in the gas phase namely, parallel displaced, T-shaped, parallel staggered and herringbone structures. The parallel displaced structure is stabilized solely by the π - π interaction, whereas the T-shaped structure mainly by the C-H.. π interaction. The former was predicted by *ab initio* calculations at the highest level of accuracy (Sinnokrot, Valeev, and Sherrill, 2002) to possess the lowest interaction energy and in good agreement with experiment (Grover, Walters, and Hui, 1987), whereas the latter was pointed out to represent a low-energy saddle point for the interconversion between parallel displaced structures.

Fast dynamics of single Benz molecule in the liquid phase ([Benz]_{liquid}) was studied in femtosecond heterodyne detected optical Kerr effect (HD-OKE) experiments in a wide temperature range (Ricci et al., 2001), from which the results at short times were interpreted by assuming that the basic microscopic system consists

of a Benz molecule librating and oscillating in a local confinement or solvent “cage”. The instantaneous cage structures and dynamics in [Benz]_{liquid} and [Benz]_{crystal} were studied in details by spectroscopic measurements (Margo et al., 2005), as well as molecular dynamic (MD) (Chelli et al., 2000) and lattice dynamic simulations (Kearley, Johnson, and Tomkinson, 2006). It was reported that, a reminiscence of crystalline structure was evident in [Benz]_{liquid}, although no preferential orientation was observed in the first coordination shell (Chelli et al., 2000). Moreover, the cages in [Benz]_{liquid} were similar in composition to those in [Benz]_{crystal}, and the majority of the cages in [Benz]_{liquid} could live several hundred femtoseconds (fs) or picoseconds (ps), depending upon the radius used to define the cage (Chelli et al., 2000).

Association of organic acids in organic solvents has been extensively studied in the past two decades using various theoretical and experimental techniques (Chocholoušová, Vacek, and Hobza, 2003; Christian, Affsprung, and Taylor, 1963; Zaugg, Steed, and Woolley, 1972; Fujii, Yamada, and Mitzuta, 1988). The self-association and hydration constants of organic acids in non-polar solvents can be obtained by distribution of an organic acid between two immiscible solvents such as water and Benz. Distribution experiments suggested the formation of microhydrates of the organic acid monomer (Van Duyne, Taylor, Christian, and Affsprung, 1967) and dimer (Wall and Rouse, 1941; Wall, 1942; Van Duyne et al., 1967; Shamsul Huq and Lodhi, 1966) in organic solvents. For small carboxylic acids such as acetic acid (AA), cyclic H-bond structures were reported to be quite stable in the gas phase, as well as in chloroform (Chocholoušová, Vacek, and Hobza, 2003), Benz (Christain, Affsprung, and Taylor, 1963) and carbon tetrachloride (Christain, Affsprung, and Taylor, 1963; Zaugg, Steed, and Woolley, 1972). It was concluded that the more

inactive the solvent, the more pronounced is the tendency of the acid to react with itself (Fujii, Yamada, and Mizuta, 1988).

Benzoic acid (BA) is an aromatic carboxylic acid with a phenyl ring and a carboxylic functional group in the same molecule. The magnitudes of the enthalpy changes for the dimerization of BA evaluated from IR vary with solvent in the order: Benz < carbon tetrachloride < cyclohexane < vapor (Allen, Watkinson, and Webb, 1966). Distribution of BA between the Benz and water phases, as well as the number of water molecules H-bonded to BA in the Benz phase, represents one of the classical problems in the area of molecular association in solutions (Wall and Rouse, 1941; Wall, 1942; Van Duyne et al., 1967; Shamsul Huq and Lodhi, 1966). It was shown that, BA exists as monomer in aqueous solutions (Wall and Rouse, 1941; Van Duyne et al., 1967). The distribution data revealed that the important associated species in Benz solution at 298 K are $(BA)_2$, the BA-H₂O 1 : 1, 1 : 2 and 2 : 1 complexes (Van Duyne et al., 1967). In order to obtain a satisfactory correlation of the results, they must be taken into account in the analysis of the distribution data. However, based on the assumption that the hydrated $(BA)_2$ can be ignored, it was proposed that a single BA molecule is hydrated by a water molecule in the Benz phase. These opposite to the assumption to neglect the probability of finding microhydrates of both BA and $(BA)_2$ in the Benz phase (Shamsul Huq and Lodhi, 1966).

Structures and stability of the cyclic H-bond planar (CHP) and side-on type (SOT) dimers of BA in aqueous solutions were studied based on the intermolecular potentials derived from the test-particle model (T-model) and MD simulations (Sagarik and Rode, 2000). It was found that, in the gas phase and dilute aqueous solution, the cyclic H-bonds in the CHP and SOT dimers can be disrupted by H-

bonding with water, as well as thermal energy fluctuation. The theoretical results agree well with the previous reports (Wall and Rouse, 1941; Van Duyne et al., 1967) and the experimental finding that the concentration of $(\text{BA})_2$ is less than 3 % of the concentration of the unionized BA (Gruenloh, Florio, Carney, Hagemeister, and Zwier, 1999; Gruenloh, Hagemeister, Carney, and Zwier, 1999). The situations in $(\text{BA})_2$ are similar to the acetic acid dimer $((\text{AA})_2)$, in which water-separated structures were suggested to dominate in the gas phase and aqueous solutions (Zaugg, Steed, and Woolley, 1972).

As the simplest aromatic compound which can form O-H... π and O-H...O H-bonds, and a prototype for structurally related subunits in larger biomolecules, such as tyrosine (Tyr) residue in proteins, phenol (PhOH) has been frequently selected as a model molecule in both experimental and theoretical investigations (Sinnokrot and Cherrill, 2004; Hunter, Singh, and Thornton, 1991). For example, theoretical methods at MP2/6-31G(d) and B3LYP/6-31G(d) levels were employed in the study of structures and stabilities of the O-H...O H-bond in $(\text{PhOH})_n$ and $(\text{H}_2\text{O})_n$, $n = 1 - 4$, as well as the PhOH-H₂O $m : n$ complexes, m and $n = 1 - 3$, and $m + n \leq 4$ (Parthasarathi, Subramanian, and Sathyamurthy, 2005). MP2/6-31G(d) results showed that $(\text{PhOH})_n$ and $(\text{H}_2\text{O})_n$ possess similar H-bond patterns, and $(\text{PhOH})_n$ are slightly more stable due to the effects of electron correlations. Moreover, it was shown that, H-bonds in the PhOH-H₂O $m : n$ complexes are similar to $(\text{H}_2\text{O})_n$.

The interplay between electrostatic and dispersion interactions has been studied through the weak interaction between the O-H group in PhOH and the polarizable π -electron clouds in Benz (Olkawa, Abe, Mikami, and Ito, 1983; Guedes et al., 2003). In the gas phase, B3LYP/6-31G(d,p) calculations revealed that, the

PhOH-Benz 1 : 1 complex is stabilized mainly by the O–H.. π H-bond, whereas in the PhOH-Benz 1 : 2 complex, the O-H group of PhOH acts simultaneously as proton donor and acceptor towards Benz molecules (Guedes et al., 2003).

Molecular association of PhOH in Benz solutions was examined in classical partition experiments, in which distributions of PhOH between Benz and water were studied at 298 K (Endo, 1926). The measurements of partition coefficients revealed that, in Benz, equilibrium could establish between PhOH and (PhOH)₃, whereas in water, PhOH is monomolecular up to at least 0.15 M. It was emphasized that, PhOH associates itself in triple molecules and not in double molecules (Endo, 1926). The existence of the monomer-trimer equilibrium was also suggested from NMR experiment (Saunders and Hyne, 1958), in which the equilibrium constant was determined in CCl₄ by measuring the hydroxyl NMR frequencies as functions of concentrations. However, Philbrick (1934) proposed the existence of (PhOH)₂ in Benz solutions, by measurements of partition coefficients of PhOH between Benz and water at concentrations in the water layer below 0.1 M. The results were confirmed by isopiestic experiments in anhydrous solutions (Lassette and Dickinson, 1939).

Dynamics of complexes involving non-covalent interactions with aromatic rings is pivotal to protein-ligand recognition (Meyer, Castellano, and Diederich, 2003). With the enthalpy of formation of only about 17 kJ mol⁻¹ (Knee, Khundkar, and Zewail, 1987), the association and dissociation of the PhOH-Benz complexes in solutions seem too rapid to measure using conventional spectroscopic methods (Zheng et al., 2005). Two-dimensional IR (2D-IR) vibrational echo spectroscopy, an ultrafast vibrational analog of two-dimensional NMR, has been developed to measure fast chemical exchange dynamics in the ground electronic state under thermal

equilibrium conditions (Zheng, Kwak, and Fayer, 2007; Kwac et al., 2006; Zheng, Kwak, Chen, Asbury, and Fayer, 2006; Finkelstein et al., 2007; Kwak, Zheng, Cang, and Fayer, 2006). Equilibrium dynamics in the PhOH-Benz complex was studied in a mixed solvent of Benz by measuring in real time the appearance of off-diagonal peaks in the 2D-IR vibrational echo spectra of the PhOH hydroxyl stretching (Kwak et al., 2006); the high-frequency hydroxyl stretching was assigned to free PhOH, whereas the low-frequency to the PhOH-Benz complex. According to the analysis of the 2D-IR spectra, the dissociation time of the PhOH-Benz 1 : 1 complex was estimated to be about 8 ps.

In order to investigate the interplay between H-bond and π - π interactions in non-aqueous environment, two chemical systems were considered in the present thesis. In the first system, structures and stabilities of cyclic H-bonds in Benz solutions were examined using $(BA)_2$ and the BA-H₂O m : n complexes, m and n = 1 - 2, as model molecules. The theoretical study began with construction of the T-model potentials for BA, Benz and the BA-H₂O complexes, followed by a series of MD simulations. The structures and stability of $(BA)_2$ and the BA-H₂O complexes in Benz solutions were studied by performing MD simulations at 280 and 298 K. The H-bond (A-H..B) complexes in Benz solutions were discussed based on the average H-bond distances ($\langle R_{A-H..B} \rangle$) and angles ($\langle \theta_{A-H..B} \rangle$), as well as the H-bond lifetimes ($\langle t_{A-H..B} \rangle$). The stability of $(BA)_2$ and the BA-H₂O complexes was also analyzed and discussed using the average solute-solute interaction energies ($\langle E_{Benz}^{sol-sol} \rangle$) and the average potential energies of Benz solutions ($\langle E_{Benz}^{pot} \rangle$) derived from MD simulations.

In the second system, the effects of weak C-H.. π , O-H.. π H-bond and π .. π interactions on structures, energetic and dynamics of (PhOH) $_n$, $n = 1 - 3$, in Benz solutions were studied. In order to acquire some basic information, the equilibrium structures and interaction energies of the PhOH-Benz $m : n$ complexes, m and $n = 1 - 2$, in the gas phase, were investigated using the T-model potentials. Then, NVE-MD simulations were performed on [(PhOH) $_n$] $_{\text{Benz}}$ at 298 K. The average three-dimensional structures and interaction energy distributions in [(PhOH) $_n$] $_{\text{Benz}}$ were visualized and analyzed based on solvent probability distribution (PD) maps and average solute-solvent and solvent-solvent interaction energy PD maps, respectively (Sagarik and Chaiyapongs, 2005; Sagarik and Dokmaisrijan, 2005; Deeying and Sagarik, 2006). The dynamics in the first solvation shell of [(PhOH) $_n$] $_{\text{Benz}}$ was analyzed and discussed using the average interaction energy PD maps and their cross section plots (Sagarik and Chaiyapongs, 2005; Sagarik and Dokmaisrijan, 2005; Deeying and Sagarik, 2006), as well as the H-bond and solvent exchange diagrams. The results were discussed in comparison with available theoretical and experimental results of the same and similar systems.

CHAPTER II

RESEARCH METHODOLOGY

Intermolecular potentials (ΔE) constitute primary information needed for all kinds of statistical mechanical simulations, e.g. MD and Monte Carlo (MC) simulations. ΔE could be computed directly from *ab initio* calculations or inferred from experimental data. While *ab initio* calculations are restricted to small molecules with high symmetry, experimental data seem not complete for polyatomic molecules. In order to approximate ΔE , it is therefore reasonable and applicable to combine information from both *ab initio* calculations and available experimental data. Such method has been developed (Böhm, Ahlrichs, Scharf, and Schiffer, 1984) and tested successfully in MD simulations on H-bond and π - π systems (Sagarik, Pongpituk, Chaiyapongs, and Sisot, 1991; Sagarik and Spohr, 1995; Sagarik and Asawakun, 1997; Sagarik and Rode, 2000; Sagarik, Chaiwongwattana, and Sisot, 2004).

In this chapter, some important aspects of the theoretical methods employed in the present thesis, e.g. the T-model and MD simulations, will be briefly summarized, with the emphasis on MD simulations conditions and analyses.

2.1 The T-model

Within the framework of the T-model, the interaction energy ($\Delta E_{\text{T-model}}$) between molecules A and B is written as a sum of the first-order interaction energy (ΔE_{SCF}^1) and a higher-order energy (ΔE^r).

$$\Delta E_{\text{T-model}} = \Delta E_{\text{SCF}}^1 + \Delta E^r \quad (1)$$

ΔE_{SCF}^1 accounts for the exchange repulsion and electrostatic energy contributions. It is computed from *ab initio* SCF calculations (Böhm and Ahlrichs, 1982) and takes the following analytical form:

$$\Delta E_{\text{SCF}}^1 = \sum_{i \in A} \sum_{j \in B} \left[\exp \left[\frac{-R_{ij} + \sigma_i + \sigma_j}{\rho_i + \rho_j} \right] + \frac{q_i q_j}{R_{ij}} \right] \quad (2)$$

i and j in Equation (2) label the sites of molecules A and B. σ_i , ρ_i and q_i are site parameters. R_{ij} is the site-site distance. The exponential parameters, σ_i and ρ_i , are responsible for the exchange repulsion and determined by probing molecules A and B with an uncharged spherical test particle. A nitrogen atom (N) in its average of terms state has been proved to be the most suitable (Böhm and Ahlrichs, 1982). Since in general molecules A and B are not spherically symmetric, molecules A and B must be probed in all possible directions by the test particle.

The higher-order energy, ΔE^r in Equation (1), represents the dispersion and polarization contributions of the T-model potential. ΔE^r could be determined from

both theoretical and experimental data. Previous experience has shown that, a calibration of the incomplete potential to the properties related to intermolecular interaction energies could be an appropriate choice. ΔE^r takes the following analytical form:

$$\Delta E^r = -\sum_{i \in A} \sum_{j \in B} C_{ij}^6 F_{ij}(R_{ij}) R_{ij}^{-6} \quad (3)$$

where

$$F_{ij}(R_{ij}) = \exp\left[-\left(1.28R_{ij}^0/R_{ij} - 1\right)^2\right], R_{ij} < 1.28R_{ij}^0 \\ = 1, \text{ elsewhere} \quad (4)$$

and

$$C_{ij}^6 = C_6 \frac{3}{2} \frac{\alpha_i \alpha_j}{(\alpha_i/N_i)^{1/2} + (\alpha_j/N_j)^{1/2}}, \quad (5)$$

R_{ij}^0 in Equation (4) is the sum of the van der Waals radii of the interacting atoms. Equation (5) is the Slater-Kirkwood relation; α_i and N_i denote the atomic polarizability and the number of valence electrons of the corresponding atom, respectively. $F_{ij}(R_{ij})$ in Equation (4) is a damping function, introduced to correct the behavior of R_{ij}^{-6} at short R_{ij} distance. Only C_6 in Equation (5) is unknown. The value of C_6 can be determined in many different ways. For $(\text{Benz})_n$ and $\text{Benz-H}_2\text{O}$ complexes, C_6 was determined by fits of the incomplete potentials, including ΔE_{SCF}^1 , to experimental second virial coefficients ($B(T)$) and second virial cross coefficients ($B_{12}(T)$) (Dymond and Smith, 1980), respectively. The agreements between the experimental and theoretical $B(T)$ in Figure 2.1 reflect the quality of the T-model potentials of Benz. For the PhOH-Benz complex, the C_6 parameter was determined by

a calibration of the incomplete potential with the interaction energy obtained from MP2/6-311G(d,p) calculations.

In the present study, the T-model parameters for BA, Benz and water were taken from Sagarik and Rode (2000) and listed in Table A.1, whereas those for PhOH from Sagarik and Asawakun (1997) and shown in Table A.2.

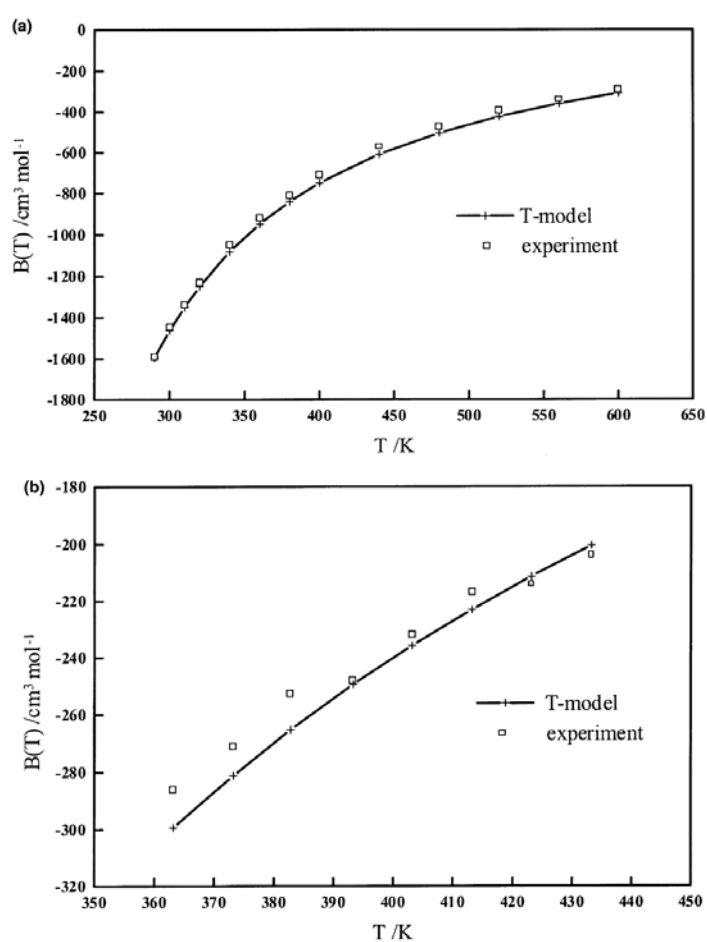


Figure 2.1 a) Second virial coefficients for Benz. b) Second virial cross-coefficients for Benz-H₂O complex.

2.2 Equilibrium structures in the gas phase

The geometries of BA and PhOH, shown in Figure 2.2 with atom numbering system, were taken from Sagarik and Rode (2000) and Sagarik and Asawakun (1997), respectively. They were kept constant throughout the calculations. Since the calculations of the minimum energy geometries of all the H-bond complexes considered followed the same procedures, they will be explained using the PhOH-Benz 1 : 1 complex as an example.

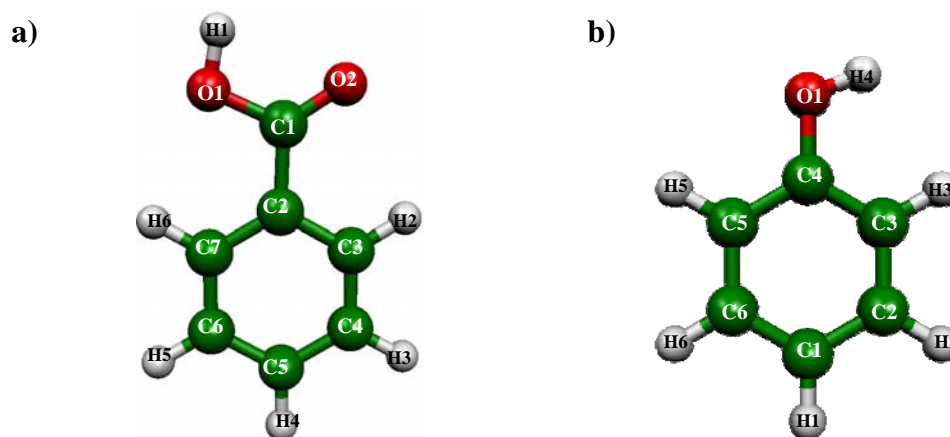


Figure 2.2 The conformations of BA and PhOH with running number.

The absolute and local minimum energy geometries of the PhOH-Benz 1 : 1 complexes were computed by placing PhOH at the origin of the Cartesian coordinate system. The coordinates of Benz were randomly generated in the vicinities of PhOH. Based on the T-model potentials (Sagarik, Chaiwongwattana, and Sisot, 2004; Sagarik and Asawakun, 1997), the absolute and local minimum energy geometries were searched using a minimization technique (Schlegel, 1982). One hundred starting configurations were employed in each geometry optimization and

some characteristic H-bond distances were computed and used in the discussions on Benz solutions.

2.3 MD simulations

The T-model parameters listed in Tables A.1 and A.2 were applied in MD simulations of $[(BA)_2]_{Benz}$ and $[BA-H_2O]_{Benz}$, as well as $[(PhOH)_n]_{Benz}$, respectively.

2.3.1 $[(BA)_2]_{Benz}$ and $[BA-H_2O]_{Benz}$

In order to obtain insights into the structure and stability of H-bonds in $[(BA)_2]_{Benz}$, as well as in the microhydrates of BA and $(BA)_2$ in Benz solutions, a series of NVE-MD simulations were conducted. The investigations included MD simulations of $[(BA)_2]_{Benz}^{T=X}$, $[1:1]_{Benz}^{T=X}$, $[1:2]_{Benz}^{T=X}$, $[2:1]_{Benz}^{T=X}$ and $[2:2]_{Benz}^{T=X}$, at $X = 280$ and 298 K. These correspond to MD- $[(BA)_2]_{Benz}^{T=X}$, MD- $[1:1]_{Benz}^{T=X}$, MD- $[1:2]_{Benz}^{T=X}$, MD- $[2:1]_{Benz}^{T=X}$ and MD- $[2:2]_{Benz}^{T=X}$, respectively. MD simulations performed at 280 K were aimed at obtaining information at the temperature slightly higher than the freezing point of liquid Benz.

For $[(BA)_2]_{Benz}^{T=X}$, the CHP dimer was chosen since it was reported to represent the most stable structure of $(BA)_2$ in the gas phase (Chocholoušová, Vacek, and Hobza, 2003; Sagarik and Rode, 2000). In MD simulations of $[(BA)_2]_{Benz}^{T=X}$, the CHP dimer and 124 Benz molecules were put in a cubic box subject to periodic boundary conditions. The density of $[(BA)_2]_{Benz}^{T=X}$ was maintained at the liquid density of 0.874 g cm^{-3} . The cutoff radius was half of the box length. The Ewald summation was employed to account for the long-range Coulomb interactions. The time step

applied in solving the equations of motion was 0.5 fs. In order to systematically follow the changes in structures and stability of H-bonds in (BA)₂, two consecutive sets of equilibration were made before property calculations took place. In the first equilibration, the CHP dimer was treated as a supermolecule, in which both BA molecules were not allowed to move in the course of MD simulations. After the solvent molecules were well equilibrated, the second equilibration was made. All molecules, including both BA in the CHP dimer, were allowed to move in the second equilibration. 20,000 MD steps were devoted to each equilibration and another 20,000 steps to property calculations. It was recognized that the cyclic H-bonds in the CHP dimer were considerably strong in Benz solution. After the second equilibration, the structures of the CHP dimer did not change substantially in the course of MD simulations. Since in the present case, the atom pair correlation functions ($g(R)$) between H-bond donor and acceptor showed only sharp peaks, it seems more informative and meaningful to analyse the structure and stability of the H-bond dimer based on the average H-bond distances ($\langle R_{A-H..B} \rangle$) and angles ($\langle \theta_{A-H..B} \rangle$), as well as the H-bond lifetimes ($\langle t_{A-H..B} \rangle$). $\theta_{A-H..B}$ is defined as the angle between the A-H bond and the line connecting atoms A and B. H-bond is considered to be strictly linear when $\langle \theta_{A-H..B} \rangle$ is 0 degree. $\langle t_{A-H..B} \rangle$ is defined as the percentage of simulation steps during which H-bond donor and acceptor are coming close enough to engage in H-bond formation. Therefore, $\langle t_{A-H..B} \rangle$ could be regarded as the probability of finding A-H..B H-bond in the course of MD simulations. Since the H-bond lifetime depends upon the degree of association as well as the dynamic behavior of the interacting molecules, it could be used to measure the stability of H-bond complex. In

the present work, H-bond donor and acceptor were considered to engage in H-bond formation when the donor-acceptor distance was shorter than 4 Å. With this H-bond distance cutoff, the standard deviation (SD) of $\langle R_{A-H..B} \rangle$ was found in the present work to be 0.36 Å at most. Structures and stability of the BA-H₂O m : n complexes, with m and n = 1 - 2, in Benz solution were investigated and analyzed using the same procedures.

2.3.2 [(PhOH)_n]_{Benz}

For [(PhOH)_n]_{Benz}, n = 1 - 3, NVE-MD simulations were performed at 298 K. MD-[(PhOH)_n]_{Benz}^{frozen} and MD-[(PhOH)_n]_{Benz}^{free} represent two scenarios in [(PhOH)_n]_{Benz}. In MD-[(PhOH)_n]_{Benz}^{frozen}, structures of (PhOH)_n were frozen at the T-model equilibrium geometries (Sagarik and Asawakun, 1997), and only Benz molecules were allowed to move. MD-[(PhOH)_n]_{Benz}^{frozen} was aimed primarily at the average three-dimensional structures and interaction energy distributions of Benz molecules in [(PhOH)_n]_{Benz}. MD-[(PhOH)_n]_{Benz}^{free} represents the situation, in which all PhOH and Benz molecules were free to move, starting from the equilibrium configurations obtained from MD-[(PhOH)_n]_{Benz}^{frozen}. MD-[(PhOH)_n]_{Benz}^{free} was aimed at structures and dynamics in [(PhOH)_n]_{Benz}.

In both MD-[(PhOH)_n]_{Benz}^{frozen} and MD-[(PhOH)_n]_{Benz}^{free}, (PhOH)_n and five hundred Benz molecules were put in a cubic box subject to periodic boundary conditions. The center of mass of (PhOH)_n was coincide with the center of the simulation box. The density of [(PhOH)_n]_{Benz} was maintained at the liquid density of 0.874 g cm⁻³, corresponding to the box length of about 42 Å. The cut-off radius was

half of the box length. The long-range Coulomb interaction was taken into account by means of the Ewald summations. Fifty thousand MD steps of 0.5 fs were devoted to equilibration and one hundred thousand steps to property calculations. The primary energetic results of interest were the average solute-solute ($\langle E_{\text{Benz}}^{\text{solu-solu}} \rangle$) and solute-solvent ($\langle E_{\text{Benz}}^{\text{solu-solv}} \rangle$) interaction energies, as well as the average potential energies of $[(\text{PhOH})_n]_{\text{Benz}}$ ($\langle E_{\text{Benz}}^{\text{pot}} \rangle$). $\langle E_{\text{Benz}}^{\text{solu-solu}} \rangle$ resulted from the average over the number of MD steps, whereas $\langle E_{\text{Benz}}^{\text{solu-solv}} \rangle$ the average over the number of MD steps and the number of solute molecules.

In order to visualize the average three-dimensional structures of solvent molecules in $[(\text{PhOH})_n]_{\text{Benz}}$, the solvent probability distribution (π -PD) maps were constructed from MD- $[(\text{PhOH})_n]_{\text{Benz}}^{\text{frozen}}$, $n = 1 - 2$. In the present study, the center of mass of Benz is denoted by π and that of PhOH by π_{Ph} . In the calculations of the π -PD maps, molecular plane of a PhOH molecule was assumed to coincide with the XY plane of the simulation box ($Z = 0 \text{ \AA}$). The volumes above and below the plane were divided into layers, with the thickness of 1 \AA . In each layer, a π -PD map was constructed from 61x61 grid intersections, by following the trajectories of the center of mass of Benz in the course of MD simulations. The π -PD maps were represented by contour lines, computed and displayed using SURFER program (Golden Software, Computer software, 1997). The densities of the contour lines reflect the probability of finding Benz in $[(\text{PhOH})_n]_{\text{Benz}}$. For simplicity, the minimum and maximum values of the contour lines, as well as the contour intervals, were chosen to be the same for all π -PD maps. Since the solvent cages in $[(\text{PhOH})_2]_{\text{Benz}}$ were complicated, additional π -

PD maps were constructed with respect to XZ and YZ planes. The molecular planes employed in MD analyses are displayed in Figure 2.3.

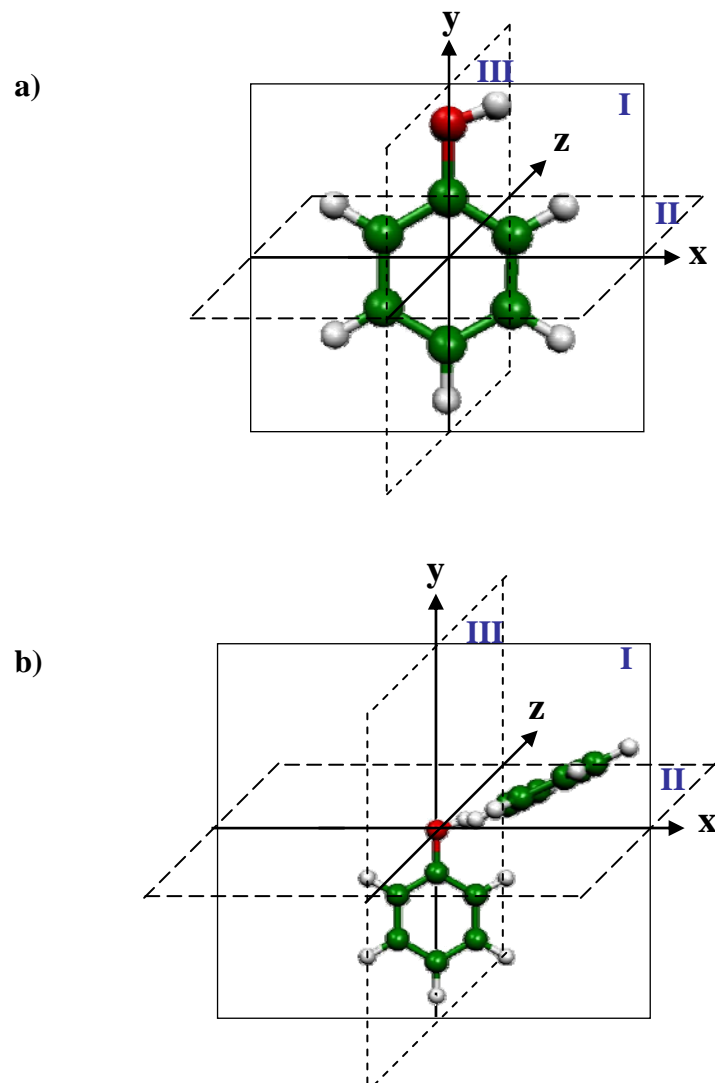


Figure 2.3 a) – b) Reference planes for PhOH and (PhOH)₂ in Benz solutions.

Based on similar approaches, the average solute-solvent and solvent-solvent interaction energy PD maps, denoted by the PB-PD and BB-PD maps, respectively, were constructed from MD-[(PhOH)_n]_{Benz}^{frozen}, n = 1 - 2. The PB-PD maps

were computed from the interaction energies between Benz at the grid intersections and $(\text{PhOH})_n$, whereas BB-PD maps from the interaction energies between Benz at the grid intersections and all other Benz molecules. The average potential energy landscapes in $[(\text{PhOH})_n]_{\text{Benz}}$ were represented by the PB-BB-PD maps, computed by combinations of the PB-PD and BB-PD maps. Because the solvent cages tend to bring about stabilization effects to $[(\text{PhOH})_n]_{\text{Benz}}$, only negative-energy contour lines were displayed on the PB-PD, BB-PD and PB-BB-PD maps. It should be noted that, since the solvent-solvent interaction energies dominate in $[(\text{PhOH})_n]_{\text{Benz}}$, the minimum and maximum values of the contours, as well as the contour intervals, on the PB-PD, BB-PD and PB-BB-PD maps must be assigned differently for clarity.

Since the dynamics of PhOH and Benz in the first solvation shell was one of the main objectives, additional MD analyses had to be made. Experience in aqueous solutions (Sagarik and Chaiyapongs, 2005; Sagarik and Dokmaisrijan, 2005; Deeying and Sagarik, 2006) showed that, although not straightforward, the dynamics of specific solvent molecules in the first solvation shell of solute could be anticipated at least qualitatively from the structures of the average potential energy landscapes. Therefore, the PB-PD, BB-PD and PB-BB-PD maps computed from MD- $[(\text{PhOH})_n]_{\text{Benz}}^{\text{frozen}}$ were further analyzed in details. Several cross section plots were generated by taking vertical slices along the predefined profile lines, through the surfaces of the PB-BB-PD maps, as well as the PB-PD and BB-PD maps, using the methods described in Sagarik and Dokmaisrijan (2005). The cross section plots derived from the longitudinal profile lines could be associated with the average potential energy barriers to solvent exchange within, as well as between, the first solvation shells ($\langle E_{\text{Benz}}^{\text{L}} \rangle$). Whereas those computed from the transverse profile lines

are connected to the average potential energy barriers to the solvent exchange between Benz molecules in the first solvation shell and the outside ($\langle E_{\text{Benz}}^{\text{T}} \rangle$).

Additional solvation structures, stability and dynamics in $[(\text{PhOH})_n]_{\text{Benz}}$, $n = 1 - 3$, were analyzed and discussed based on the results of MD- $[(\text{PhOH})_n]_{\text{Benz}}^{\text{free}}$, from which some atom-atom pair correlation functions ($g(R)$) and the average running coordination numbers ($n(R)$) related to the π - π interaction, the C-H.. π , O-H.. π and O-H..O H-bonds were computed and employed in the discussion. Because large-amplitude nuclear motions, which could lead to solvent structure reorganization, were pointed out to be one of the main reasons for the non-rigidity in aromatic van der Waal clusters (Sun and Bernstein, 1996), they were investigated in the present study. As the O-H..O and O-H.. π H-bonds, as well as the π - π interactions, are responsible for molecular associations in $[(\text{PhOH})_n]_{\text{Benz}}$, the dynamics at short time could be investigated through their vibrational behaviors. In the present case, the H-bond exchange diagrams, showing the distance between the oxygen atom of PhOH and the center of mass of a specific Benz molecule as a function of MD simulation time, were constructed. The vibrational frequencies of the O-H.. π H-bond were computed, by performing fast Fourier transformations (FFT) (Borse, 1997) on the H-bond exchange curves. Characteristic large-amplitude vibrational frequencies were approximated and discussed based on the FFT results.

2.4 Computer softwares and facilities

All the calculations in the present study were performed at the School of Chemistry and School of Mathematics, Institute of Science, Suranaree University of Technology (SUT). The following computers and computational chemistry softwares packages were used.

- LINUX cluster with eight nodes and Red Hat Enterprise.
- COLUMBUS system programs (Ahlrichs et al., 1985).
- Gaussian 03 package (Frisch et al., Computer software, 2006).
- Moldy MD simulations program (Refson, Computer software, 1996).
- SURFER contouring program (Golden Software, Computer software, 1997).
- AMBER version 6 (Case et al., Computer software, 1999) etc.

CHAPTER III

RESULTS AND DISCUSSION

Although the main objectives of the present thesis were to investigate structures, energetic and dynamics of clusters of aromatic compounds in non-aqueous environment, some results in the gas phase (Sagarik and Rode, 2000) had to be discussed to ensure that the computed T-model potentials are accurate enough for the applications in the present MD simulations. Characteristic H-bond and π - π distances will be used in the discussions of the non-aqueous solutions.

3.1 (BA)₂ and BA-H₂O complexes

3.1.1 Structures and energetic in the gas phase

Based on the T-model potentials discussed in the previous chapter, Sagarik and Rode (2000) presented equilibrium structures and interaction energies of (BA)₂ and BA-H₂O complexes. The absolute minimum energy geometry of (BA)₂ was reported to be the CHP dimer, with the interaction energy of -47.0 kJ mol⁻¹. The only local minimum energy geometry was the SOT dimer, with interaction energy of -31.1 kJ mol⁻¹. The structures of the CHP and SOT dimers are shown in Figure 3.1. The absolute and local minimum energy geometries are in accordance with the experimental and theoretical results in the gas phase (Cieplak, Pawlowski, and Wieckowska, 1992; Neumann et al., 1998; Meijer, de Vries, Hunziker, and Wendt, 1990). The molecular mechanical program AMBER, with the charges of BA obtained

from a fit to the electrostatic potential around the molecule, predicted a similar dimer to possess the interaction energy of only $-33.4 \text{ kJ mol}^{-1}$ (Cieplak, Pawlowski, and Wieckowska, 1992).

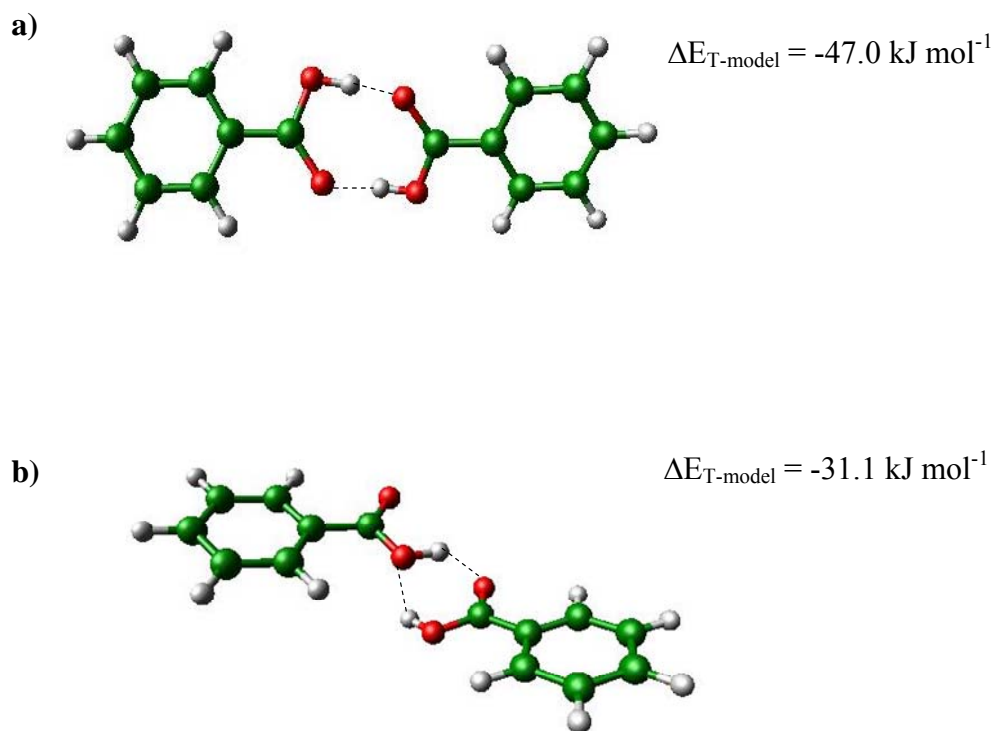


Figure 3.1 Structures of the CHP and SOT dimers computed from the T-model potentials.

Equilibrium structures and interaction energies of the BA-H₂O 1 : 1, 1 : 2, 2 : 1 and 2 : 2 complexes were also reported by Sagarik and Rode (2000). The absolute and two low-lying energy geometries of the BA-H₂O complexes are shown in Figures 3.2, 3.3, 3.4 and 3.5, respectively.

The T-model potentials predicted a CHP structure to be the absolute minimum energy geometry of the BA-H₂O 1 : 1 complex, structure **a** in Figure 3.2. Structure **a** consists of two H-bonds, in which water acts as proton donor towards C=O and as proton acceptor towards O-H of BA. The interaction energy in this case is -32.3 kJ mol⁻¹. Structure **b** is -15.2 kJ mol⁻¹ less stable than structure **a**. It is stabilized by C=O..H-O and C-H..O H-bonds. Structure **c** possesses the interaction energy of only -9.7 kJ mol⁻¹.

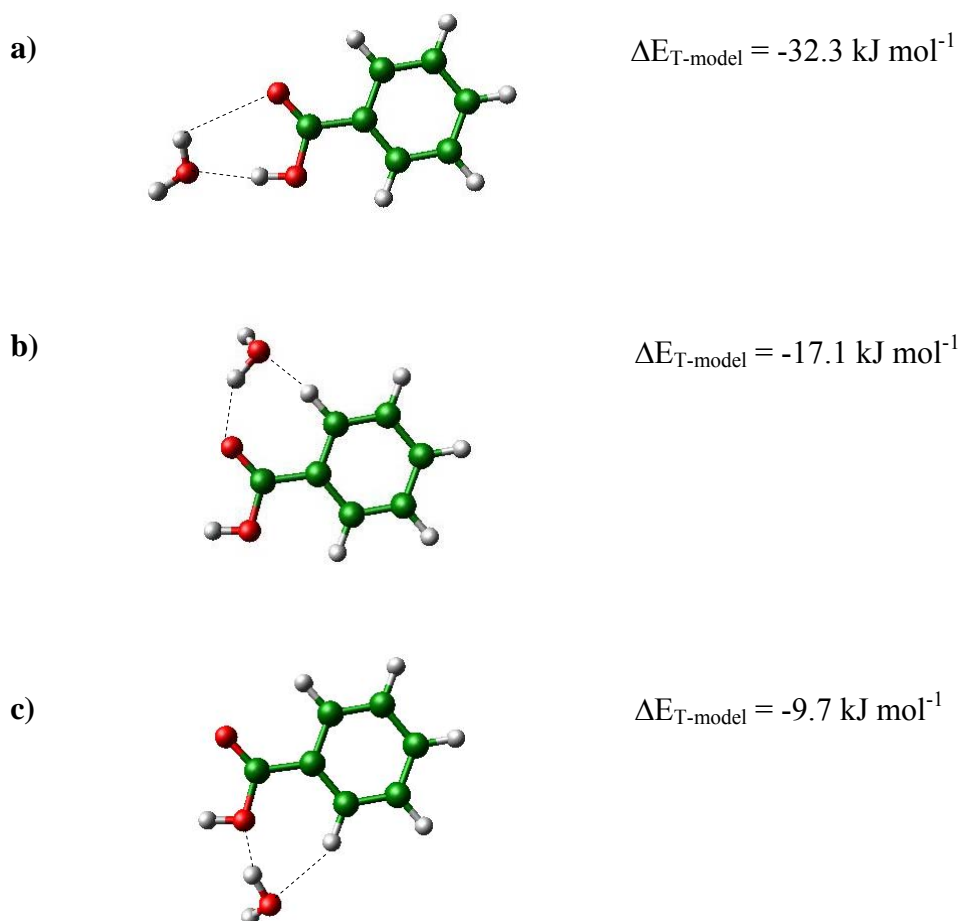


Figure 3.2 The absolute and two local minimum energy geometries of the BA-H₂O 1 : 1 complexes computed from the T-model potentials.

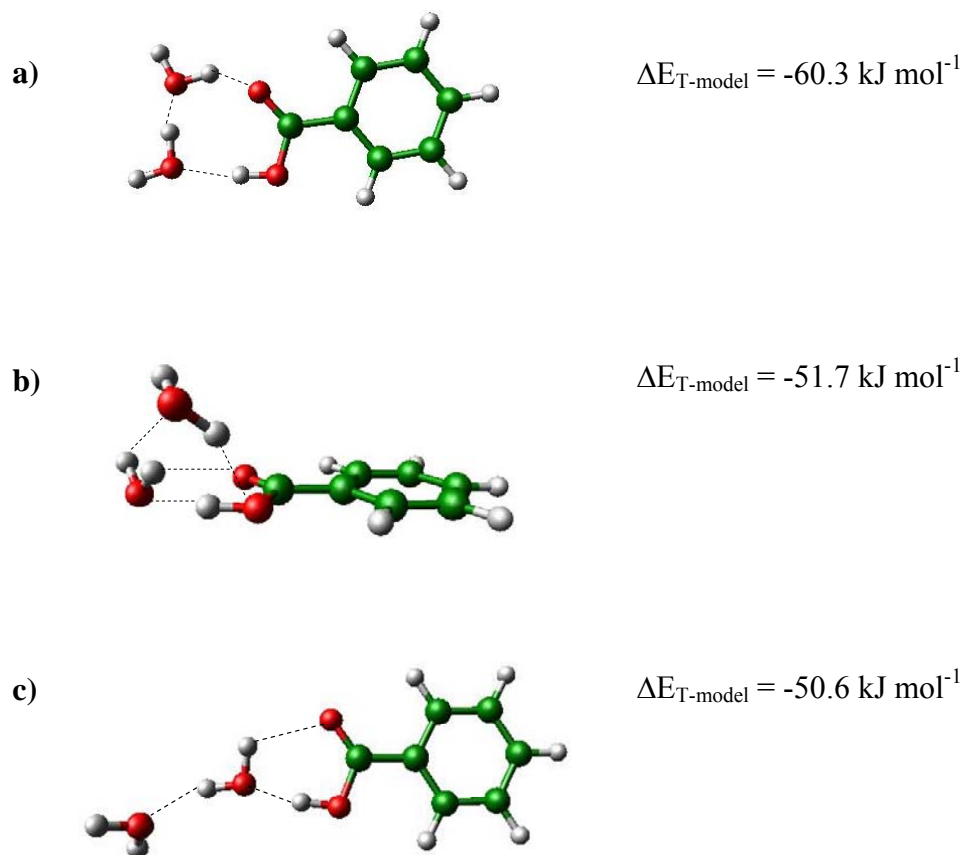


Figure 3.3 The absolute and two local minimum energy geometries of the BA-H₂O 1 : 2 complexes computed from the T-model potentials.

For the BA-H₂O 1 : 2 complexes, the COOH group is still the most preferential binding site for water. The absolute minimum energy geometry of the BA-H₂O 1 : 2 complexes predicted by the T-model was structure **a** in Figure 3.3. Structure **a** consists of three planar H-bonds, with the interaction energy of $-60.3 \text{ kJ mol}^{-1}$. Structures **b** and **c** have a unit resembling the absolute minimum energy geometry of the BA-H₂O 1 : 1 complex. The T-model suggested that structures **b** and **c** possess comparable interaction energy, $-51.7 \text{ kJ mol}^{-1}$ and $-50.6 \text{ kJ mol}^{-1}$,

respectively. Structure **b** is stabilized by four cyclic H-bonds, whereas structure **c** by three H-bonds.

For the BA-H₂O 2 : 1 complexes, the planar structure, in which water acts simultaneously as proton donor and acceptor bridging the C=O and O-H groups of both BA molecules, was found to be the absolute minimum energy geometry, structure **a** in Figure 3.4. The interaction energy of structure **a** is -66.9 kJ mol⁻¹. The stability of structures **b** is comparable to structure **a**, whereas structure **c** is slightly less stable than structures **a** and **b**. Structures **b** and **c** possess a unit resembling the absolute minimum energy geometry of the BA-H₂O 1 : 1 complex. Structures **a** and **b** can be constructed by breaking one H-bond of the CHP dimer and inserting a water molecule between the C=O and O-H groups, whereas structure **c** can be obtained by inserting a water molecule in the SOT dimer.

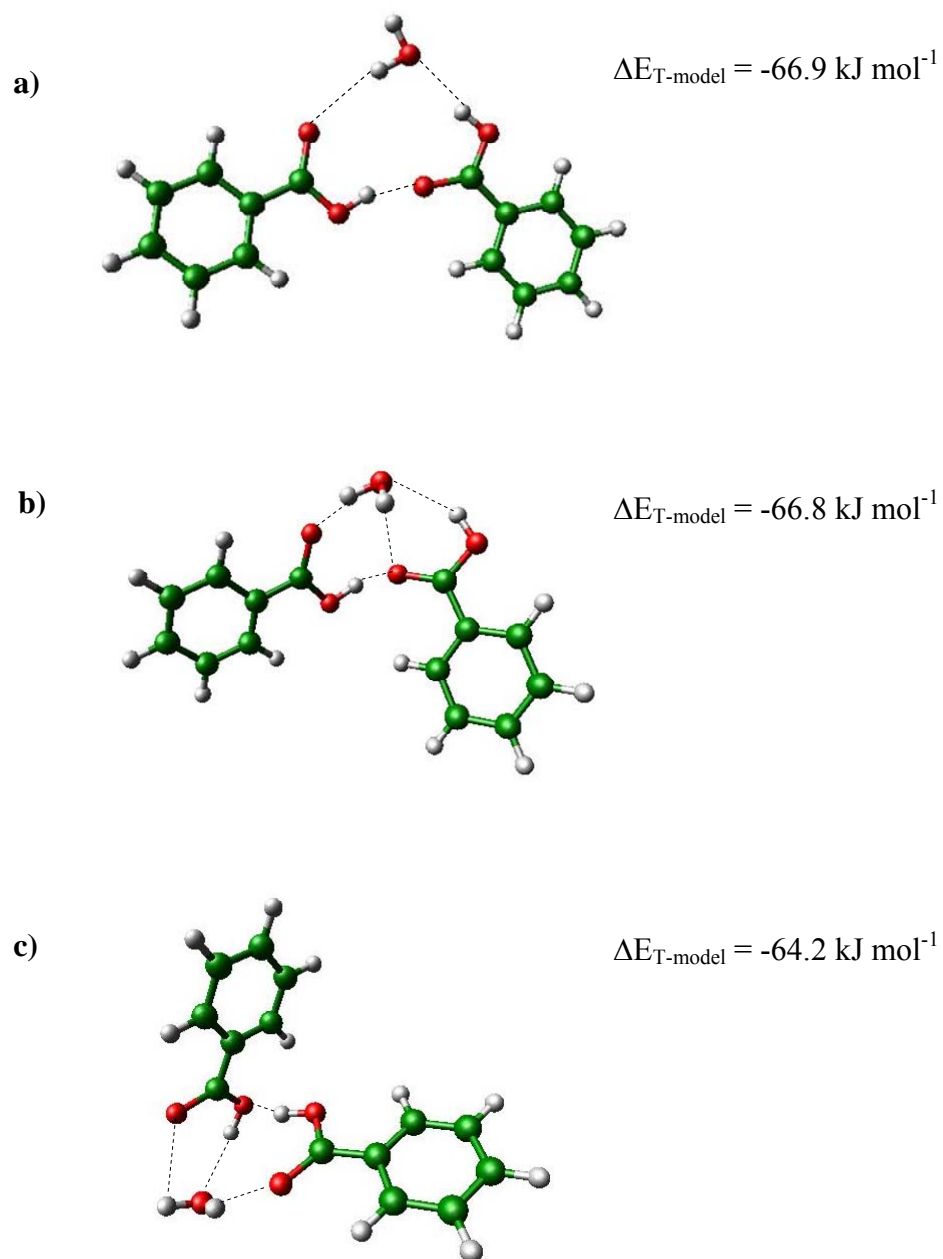


Figure 3.4 The absolute and two local minimum energy geometries of the BA-H₂O 2 : 1 complexes computed from the T-model potentials.

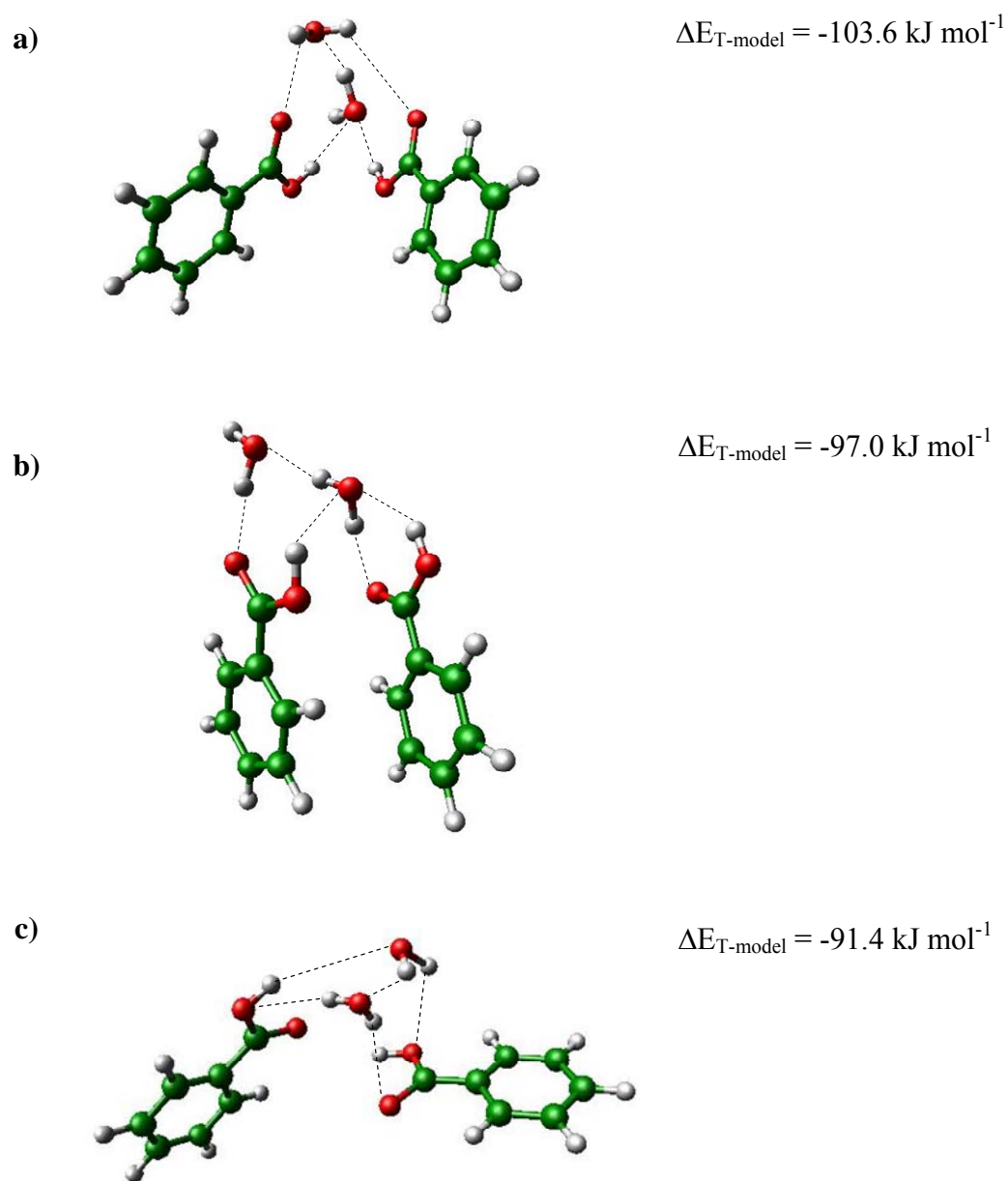


Figure 3.5 The absolute and two local minimum energy geometries of the BA-H₂O 2 : 2 complexes computed from the T-model potentials.

A herringbone structure appeared to be the absolute minimum energy geometry of the BA-H₂O 2 : 2 complexes, structure **a** in Figure 3.5. Structure **a** consists of a unit resembling the absolute minimum energy geometry of the water dimer, with the interaction energy of -103.6 kJ mol⁻¹. Including two water molecules in the BA dimer seems to increase the flexibility of the H-bonded cluster, and hence the possibility to form the π - π interaction.

3.1.2 MD simulations of benzene solutions

In this section, structures and stability as well as some dynamic behaviors of the H-bond clusters in Benz solutions derived from MD simulations are discussed. Comments are made on the results obtained from distribution experiments, especially the situations in Benz solutions. The energetic results obtained from MD simulations at 280 and 298 K are summarized in Table 3.1, whereas the average H-bond distances ($\langle R_{A-H..B} \rangle$), angles ($\langle \theta_{A-H..B} \rangle$) and lifetimes ($\langle t_{A-H..B} \rangle$) are listed in Table 3.2.

MD-[(BA)₂]_{Benz}^{T=298}

The results of MD-[(BA)₂]_{Benz}^{T=298} suggest that the cyclic H-bonds in (BA)₂ are very associated in pure Benz, with $\langle t_{O1-H1..O2} \rangle$ (1-2) and (2-1) about 100%. The CHP structure was changed slightly in the course of MD simulations. $\langle R_{O1-H1..O2} \rangle$ (1-2) and $\langle E_{Benz}^{sol-sol} \rangle$ derived from MD-[(BA)₂]_{Benz}^{T=298} are 2.9 Å and -39.9 kJ mol⁻¹, respectively. The average H-bond distance is only 0.1 Å longer than the gas-phase structure proposed by Sagarik and Rode (2000). $\langle E_{Benz}^{sol-sol} \rangle$ is about 7 kJ mol⁻¹ higher than the interaction energy of the CHP dimer in the gas phase and

comparable with the enthalpy of dimerization in Benz derived from experiment -37.6 kJ mol^{-1} (Shamsul Huq and Lodhi, 1966).

MD-[1:1]_{Benz}^{T=X}

The gas phase structure of the BA-H₂O 1 : 1 complex, represented by the O1-H1 group of BA acting as proton donor toward oxygen of water, did not change much in the course of MD simulations. The results of MD-[1:1]_{Benz}^{T=298} reveal that the O1-H1..Ow H-bond is quite strong in Benz. The average H-bond interaction energy ($\langle E_{\text{Benz}}^{\text{sol-sol}} \rangle$) in [1:1]_{Benz}^{T=298} is -21.0 kJ mol^{-1} , compared with the gas phase of -32.3 kJ mol^{-1} . The statistical analysis of H-bond in structure **b** in Table 3.2, shows that, water spends most of the time at the hydroxyl group of BA, with the average H-bond lifetime ($\langle t_{\text{O1-H1..Ow}} \rangle (2-1)$) of about 100%. $\langle R_{\text{O1-H1..Ow}} \rangle (2-1)$ and $\langle \theta_{\text{O1-H1..Ow}} \rangle (2-1)$ derived from MD-[1:1]_{Benz}^{T=298} are 2.9 Å and 21.4 degree, respectively. For the BA-H₂O 1 : 1 complex, the probability of finding cyclic H-bond structure could be computed from $\langle t_{\text{Ow-Hw..O2}} \rangle (1-2)$. In [1:1]_{Benz}^{T=298}, $\langle t_{\text{Ow-Hw..O2}} \rangle (1-2)$ is about 22%.

The MD results on [1:1]_{Benz}^{T=280} and [1:1]_{Benz}^{T=298} are virtually the same. At lower temperature, the degree of H-bond association is slightly higher as expected. The probability of finding cyclic H-bond structure ($\langle t_{\text{Ow-Hw..O2}} \rangle (1-2)$) increases to 35%. $\langle E_{\text{Benz}}^{\text{solu-solu}} \rangle$ of [1:1]_{Benz}^{T=280} is -22.9 kJ mol^{-1} , with $\langle R_{\text{O1-H1..Ow}} \rangle (2-1)$ and $\langle \theta_{\text{O1-H1..Ow}} \rangle (2-1)$ of 2.9 Å and 20.8 degree, respectively.

MD-[1:2]_{Benz}^{T=X}

For MD-[1:2]_{Benz}^{T=280} and MD-[1:2]_{Benz}^{T=298}, the MD results are quite different. Two forms of the BA-H₂O complex dominate in Benz solutions. In the course of MD-[1:2]_{Benz}^{T=298}, the gas phase cyclic structure proposed by Sagarik and Rode, (2000), employed as the starting geometry, was converted into a partially open H-bond structure, resembling in [1:1]_{Benz}^{T=298}. The probability of finding the cyclic BA-H₂O 1 : 1 like structure ($\langle t_{Ow-Hw..O2} \rangle (2-3)$) is about 26%. The H-bond lifetime ($\langle t_{O1-H1..Ow} \rangle (3-2)$) for structure **d** in Table 3.2 indicates that, the O1-H1..Ow H-bond in [1:2]_{Benz}^{T=298} is less associated compared to [1:1]_{Benz}^{T=298}, with a slightly longer $\langle R_{O1-H1..Ow} \rangle (3-2)$.

The presence of $\langle t_{Ow-Hw..Ow} \rangle (1-2)$ and $\langle t_{Ow-Hw..Ow} \rangle (2-1)$ reflects the possibility for the H-bond donor-acceptor pair exchange between water molecules in [1:2]_{Benz}^{T=298}. This dynamic process could be regarded as non-mutual H-bond exchange as in NMR spectroscopy (Sagarik and Rode, 2000). The non-mutual H-bond exchange leads in this case to the total probability of the Ow-Hw..Ow H-bond formation of about 41%. $\langle E_{Benz}^{solu-solu} \rangle$ for [1:2]_{Benz}^{T=298} is -23.1 kJ mol⁻¹, slightly lower than [1:1]_{Benz}^{T=298}. In the gas phase, a similar BA-H₂O 1 : 2 complex was reported to possess the interaction energy of -50.6 kJ mol⁻¹.

The gas phase cyclic structure did not change appreciably in the course of MD-[1:2]_{Benz}^{T=280}. The values of $\langle E_{Benz}^{solu-solu} \rangle$ in Table 3.1 and $\langle t_{A-H..B} \rangle$ in Table 3.2 reveal that, the H-bonds in the BA-H₂O 1 : 2 complex become more associated and the molecular motions are rather restricted at lower temperature. Consequently, the

probability of the non-mutual H-bond exchange is disappeared at 280 K. At this temperature, however, there exists another type of H-bond exchange process, in which a water molecule executes rotation leading to the H-bond donor exchange within the same water molecule. This dynamics exchange is regarded as mutual H-bond exchange in NMR spectroscopy. In this case, the total probability of the Ow-Hw..Ow H-bond formation ($\langle t_{\text{Ow-Hw..Ow}} \rangle (1-2)$) increases to about 73%. The mutual H-bond exchange also leads to an increase in the total probability of the cyclic H-bond formation ($\langle t_{\text{Ow-Hw..O2}} \rangle (2-3)$) to about 90%. $\langle E_{\text{Benz}}^{\text{solu-solu}} \rangle$ for $[1:2]_{\text{Benz}}^{T=280}$ is $-41.0 \text{ kJ mol}^{-1}$, compared with $-60.3 \text{ kJ mol}^{-1}$ in the gas phase. The probability of finding the cyclic BA-H₂O 1 : 1 like structure in $[1:2]_{\text{Benz}}^{T=280}$ seems to be decreased. The total probability of the Ow-Hw..O2 H-bond formation ($\langle t_{\text{Ow-Hw..O2}} \rangle (1-3)$) in $[1:2]_{\text{Benz}}^{T=280}$ is only about 22%.

MD-[2:1]_{Benz}^{T=X}

In Benz solution, the probability of breaking H-bonds in the CHP dimer by water is evident from the MD-[2:1]_{Benz}^{T=280} and MD-[2:1]_{Benz}^{T=298}. On average, the gas phase structure applied as the starting configuration, did not changed substantially in the course of MD-[2:1]_{Benz}^{T=X}. The O1-H1..Ow, O1-H1..O2 and Ow-Hw..O2 H-bonds are still responsible for the molecular associations as in the gas phase. However, dynamic H-bond exchanges take place in $[2:1]_{\text{Benz}}^{T=280}$ and $[2:1]_{\text{Benz}}^{T=298}$. At 298 K, the O1-H1..O2 and O1-H1..Ow H-bonds are the two major contributors for the cluster association. $\langle t_{\text{O1-H1..O2}} \rangle (1-2)$ and $\langle t_{\text{O1-H1..Ow}} \rangle (2-3)$ are about 80 and 100%,

respectively. Besides, there exists the possibility for the non-mutual H-bond exchange between BA molecules. The total probability of the O1-H1..O1 H-bond formation ($\langle t_{\text{O1-H1..O1}} \rangle (1-2)$ and $\langle t_{\text{O1-H1..O1}} \rangle (2-1)$) is about 42%. Similarly, due to the mutual H-bond exchange, the total probability of the Ow-Hw..O2 H-bond formation ($\langle t_{\text{Ow-Hw..O2}} \rangle (3-1)$) increase to about 67% at 298 K. Since water molecule could form the cyclic BA-H₂O 1 : 1 like complex with both BA molecules, the corresponding probabilities could be estimated using $\langle t_{\text{Ow-Hw..O2}} \rangle (3-2)$ and $\langle t_{\text{O1-H1..Ow}} \rangle (1-3)$. At 298 K, they are about 18 and 61%, respectively. Due to the restriction in molecular motions at lower temperature, the probability of the non-mutual H-bond exchange is disappeared at 280 K. The O1-H1..O2 and O1-H1..Ow H-bonds become very associated, with $\langle t_{\text{O1-H1..O2}} \rangle (1-2)$ and $\langle t_{\text{O1-H1..Ow}} \rangle (2-3)$ of approximately 100%. The cyclic H-bond structure in Table 3.2 seems to occupy about 91% of the simulation time, as can be seen from the values of $\langle t_{\text{Ow-Hw..O2}} \rangle (3-1)$. At 280 K, water tends to form the cyclic BA-H₂O 1 : 1 like complex with only one BA molecule. The total probability of the Ow-Hw..O2 H-bond formation ($\langle t_{\text{Ow-Hw..O2}} \rangle (3-2)$) in this case is about 31%. $\langle E_{\text{Benz}}^{\text{solu-solu}} \rangle$ in $[2:1]_{\text{Benz}}^{T=280}$ and $[2:1]_{\text{Benz}}^{T=298}$ are -56.2 and -50.8 kJ mol⁻¹, respectively, compared with the interaction energy in the gas phase of -66.9 kJ mol⁻¹.

MD-[2:2]_{Benz}^{T=X}

Due to the increase in the H-bond cluster size, the situation in $[2:2]_{\text{Benz}}^{T=X}$ are quite different from $[2:1]_{\text{Benz}}^{T=X}$. In the course of MD-[2:2]_{Benz}^{T=298}, the gas phase

structure of the BA-H₂O 2 : 2 complex was weakened and transformed into the structure **h** in Table 3.2. At 298 K, water molecule tends to H-bond directly to each BA. No direct evidence shows the existence of the Ow-Hw..Ow H-bond in $[2:2]_{\text{Benz}}^{T=298}$. The MD- $[2:2]_{\text{Benz}}^{T=298}$ results in Table 3.2 also indicate that, on average, both BA molecules link together through the O1-H1..O2 H-bond, with $\langle t_{\text{O1-H1..O2}} \rangle (1-2)$ of about 69%. In $[2:2]_{\text{Benz}}^{T=298}$, there exists the probability of the O1-H1..O1 H-bond formation ($\langle t_{\text{O1-H1..O1}} \rangle (1-2)$) of about 29%. The probability of the BA-H₂O 1 : 1 like complex formation could be inferred from $\langle t_{\text{O1-H1..Ow}} \rangle (2-4)$ and $\langle t_{\text{Ow-Hw..O2}} \rangle (3-1)$. They are about 94 and 89%, respectively. The total probability of the cyclic BA-H₂O 1 : 1 like complex formation, inferred from $\langle t_{\text{Ow-Hw..O2}} \rangle (4-2)$, is about 41%. $\langle E_{\text{Benz}}^{\text{solu-solu}} \rangle$ derived from MD- $[2:2]_{\text{Benz}}^{T=298}$ is -54.1 kJ mol⁻¹.

The average H-bond structure in $[2:2]_{\text{Benz}}^{T=280}$ is similar to $[2:1]_{\text{Benz}}$. However, in this case, the O1-H1..O1 H-bond is responsible for the weak linkage between the two BA molecules. The probability of the O1-H1..O1 H-bond formation ($\langle t_{\text{O1-H1..O1}} \rangle (1-2)$) is only about 50%. On average, only one water molecule forms cyclic H-bonds with both BA molecules, with a particularly strong preference of the O1-H1..Ow H-bond. The results of MD- $[2:2]_{\text{Benz}}^{T=280}$ indicate further that, in $[2:2]_{\text{Benz}}^{T=280}$, water molecules form strong cluster among themselves. The presence of the mutual H-bond exchange results in the probability of the Ow-Hw..Ow H-bond formation of about 85%. Since the H-bond between water molecules are quite strong, the existence of $\langle t_{\text{Ow-Hw..O2}} \rangle (4-2)$ reflects the probability of finding the cyclic BA-H₂O 1 : 2

complex, structure **e** in Table 3.2. The total probability in this case is about 31%.

$\langle E_{\text{Benz}}^{\text{solu-solu}} \rangle$ for $[2:2]_{\text{Benz}}^{T=280}$ is slightly higher than $[2:2]_{\text{Benz}}^{T=298}$. The value of $\langle t_{\text{Ow-Hw..O2}} \rangle (3-2)$ reveals a small probability to detect the cyclic BA-H₂O 1 : 1 like structure in $[2:2]_{\text{Benz}}^{T=280}$.

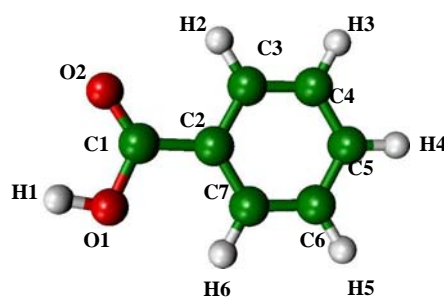
Table 3.1 The MD results on (BA)₂ and BA-H₂O complexes in Benz solutions.

The number of Benz molecules in $[(\text{BA})_2]_{\text{Benz}}^{T=298}$, $[1:1]_{\text{Benz}}^{T=X}$ and $[1:2]_{\text{Benz}}^{T=X}$ are 124 and those in $[2:1]_{\text{Benz}}^{T=X}$ and $[2:2]_{\text{Benz}}^{T=X}$ are 122, X = 280 and 298 K.

MD	L (Å)	$\langle E_{\text{Benz}}^{\text{pot}} \rangle$	$\langle E_{\text{Benz}}^{\text{solu-solu}} \rangle$
MD- $[(\text{BA})_2]_{\text{Benz}}^{T=298}$	26.6	-36.7	-39.9
MD- $[1:1]_{\text{Benz}}^{T=298}$	26.5	-37.2	-21.0
MD- $[1:1]_{\text{Benz}}^{T=280}$	26.5	-37.5	-22.9
MD- $[1:2]_{\text{Benz}}^{T=298}$	26.5	-37.3	-23.1
MD- $[1:2]_{\text{Benz}}^{T=280}$	26.5	-37.9	-41.0
MD- $[2:1]_{\text{Benz}}^{T=298}$	26.5	-37.5	-50.8
MD- $[2:1]_{\text{Benz}}^{T=280}$	26.5	-37.8	-56.2
MD- $[2:2]_{\text{Benz}}^{T=298}$	26.5	-37.8	-54.1
MD- $[2:2]_{\text{Benz}}^{T=280}$	26.5	-38.4	-51.1

Table 3.2 Some average H-bond distances ($\langle R_{A-H..B} \rangle$) and angles ($\langle \theta_{A-H..B} \rangle$), as well as the H-bond lifetimes ($\langle t_{A-H..B} \rangle$), derived from MD simulations. Only solute clusters are shown in the table.

The numbering system for the carboxylic acid is



SD = standard deviation

(A-H..B) = H-bond donor-acceptor pair between molecules A and B

Distance and angle are in Å and degree, respectively.

	MD - [(BA) ₂] _{Benz} ^{T=298}		SD	
O1-H1..O2	$\langle R_{O1-H1..O2} \rangle$	2.9	0.2	a) 1) 2)
(1 - 2) and	$\langle \theta_{O1-H1..O2} \rangle$	18.0	9.0	
(2 - 1)	$\langle t_{O1-H1..O2} \rangle$	100.0	-	

Table 3.2 (Continued).

		MD-[1:1] _{Benz} ^{T=298}		SD	
O1-H1..Ow	$\langle R_{O1-H1..Ow} \rangle$	2.9	0.2		
(2-1)	$\langle \theta_{O1-H1..Ow} \rangle$	21.4	10.1		
	$\langle t_{O1-H1..Ow} \rangle$	100.0	-		
Ow-Hw..O2	$\langle R_{Ow-Hw..O2} \rangle$	2.9	0.2		
(1-2)	$\langle \theta_{Ow-Hw..O2} \rangle$	44.1	7.6		
	$\langle t_{Ow-Hw..O2} \rangle$	21.5	-		
		MD-[1:1] _{Benz} ^{T=280}		SD	
O1-H1..Ow	$\langle R_{O1-H1..Ow} \rangle$	2.9	0.1		
(2-1)	$\langle \theta_{O1-H1..Ow} \rangle$	20.8	10.4		
	$\langle t_{O1-H1..Ow} \rangle$	98.7	-		
Ow-Hw..O2	$\langle R_{Ow-Hw..O2} \rangle$	2.9	0.2		
(1-2)	$\langle \theta_{Ow-Hw..O2} \rangle$	44.4	7.5		
	$\langle t_{Ow-Hw..O2} \rangle$	34.8	-		

Table 3.2 (Continued).

		MD-[1:2] _{Benz} ^{T=298}	SD
O1-H1..Ow	$\langle R_{O1-H1..Ow} \rangle$	3.0	0.3
(3-2)	$\langle \theta_{O1-H1..Ow} \rangle$	24.1	10.4
	$\langle t_{O1-H1..Ow} \rangle$	77.2	-
Ow-Hw..O2	$\langle R_{Ow-Hw..O2} \rangle$	3.1	0.3
(2-3)	$\langle \theta_{Ow-Hw..O2} \rangle$	38.9	11.9
	$\langle t_{Ow-Hw..O2} \rangle$	26.4	-
Ow-Hw..Ow	$\langle R_{Ow-Hw..Ow} \rangle$	3.1	0.2
(2-1)	$\langle \theta_{Ow-Hw..Ow} \rangle$	28.4	14.8
	$\langle t_{Ow-Hw..Ow} \rangle$	28.2	-
Ow-Hw..Ow	$\langle R_{Ow-Hw..Ow} \rangle$	3.1	0.2
(1-2)	$\langle \theta_{Ow-Hw..Ow} \rangle$	31.1	15.4
	$\langle t_{Ow-Hw..Ow} \rangle$	12.6	-

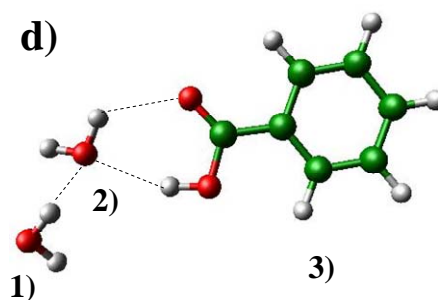


Table 3.2 (Continued).

		MD-[1:2]_{Benz}^{T=280}		SD	
O1-H1..Ow	$\langle R_{O1-H1..Ow} \rangle$	2.9	0.2		
(3-1)	$\langle \theta_{O1-H1..Ow} \rangle$	17.4	9.4		
	$\langle t_{O1-H1..Ow} \rangle$	100.0	-		
Ow-Hw..O2	$\langle R_{Ow-Hw..O2} \rangle$	3.1	0.3		
(2-3)	$\langle \theta_{Ow-Hw..O2} \rangle$	31.4	12.8		
	$\langle t_{Ow-Hw..O2} \rangle$	50.7	-		
Ow-Hw..O2	$\langle R_{Ow-Hw..O2} \rangle$	3.1	0.3		
(2-3)	$\langle \theta_{Ow-Hw..O2} \rangle$	29.6	13.1		
	$\langle t_{Ow-Hw..O2} \rangle$	39.6	-		
Ow-Hw..O2	$\langle R_{Ow-Hw..O2} \rangle$	3.0	0.3		
(1-3)	$\langle \theta_{Ow-Hw..O2} \rangle$	47.8	6.9		
	$\langle t_{Ow-Hw..O2} \rangle$	11.0	-		
Ow-Hw..O2	$\langle R_{Ow-Hw..O2} \rangle$	3.1	0.2		
(1-3)	$\langle \theta_{Ow-Hw..O2} \rangle$	47.4	8.2		
	$\langle t_{Ow-Hw..O2} \rangle$	11.1	-		
Ow-Hw..Ow	$\langle R_{Ow-Hw..Ow} \rangle$	3.2	0.3		
(1-2)	$\langle \theta_{Ow-Hw..Ow} \rangle$	28.9	13.5		
	$\langle t_{Ow-Hw..Ow} \rangle$	39.5	-		
Ow-Hw..Ow	$\langle R_{Ow-Hw..Ow} \rangle$	3.3	0.3		
(1-2)	$\langle \theta_{Ow-Hw..Ow} \rangle$	26.2	13.8		
	$\langle t_{Ow-Hw..Ow} \rangle$	33.8	-		

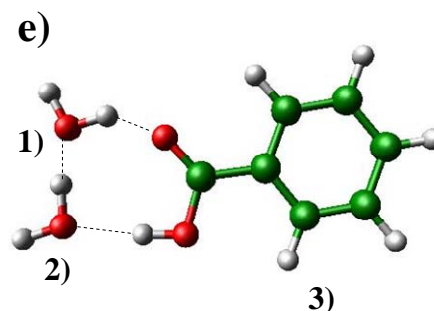


Table 3.2 (Continued).

	MD-[2:1]_{Benz}^{T=298}	SD	
O1-H1..O1	$\langle R_{O1-H1..O1} \rangle$	3.6	0.3
(1-2)	$\langle \theta_{O1-H1..O1} \rangle$	39.1	9.5
	$\langle t_{O1-H1..O1} \rangle$	29.7	-
O1-H1..O1	$\langle R_{O1-H1..O1} \rangle$	3.7	0.3
(2-1)	$\langle \theta_{O1-H1..O1} \rangle$	47.0	6.0
	$\langle t_{O1-H1..O1} \rangle$	12.2	-
O1-H1..O2	$\langle R_{O1-H1..O2} \rangle$	3.1	0.3
(1-2)	$\langle \theta_{O1-H1..O2} \rangle$	24.9	15.1
	$\langle t_{O1-H1..O2} \rangle$	80.1	-
O1-H1..Ow	$\langle R_{O1-H1..Ow} \rangle$	3.2	0.4
(1-3)	$\langle \theta_{O1-H1..Ow} \rangle$	27.2	16.2
	$\langle t_{O1-H1..Ow} \rangle$	61.4	-
O1-H1..Ow	$\langle R_{O1-H1..Ow} \rangle$	2.9	0.2
(2-3)	$\langle \theta_{O1-H1..Ow} \rangle$	18.1	9.2
	$\langle t_{O1-H1..Ow} \rangle$	100.0	-
Ow-Hw..O2	$\langle R_{Ow-Hw..O2} \rangle$	3.0	0.2
(3-2)	$\langle \theta_{Ow-Hw..O2} \rangle$	45.4	9.0
	$\langle t_{Ow-Hw..O2} \rangle$	18.3	-
Ow-Hw..O2	$\langle R_{Ow-Hw..O2} \rangle$	3.0	0.3
(3-1)	$\langle \theta_{Ow-Hw..O2} \rangle$	26.0	13.5
	$\langle t_{Ow-Hw..O2} \rangle$	27.8	-

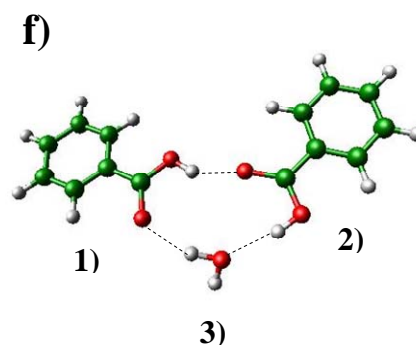


Table 3.2 (Continued).

		MD-[2:1]_{Benz}^{T=298}		SD	
Ow-Hw..O2	$\langle R_{Ow-Hw..O2} \rangle$	3.1		0.3	
(3 - 1)	$\langle \theta_{Ow-Hw..O2} \rangle$	36.6		12.9	
	$\langle t_{Ow-Hw..O2} \rangle$	39.6		-	
		MD-[2:1]_{Benz}^{T=280}		SD	
O1-H1..O2	$\langle R_{O1-H1..O2} \rangle$	2.9		0.2	
(1 - 2)	$\langle \theta_{O1-H1..O2} \rangle$	18.5		10.5	
	$\langle t_{O1-H1..O2} \rangle$	100.0		-	
O1-H1..Ow	$\langle R_{O1-H1..Ow} \rangle$	2.9		0.2	
(2 - 3)	$\langle \theta_{O1-H1..Ow} \rangle$	13.5		7.5	
	$\langle t_{O1-H1..Ow} \rangle$	100.0		-	
Ow-Hw ..O2	$\langle R_{Ow-Hw..O2} \rangle$	3.1		0.2	
(3 - 2)	$\langle \theta_{Ow-Hw..O2} \rangle$	48.1		6.8	
	$\langle t_{Ow-Hw..O2} \rangle$	18.2		-	
Ow-Hw ..O2	$\langle R_{Ow-Hw..O2} \rangle$	3.0		0.2	
(3 - 2)	$\langle \theta_{Ow-Hw..O2} \rangle$	48.9		6.0	
	$\langle t_{Ow-Hw..O2} \rangle$	13.0		-	
Ow-Hw..O2	$\langle R_{Ow-Hw..O2} \rangle$	3.3		0.3	
(3 - 1)	$\langle \theta_{Ow-Hw..O2} \rangle$	21.0		10.9	
	$\langle t_{Ow-Hw..O2} \rangle$	59.6		-	

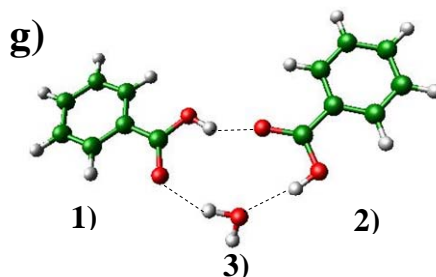


Table 3.2 (Continued).

		MD-[2:1]_{Benz}^{T=280}		SD	
Ow-Hw..O2	$\langle R_{Ow-Hw..O2} \rangle$	3.3		0.3	
(3-1)	$\langle \theta_{Ow-Hw..O2} \rangle$	20.0		11.6	
	$\langle t_{Ow-Hw..O2} \rangle$	31.4		-	
		MD-[2:2]_{Benz}^{T=298}		SD	
O1-H1..O1	$\langle R_{O1-H1..O1} \rangle$	3.2		0.3	
(1-2)	$\langle \theta_{O1-H1..O1} \rangle$	17.8		11.6	
	$\langle t_{O1-H1..O1} \rangle$	29.0		-	
O1-H1..O2	$\langle R_{O1-H1..O2} \rangle$	3.0		0.3	
(1-2)	$\langle \theta_{O1-H1..O2} \rangle$	22.8		12.3	
	$\langle t_{O1-H1..O2} \rangle$	69.4		-	
O1-H1..Ow	$\langle R_{O1-H1..Ow} \rangle$	2.9		0.2	
(2-4)	$\langle \theta_{O1-H1..Ow} \rangle$	22.0		11.4	
	$\langle t_{O1-H1..Ow} \rangle$	93.6		-	
Ow-Hw..O2	$\langle R_{Ow-Hw..O2} \rangle$	2.9		0.2	
(4-2)	$\langle \theta_{Ow-Hw..O2} \rangle$	44.4		7.5	
	$\langle t_{Ow-Hw..O2} \rangle$	29.4		-	

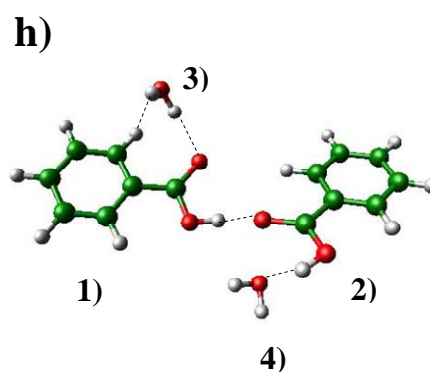


Table 3.2 (Continued).

		MD-[2:2]_{Benz}^{T=298}		SD	
Ow-Hw..O2	$\langle R_{Ow-Hw..O2} \rangle$	3.0	0.2		
(4-2)	$\langle \theta_{Ow-Hw..O2} \rangle$	45.6	7.5		
	$\langle t_{Ow-Hw..O2} \rangle$	11.2	-		
Ow-Hw..O2	$\langle R_{Ow-Hw..O2} \rangle$	3.2	0.3		
(3-1)	$\langle \theta_{Ow-Hw..O2} \rangle$	27.3	13.9		
	$\langle t_{Ow-Hw..O2} \rangle$	49.3	-		
Ow-Hw..O2	$\langle R_{Ow-Hw..O2} \rangle$	3.1	0.3		
(3-1)	$\langle \theta_{Ow-Hw..O2} \rangle$	29.0	14.2		
	$\langle t_{Ow-Hw..O2} \rangle$	39.9	-		
		MD-[2:2]_{Benz}^{T=280}		SD	
O1-H1..O1	$\langle R_{O1-H1..O1} \rangle$	3.0	0.2		
(1-2)	$\langle \theta_{O1-H1..O1} \rangle$	24.7	11.2		
	$\langle t_{O1-H1..O1} \rangle$	50.4	-		
O1-H1..Ow	$\langle R_{O1-H1..Ow} \rangle$	2.9	0.2		
(2-3)	$\langle \theta_{O1-H1..Ow} \rangle$	16.6	8.9		
	$\langle t_{O1-H1..Ow} \rangle$	100.0	-		
O1-H1..Ow	$\langle R_{O1-H1..Ow} \rangle$	3.5	0.3		
(2-4)	$\langle \theta_{O1-H1..Ow} \rangle$	39.6	10.4		
	$\langle t_{O1-H1..Ow} \rangle$	14.6	-		

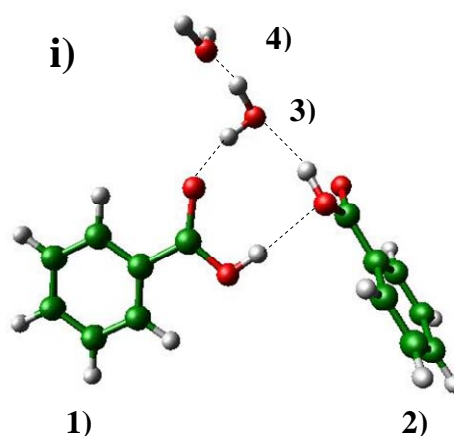


Table 3.2 (Continued).

		MD-[2:2]_{Benz}^{T=280}	SD
Ow-Hw..O2	$\langle R_{Ow-Hw..O2} \rangle$	3.2	0.3
(3-1)	$\langle \theta_{Ow-Hw..O2} \rangle$	35.2	12.0
	$\langle t_{Ow-Hw..O2} \rangle$	16.9	-
Ow-Hw..O2	$\langle R_{Ow-Hw..O2} \rangle$	3.0	0.3
(3-2)	$\langle \theta_{Ow-Hw..O2} \rangle$	43.7	9.3
	$\langle t_{Ow-Hw..O2} \rangle$	14.0	-
Ow-Hw..O2	$\langle R_{Ow-Hw..O2} \rangle$	3.0	0.2
(4-2)	$\langle \theta_{Ow-Hw..O2} \rangle$	28.8	13.9
	$\langle t_{Ow-Hw..O2} \rangle$	17.8	-
Ow-Hw..O2	$\langle R_{Ow-Hw..O2} \rangle$	3.1	0.3
(4-2)	$\langle \theta_{Ow-Hw..O2} \rangle$	32.9	14.1
	$\langle t_{Ow-Hw..O2} \rangle$	12.8	-
Ow-Hw..Ow	$\langle R_{Ow-Hw..Ow} \rangle$	3.2	0.2
(3-4)	$\langle \theta_{Ow-Hw..Ow} \rangle$	29.2	13.8
	$\langle t_{Ow-Hw..Ow} \rangle$	39.3	-
Ow-Hw..Ow	$\langle R_{Ow-Hw..Ow} \rangle$	3.2	0.3
(3-4)	$\langle \theta_{Ow-Hw..Ow} \rangle$	30.0	14.1
	$\langle t_{Ow-Hw..Ow} \rangle$	45.7	-

As mentioned in the introduction that the partition of BA between the Benz and water phases represents one of the classical problems in the area of molecular association in solutions. At least three important observations in the Benz phase were addressed from experiments (Wall and Rouse, 1941; Van Duyne et al., 1967; Shamsul Huq and Lodhi, 1966). They concerned primarily with the structures of the solute clusters, the number of water molecule H-bonding directly at BA and the possibility for water molecules to self-associate in the Benz phase. It was proposed that part of water which dissolves together with BA in the Benz phase is not H-bonded together and water molecules in the Benz phase prefer to H-bond directly with BA. Based on the assumption that the hydrated $(BA)_2$ can be ignored, it was shown that the concentration of H-bonded water increases along with the increase of the BA monomer. With this experimental information, the BA-H₂O 1 : 1 complex was existed in dilute Benz solution. Different observations and interpretations were reported by Van Duyne et al. (1967) in which the authors claimed that the excess of water solubility could be explained in terms of the self-association of water molecules in the Benz phase. They also pointed out that two water molecules hydrate a single BA molecule as well as $(BA)_2$ in the Benz phase.

Based on the information obtained from MD simulations, some comments on the situations in the Benz phase could be made. The present MD results show that nearly all H-bond complexes proposed in experiment (Van Duyne et al., 1967) exist in the Benz phase, with different lifetimes. The probabilities of finding these H-bond complexes depend mainly on their size and temperature. The cyclic BA-H₂O 1 : 1 like complex seems to exist more or less in all Benz solutions considered. The MD results also suggest self-associations of water in $[1:2]_{Benz}^{T=280}$ and $[1:2]_{Benz}^{T=298}$ and $[2:2]_{Benz}^{T=280}$.

However, due to the strength of the O1-H1-Ow H-bond, the water clusters tend not to be isolated from BA. From the MD results on $[2:2]_{\text{Benz}}^{T=298}$, water molecules could also stay separate from each other. This agrees well with the experimental observation that part of water molecules dissolving together with BA is not H-bonded together. General trends are observed when the temperature is lowered from 298 to 280 K namely, the solute clusters become more associated, accompanied by some structural changes especially for large clusters. The temperature effects on the structures and stability of the BA-H₂O complexes has never been addressed in detail in the previous theoretical and experimental reports (Wall and Rouse, 1941; Van Duyne et al., 1967; Shamsul Huq and Lodhi, 1966). One could anticipate that different conclusions made from experiments are not completely disagreed. They could be attributed to limitations, conditions and approximations adopted in experiments, as well as the lack of microscopic information. Therefore, modern high-resolution spectroscopic techniques are required to investigate the structures and stability of the BA-H₂O complexes in Benz solutions in details.

3.2 PhOH-Benz complexes

3.2.1 Structures and energetic in the gas phase

The absolute and some low-lying minimum energy geometries of the PhOH-Benz $m : n$ complexes, m and $n = 1 - 2$, obtained from the T-model potentials (Sagarik, Chaiwongwattana, and Sisot, 2004; Sagarik and Asawakun, 1997), are displayed in Figures 3.6 to 3.8. In Figure 3.6, the absolute minimum energy geometry of the PhOH-Benz 1 : 1 complex is represented by structure **a**, in which the O-H group of PhOH acts as proton donor towards the π -electron cloud of Benz, with the

interaction energy ($\Delta E_{T\text{-model}}$) of $-19.5 \text{ kJ mol}^{-1}$ and the O-H.. π and $\pi_{\text{Ph}}\text{-}\pi$ distances of 3.4 and 5.4 Å, respectively. The $\pi_{\text{Ph}}\text{-}\pi$ distance in structure **a** lies within the range reported based on B3LYP/6-311G(d) and interaction energy in good agreement with the T-shaped structure obtained from the best *ab initio* calculations at SOS-MP2/6-311++G(d,p) of $-21.1 \text{ kJ mol}^{-1}$ (Guedes et al., 2003; Kwak et al., 2006) and the picosecond photofragment spectroscopy (Knee, Khundkar, and Zewail, 1987). Structures **b** and **c** are two local minimum energy geometries, with $\Delta E_{T\text{-model}}$ of -13.5 and -9.3 kJ mol^{-1} , respectively. Structure **b** shows a possibility for the oxygen atom and the π -electron cloud of PhOH to act as proton acceptor towards the C-H groups of Benz, with the C-H..O and C-H.. π_{Ph} H-bond distances of 3.4 and 4.0 Å, respectively. Structure **c** is stabilized solely by the C-H.. π H-bonds, with the C-H.. π and $\pi_{\text{Ph}}\text{-}\pi$ distances of 3.8 and 4.9 Å, respectively.

A compact H-bond cluster formed from the O-H.. π , C-H..O, C-H.. π and C-H.. π_{Ph} H-bonds represents the absolute minimum energy geometry of the PhOH-Benz 1 : 2 complex, structure **a** in Figure 3.7. Structure **a** possesses $\Delta E_{T\text{-model}}$ of $-41.6 \text{ kJ mol}^{-1}$, with the H-bond distances similar to those in the PhOH-Benz 1 : 1 complexes. The H-bonds in structure **a** are slightly more complicated than those presumed from supersonic jet spectroscopy (Olkawa et al., 1983). Structure **b** is about 11 kJ mol^{-1} less stable than structure **a**. In structure **b**, the oxygen atom of PhOH acts as proton acceptor towards two C-H groups of Benz, with the C-H..O H-bond distances of 3.3 Å. The O-H.. π H-bond in structure **c** is similar to structure **a** of the PhOH-Benz 1 : 1 complex, whereas the C-H.. π H-bond resembles the T-shaped structure in (Benz)₂ (Sinnokrot and Sherrill, 2004). Structure **c** is slightly less stable than structure **b**, with

$\Delta E_{T\text{-model}}$ of $-28.8 \text{ kJ mol}^{-1}$ and the O-H.. π and C-H.. π H-bond distances of 3.4 and 3.8 Å, respectively.

Since H-bonds in the PhOH-Benz 2 : 1 and 2 : 2 complexes are not substantially different from those in the PhOH-Benz 1 : 1 and 1 : 2 complexes, from which all characteristic H-bond structures were explained, Figure 3.8 will not be discussed in details. Comparison of the results obtained in this section with those from experiments (Knee, Khundkar, and Zewail, 1987; Olkawa et al., 1983) and *ab initio* calculations (Grover, Walters, and Hui, 1987; Kwak et al., 2006) showed that the T-model potentials (Sagarik, Chaiwongwattana, and Sisot, 2004; Sagarik and Asawakun, 1997) are accurate enough for further application in MD simulations.

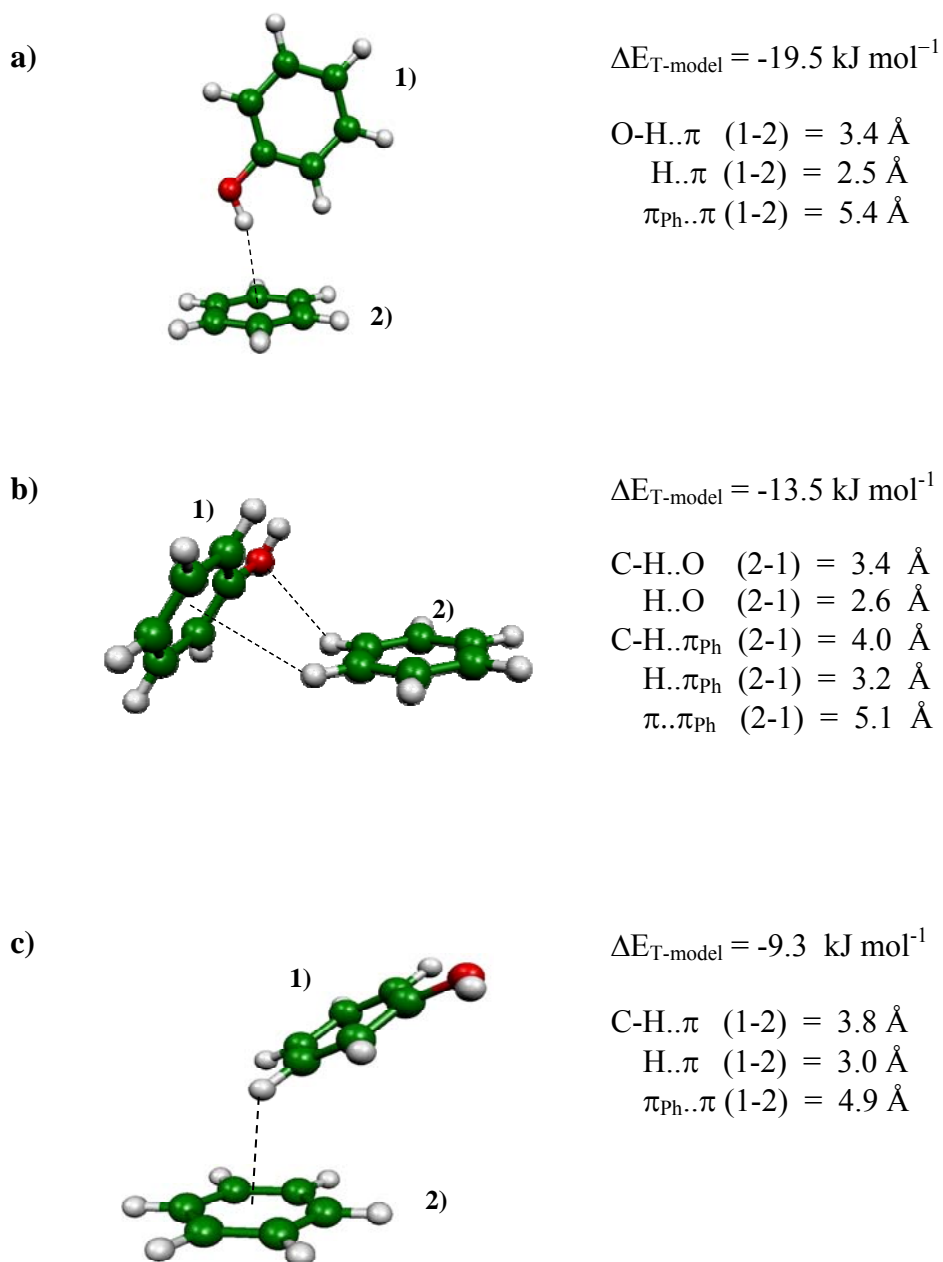


Figure 3.6 Equilibrium structures and interaction energies of the PhOH-Benz 1 : 1 complexes in the gas phase, computed from the T-model potentials.

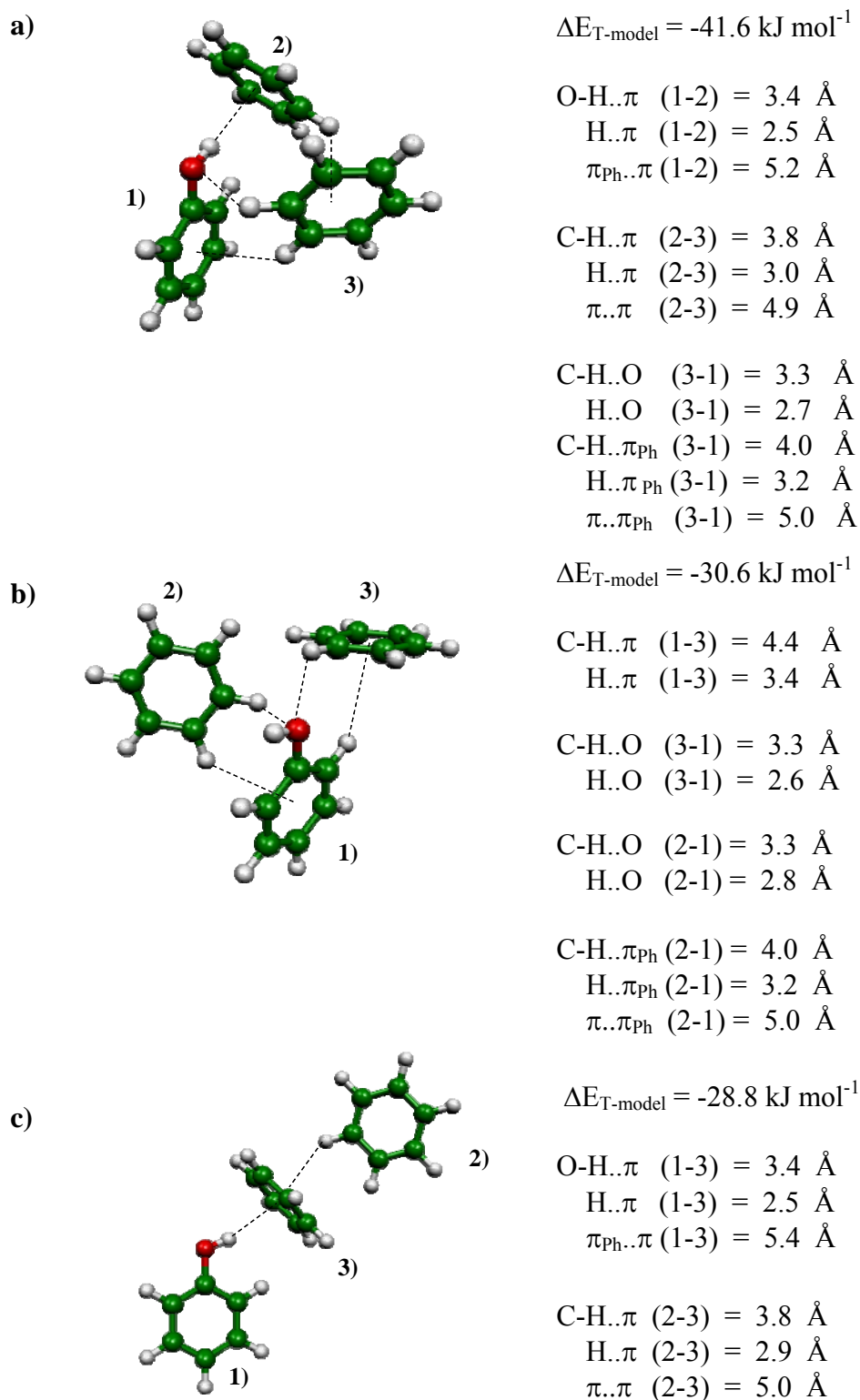


Figure 3.7 Equilibrium structures and interaction energies of the PhOH-Benz 1 : 2 complexes in the gas phase, computed from the T-model potentials.

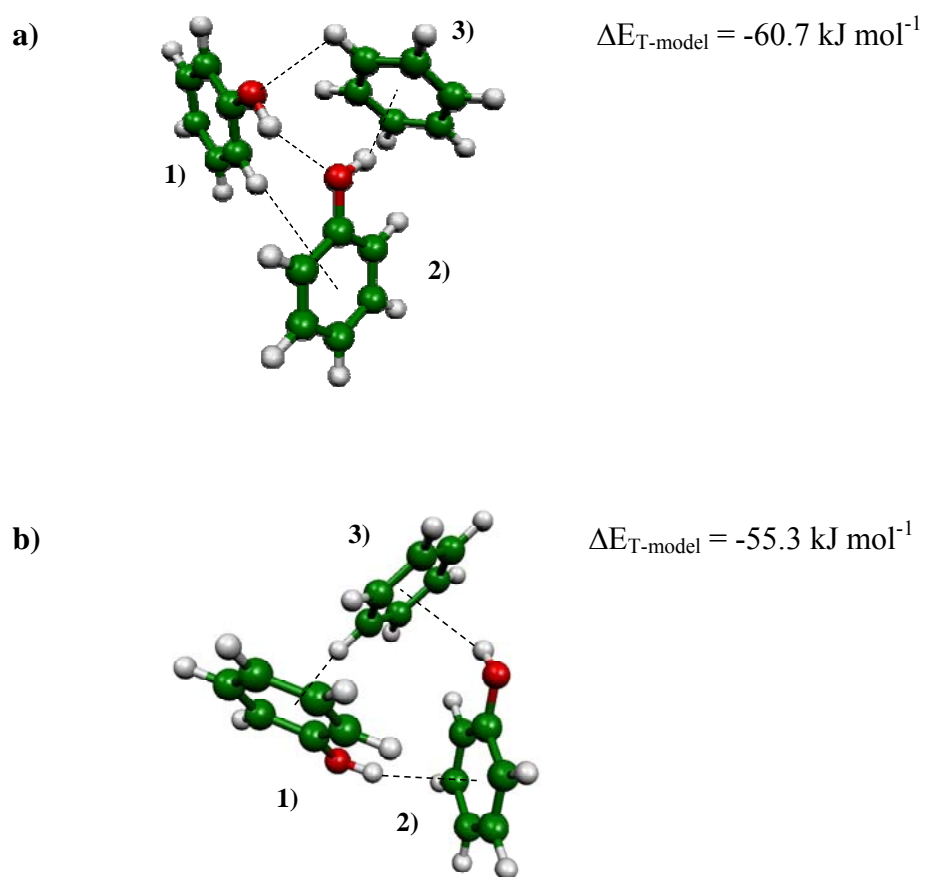


Figure 3.8 Equilibrium structures and interaction energies of the PhOH-Benz complexes in the gas phase, computed from the T-model potentials. a) – b) The PhOH-Benz 2 : 1 complexes. c) – e) The PhOH-Benz 2 : 2 complexes.

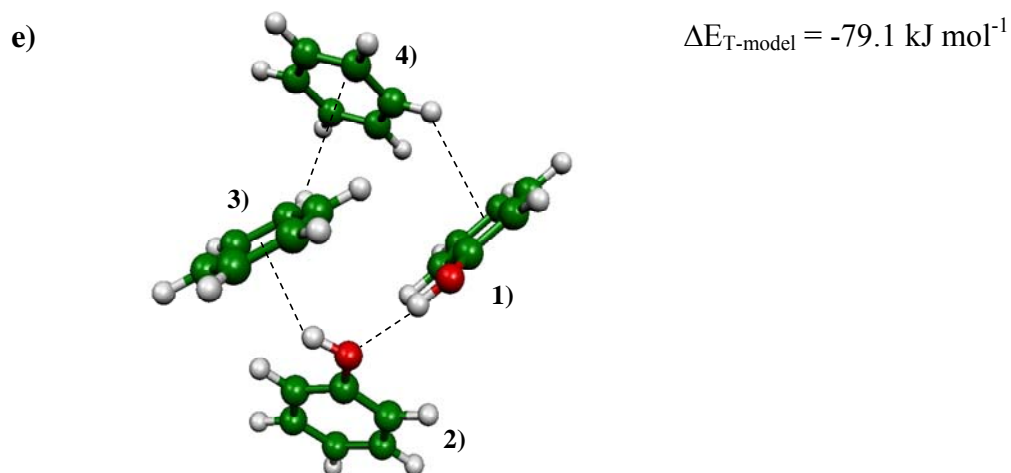
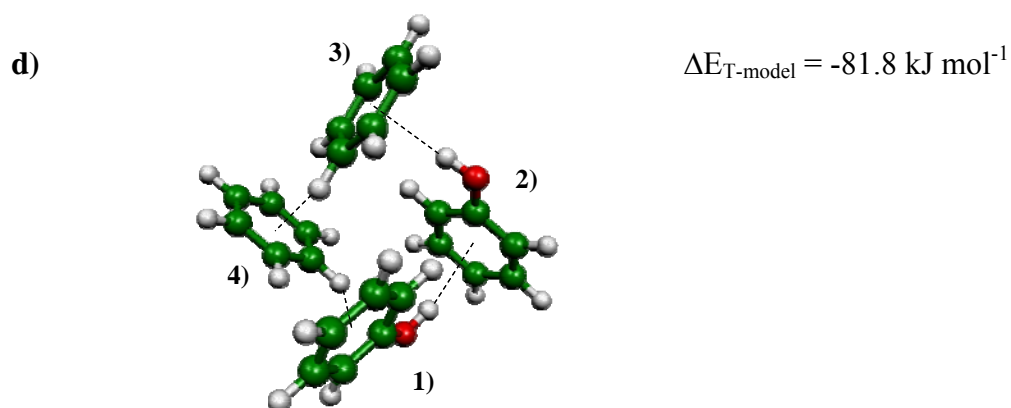
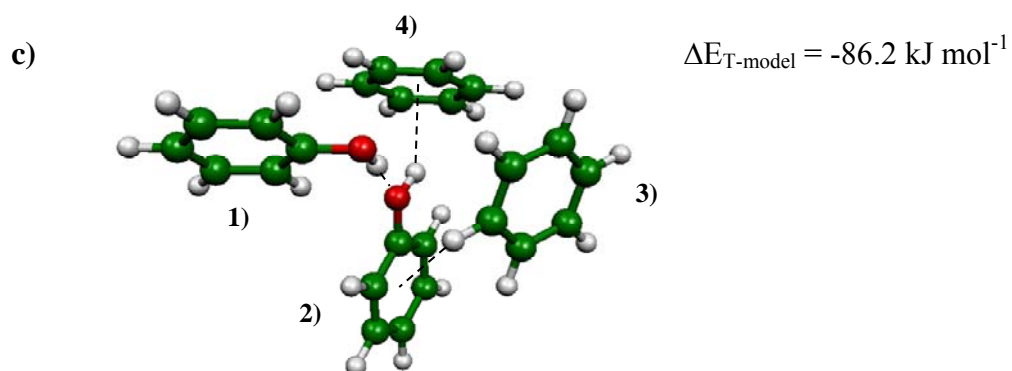


Figure 3.8 (Continued).

3.2.2 MD simulations of benzene solutions

The T-model potentials were employed in MD simulations of $[(\text{PhOH})_n]_{\text{Benz}}$, $n = 1 - 3$, at 298 K. $\langle E_{\text{Benz}}^{\text{pot}} \rangle$, $\langle E_{\text{Benz}}^{\text{solu-solu}} \rangle$ and $\langle E_{\text{Benz}}^{\text{solu-solv}} \rangle$ obtained from MD- $[(\text{PhOH})_n]_{\text{Benz}}^{\text{frozen}}$ and MD- $[(\text{PhOH})_n]_{\text{Benz}}^{\text{free}}$ are summarized in Table 3.3. In order to limit the number of figures, only selected g(R), π -PD, PB-PD and PB-BB-PD maps are displayed. High-density contours on the PD maps are labeled with capital letters.

The average interaction energies in Table 3.3 show both expected and unexpected trends in $[(\text{PhOH})_n]_{\text{Benz}}$. Due to large number of Benz molecules, $\langle E_{\text{Benz}}^{\text{pot}} \rangle$ are nearly the same for all MD simulations, and since the degree of freedom in MD- $[(\text{PhOH})_n]_{\text{Benz}}^{\text{free}}$ is higher than MD- $[(\text{PhOH})_n]_{\text{Benz}}^{\text{frozen}}$, $\langle E_{\text{Benz}}^{\text{solu-solv}} \rangle$ is about twice higher, -58.1 and -106.0 kJ mol⁻¹, respectively. As only one O-H group could act as proton donor towards Benz molecules in both MD- $[(\text{PhOH})_2]_{\text{Benz}}^{\text{frozen}}$ and MD- $[(\text{PhOH})_2]_{\text{Benz}}^{\text{free}}$, $\langle E_{\text{Benz}}^{\text{solu-solv}} \rangle$ are not substantially different, the former is about 5 kJ mol⁻¹ higher than the latter. The energetic results seem to be more complicated in MD- $[(\text{PhOH})_2]_{\text{Benz}}^{\text{free}}$, in which $\langle E_{\text{Benz}}^{\text{solu-solv}} \rangle$ is about 21 kJ mol⁻¹ lower than MD- $[(\text{PhOH})_2]_{\text{Benz}}^{\text{frozen}}$, and $\langle E_{\text{Benz}}^{\text{solu-solu}} \rangle = -2.3$ kJ mol⁻¹. These represent direct evidences for substantial changes in H-bond structures in MD- $[(\text{PhOH})_2]_{\text{Benz}}^{\text{free}}$; an increase in solute-solvent interaction is accompanied by a decrease in solute-solute interaction, leading to some solvent-separated structures. The situations seem to be less complicated in MD- $[(\text{PhOH})_3]_{\text{Benz}}^{\text{free}}$, in which $\langle E_{\text{Benz}}^{\text{solu-solu}} \rangle$ is about 64% of $\Delta E_{\text{T-model}}$ of $(\text{PhOH})_3$ in the gas

phase (Sagarik and Asawakun, 1997), and $\langle E_{\text{Benz}}^{\text{solu-solv}} \rangle = -98.0 \text{ kJ mol}^{-1}$. These indicate that, on average, the three H-bonds in $(\text{PhOH})_3$ did not change substantially in the course of MD- $[(\text{PhOH})_3]_{\text{Benz}}^{\text{free}}$. The formations of solvent-separated structures in $[(\text{PhOH})_2]_{\text{Benz}}$ and close-contact trimers in $[(\text{PhOH})_3]_{\text{Benz}}$ will be discussed in detail in the forth coming subsections.

Table 3.3 Energetic results obtained from MD- $[(\text{PhOH})_n]_{\text{Benz}}^{\text{frozen}}$ and MD- $[(\text{PhOH})_n]_{\text{Benz}}^{\text{free}}$, $n = 1 - 3$. Energies are in kJ mol^{-1} .

	$\langle E_{\text{Benz}}^{\text{pot}} \rangle$	$\langle E_{\text{Benz}}^{\text{solu-solu}} \rangle$	$\langle E_{\text{Benz}}^{\text{solu-solv}} \rangle$
MD- $[(\text{PhOH})]_{\text{Benz}}^{\text{frozen}}$	-35.4	-	-106.0
MD- $[(\text{PhOH})]_{\text{Benz}}^{\text{free}}$	-35.3	-	-58.1
MD- $[(\text{PhOH})_2]_{\text{Benz}}^{\text{frozen}}$	-35.5	-	-101.0
MD- $[(\text{PhOH})_2]_{\text{Benz}}^{\text{free}}$	-35.5	-2.3	-123.4
MD- $[(\text{PhOH})_3]_{\text{Benz}}^{\text{free}}$	-35.4	-51.8	-98.0

MD-[PhOH]_{Benz}

The average three-dimensional structures and interaction energy distributions of solvent molecules obtained from MD-[PhOH]_{Benz}^{frozen} are shown in Figure 3.9. The values of the highest probabilities at the labeled contours on the π -PD maps ($\langle P^{\pi\text{-PD}} \rangle_{\text{max}}$), together with the corresponding lowest-average interaction energies on the PB-PD, BB-PB and PB-BB-PD maps, denoted by $\langle \Delta E_{\text{Benz}}^{\text{PB-PD}} \rangle_{\text{min}}$, $\langle \Delta E_{\text{Benz}}^{\text{BB-PD}} \rangle_{\text{min}}$ and $\langle \Delta E_{\text{Benz}}^{\text{PB-BB-PD}} \rangle_{\text{min}}$, respectively, are summarized in Table 3.4.

The π -PD maps in Figures 3.9a) to 3.9d) reveal that, on average, at least three Benz molecules stay in the vicinity the O-H group of PhOH, labeled with **A** ($Z = -0.5 - 0.5 \text{ \AA}$), **B** ($Z = 2.0 - 3.0 \text{ \AA}$) and **C** ($Z = -0.5 - 0.5 \text{ \AA}$). It is obvious that, the π -electron clouds of Benz molecules at **A** and **B** act as proton acceptor towards the O-H and C-H groups of PhOH, respectively, whereas a C-H group of Benz at **C** acts as proton donor towards the oxygen atom of PhOH. Table 3.4 shows that, Benz molecules at **A**, **B** and **C** possess $\langle \Delta E_{\text{Benz}}^{\text{PB-PD}} \rangle_{\text{min}}$ of -17.3, -11.7 and -9.8 kJ mol⁻¹, respectively. Comparison of $\Delta E_{\text{T-model}}$ in Figure 3.6 and $\langle \Delta E_{\text{Benz}}^{\text{PB-PD}} \rangle_{\text{min}}$ suggests a possibility for a C-H group of Benz at **B** to act as proton donor towards the oxygen atom of PhOH.

Table 3.4 The highest probabilities at the labeled contours on the π -PD maps ($\langle P^{\pi\text{-PD}} \rangle_{\text{max}}$) in Figure 3.9, together with the corresponding lowest average interaction energies ($\langle \Delta E_{\text{Benz}}^X \rangle_{\text{min}}$) obtained from MD-[PhOH]_{Benz}^{frozen}. Energies are in kJ mol^{-1} and $X = \text{PB-PD}$, BB-PD or PB-BB-PD .

	$\langle P^{\pi\text{-PD}} \rangle_{\text{max}}$	$\langle \Delta E_{\text{Benz}}^{\text{PB-PD}} \rangle_{\text{min}}$	$\langle \Delta E_{\text{Benz}}^{\text{BB-PD}} \rangle_{\text{min}}$	$\langle \Delta E_{\text{Benz}}^{\text{PB-BB-PD}} \rangle_{\text{min}}$
$Z = -0.5 - 0.5 \text{ \AA}$				
A	0.10	-17.3	-74.2	-83.7
C	0.04	-7.3	-79.7	-81.4
$Z = 0.0 - 1.0 \text{ \AA}$				
A	0.08	-16.1	-78.3	-94.4
C	0.03	-7.5	-77.2	-82.1
$Z = 1.0 - 2.0 \text{ \AA}$				
A	0.03	-16.1	-73.0	-83.1
B	0.03	-10.8	-72.9	-82.9
C	0.02	-7.9	-76.4	-88.2
$Z = 2.0 - 3.0 \text{ \AA}$				
A	0.04	-9.5	-76.9	-91.5
B	0.11	-11.7	-75.0	-86.1
C	0.03	-9.8	-74.8	-82.5

The preferential solvation order according to $\langle P^{\pi\text{-PD}} \rangle_{\text{max}}$ and the average interaction energy orders based on the absolute values of $\langle \Delta E_{\text{Benz}}^{\text{PB-PD}} \rangle_{\text{min}}$, $\langle \Delta E_{\text{Benz}}^{\text{BB-PD}} \rangle_{\text{min}}$ and $\langle \Delta E_{\text{Benz}}^{\text{PB-BB-PD}} \rangle_{\text{min}}$ in Table 3.4 can be written as:

$$\langle P^{\pi\text{-PD}} \rangle_{\text{max}}: \quad \mathbf{B} > \mathbf{A} > \mathbf{C}$$

$$\langle \Delta E_{\text{Benz}}^{\text{PB-PD}} \rangle_{\text{min}}: \quad \mathbf{A} > \mathbf{B} > \mathbf{C}$$

$$\langle \Delta E_{\text{Benz}}^{\text{BB-PD}} \rangle_{\text{min}}: \quad \mathbf{C} > \mathbf{A} > \mathbf{B}$$

$$\langle \Delta E_{\text{Benz}}^{\text{PB-BB-PD}} \rangle_{\text{min}}: \quad \mathbf{A} > \mathbf{C} > \mathbf{B}$$

It should be noted that, the preferential solvation order and the average interaction energy orders in the present case, as well as in many cases (Sagarik and Chaiyapongs, 2005; Sagarik and Dokmaisrijan, 2005; Deeying and Sagarik, 2006), are different. This is due to the fact that, the π -PD maps show relative probabilities that, a specific “position” in the first solvation shell of PhOH is occupied by Benz molecules, whereas the minima on the average potential energy landscapes, such as $\langle \Delta E_{\text{Benz}}^{\text{PB-BB-PD}} \rangle_{\text{min}}$, represent “low-lying interaction energy states”, probed in the course of MD simulations. In other words, Benz molecules at the position with the highest $\langle P^{\pi\text{-PD}} \rangle_{\text{max}}$ need not possess the lowest $\langle \Delta E_{\text{Benz}}^{\text{PB-BB-PD}} \rangle_{\text{min}}$. Since the occupancies of the interaction energy states depend upon dynamics of individual solvent molecules, which could be described by structures of the average potential energy landscapes, it is necessary to include them in the discussion of $[(\text{PhOH})_n]_{\text{Benz}}$ (Sagarik and Chaiyapongs, 2005; Sagarik and Dokmaisrijan, 2005; Deeying and Sagarik, 2006). The cross section plots were constructed for this purpose. They show

both the average potential energy barriers interconnecting interaction the energy states and the average potential energy wells, in which solvent molecules are confined. The latter could be related to the “average cage potentials” (Magro et al., 2005). Figures 3.9e) and 3.9f) are examples of the average potential energy landscapes and cross section plots obtained from MD-[PhOH]_{Benz}^{frozen}. The cross section plots indicate that, the average potential energy barriers at **A**, **B** and **C** are quite high, in both longitudinal and transverse directions, e.g. about 120 kJ mol⁻¹ at **A** in Figures 3.9f) (I) and (II). However, a possibility for the solvent exchange within the first solvation shell is evident from the PB-PD and PB-BB-PD maps in Figure 3.9d) ($Z = 2.0 - 3.0 \text{ \AA}$), and the corresponding cross section plots in Figure 3.9f) (IV), in which an energy channel connecting **B** and **C**, and a moderate energy barrier to Benz exchange, are recognized, respectively. All the cross section plots in Figures 3.9e) and 3.9f) reveal that, the size and shape of the average potential energy wells are determined nearly exclusively by the average solvent-solvent interactions. These could restrict translational motion of Benz in the first solvation shell of PhOH, especially in the transverse direction. One could, therefore, conclude that, Benz molecules at **A**, **B** and **C** form a part of a quite well-defined local solvent cage at the O-H group of PhOH. The qualitative interpretation of dynamics of individual solvent molecules in connection to the average potential energy landscapes is similar to Rabani, Gezelter, and Berne (1997) by which molecular translation in the liquid phase characterized by the average potential energy landscapes was proposed to occur through jumps between basins separated by high-energy barriers, and the identity of the solvent cage should be more related to the multi-minimum basin itself, rather than to single actual configuration.

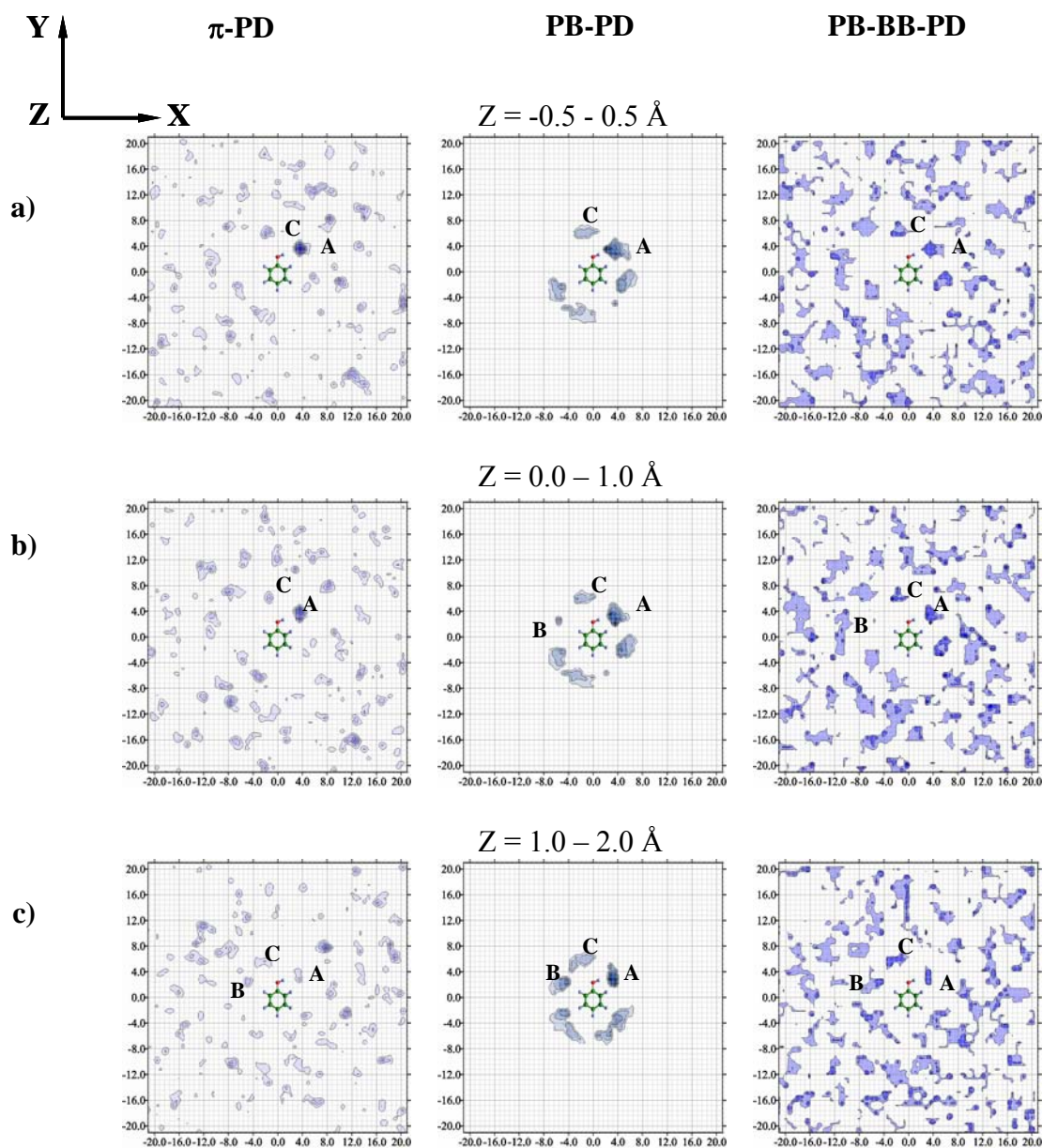
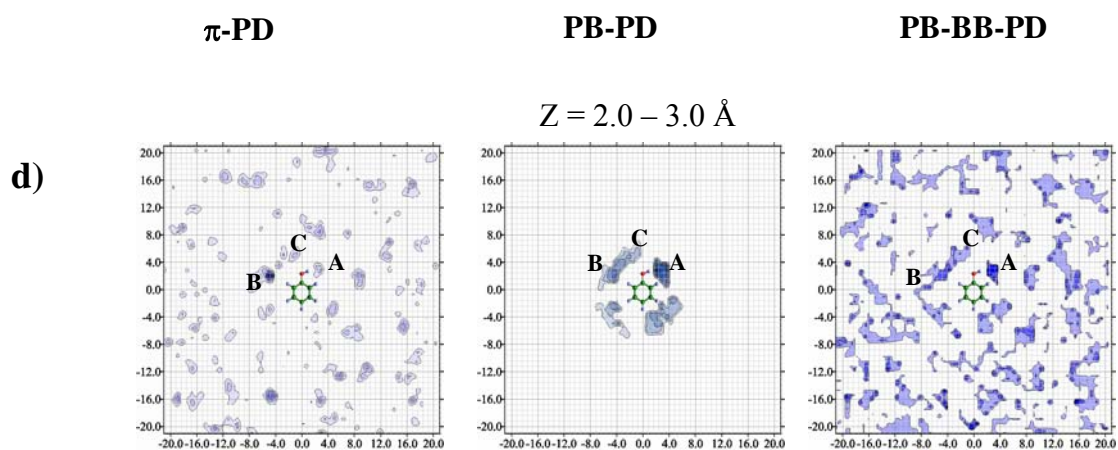


Figure 3.9 Structural and energetic results obtained from MD-[PhOH]_{Benz}^{frozen}. X-, Y- and Z-axes are in Å, energies in kJ mol⁻¹. a) – d) The π -PD, PB-PD and PB-BB-PD maps. e) – f) Average potential energy landscapes and the cross section plots computed from longitudinal and transverse profile lines. _____ PB-BB-PD cross section plot. - - - - - PB-PD cross section plot. - - - - - BB-PD cross section plot.



e) $Z = -0.5 - 0.5 \text{ \AA}$

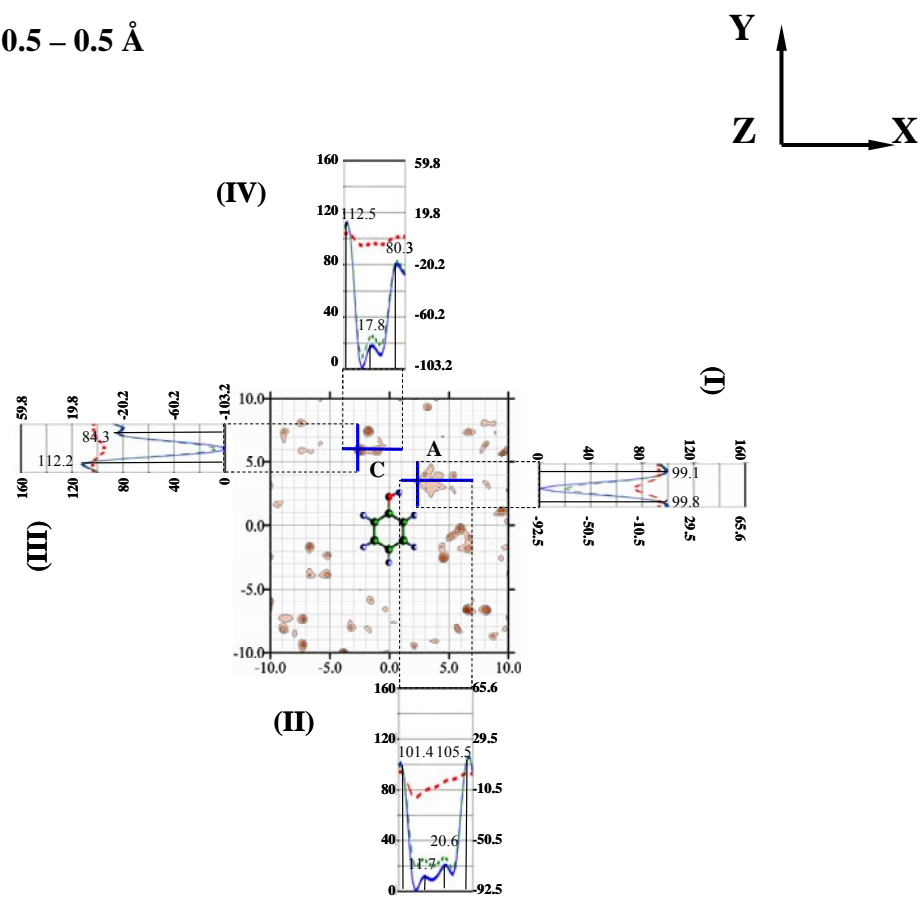


Figure 3.9 (Continued).

f) $Z = 2.0$ 3.0 \AA

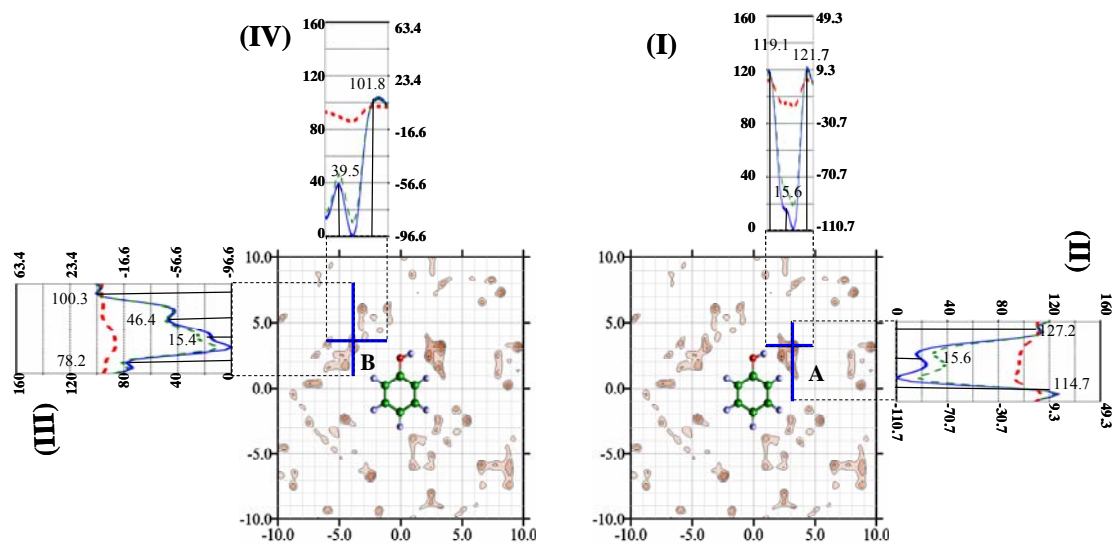
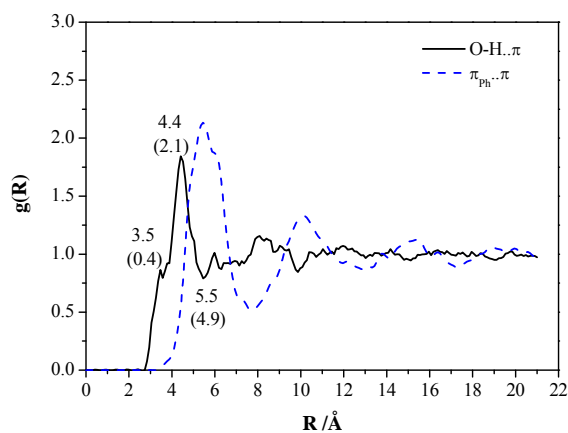


Figure 3.9 (Continued).

a)



b)

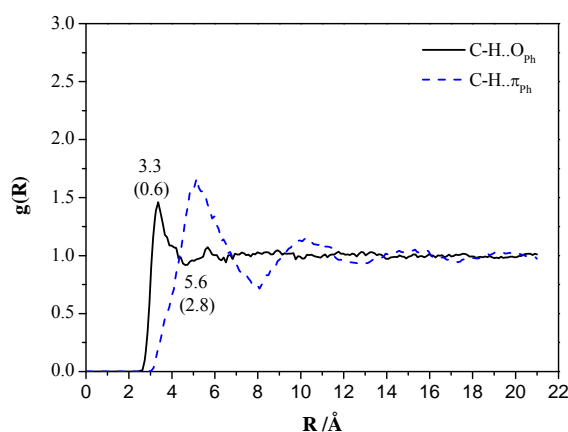


Figure 3.10 Structural and dynamic results obtained from MD-[PhOH]_{Benz}^{free}. a) – b)

$g(R)$; characteristic distances given with $n(R)$ in parentheses. c) Example of H-bond

exchange diagram. d) Fourier transformations of the O-H... π H-bond and $\pi_{\text{ph}}...$ π

distances. $\tau_{\text{O-H}\dots\pi}^{\text{PhOH-Benz}}$ = the lifetime of the PhOH-Benz complex computed from FFT of

the O-H... π H-bond distance. $\tau_{\pi_{\text{ph}}\dots\pi}^{\text{PhOH-Benz}}$ = the lifetime of the PhOH-Benz complex

computed from FFT of the $\pi_{\text{ph}}...$ π distance.

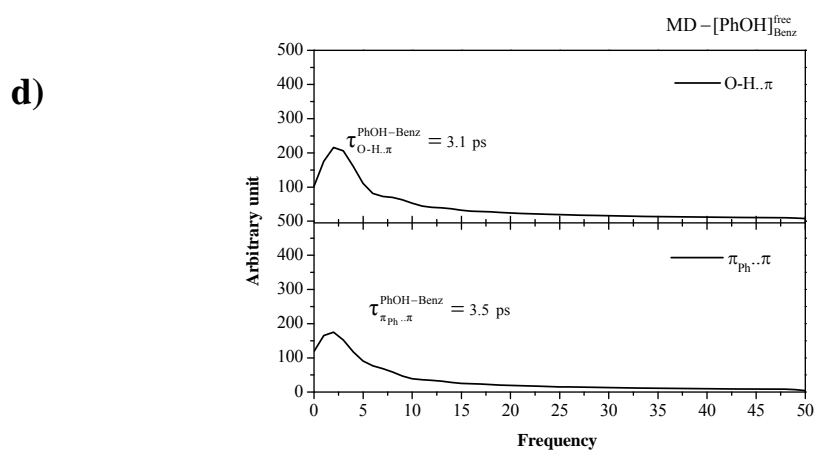
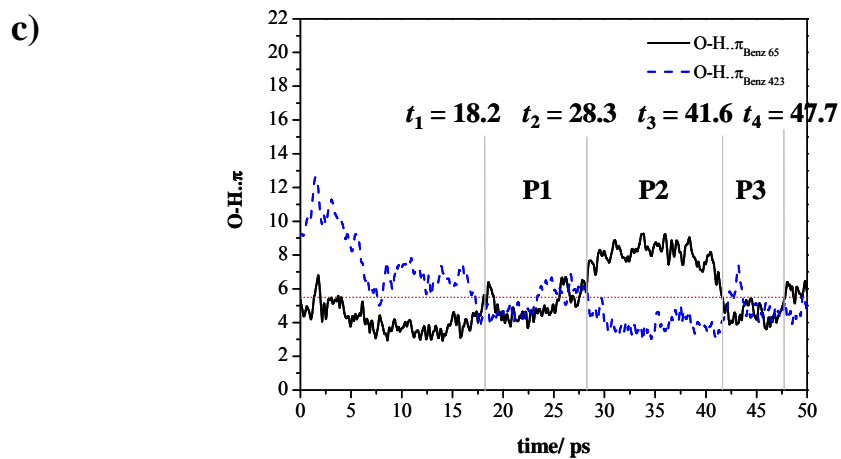


Figure 3.10 (Continued).

It appeared in general that, all structural information obtained from MD- $[\text{PhOH}]_{\text{Benz}}^{\text{free}}$ could be interpreted reasonably well based on the results of the PhOH-Benz 1 : 1 and 1 : 2 complexes in Figures 3.6 and 3.7. $g(R_{\text{O-H}\cdot\pi})$ in Figure 3.10a) shows the main peak at $R_{\text{O-H}\cdot\pi} = 4.4 \text{ \AA}$, with a small shoulder at $R_{\text{O-H}\cdot\pi} = 3.5 \text{ \AA}$, and according to $n(R_{\text{O-H}\cdot\pi})$ at the first minimum ($R_{\text{O-H}\cdot\pi} = 5.5 \text{ \AA}$), about five Benz molecules are in the first solvation shell of the O-H group. Since the main peak of $g(R_{\text{C-H}\cdot\text{O}})$ in Figure 3.10b) is seen at $R_{\text{C-H}\cdot\text{O}} = 3.3 \text{ \AA}$, one could conclude that, the main peak and small shoulder of $g(R_{\text{O-H}\cdot\pi})$ correspond to structures **b** and **a** in Figure 3.6, respectively. The predominance of the C-H.. O_{ph} H-bond in $[\text{PhOH}]_{\text{Benz}}$ was also suggested based on experiments in Philbrick (1934). Additionally in Figure 3.10a), $n(R_{\text{O-H}\cdot\pi}) = 2.1$ at the first maximum ($R_{\text{O-H}\cdot\pi} = 4.4 \text{ \AA}$) indicates that, in $[\text{PhOH}]_{\text{Benz}}$, two Benz molecules are in close contact with the O-H group, with the H-bond structures similar to structures **b** and **a** in Figure 3.7. These support the three-dimensional structures of solvent obtained from the π -PD maps and the preferential solvation order according to $\langle P^{\pi\text{-PD}} \rangle_{\text{max}}$.

Due to deep average potential energy wells, Benz molecules in the inner and outer shells of the O-H group seem not exchange as fast as water solvent (Sagarik and Dokmaisrijan, 2005; Deeying and Sagarik, 2006). The H-bond exchange diagram in Figure 3.10c) demonstrates the exchange of Benz 65 and Benz 423 in the course of MD- $[\text{PhOH}]_{\text{Benz}}^{\text{free}}$. At $t_1 = 18.2 \text{ ps}$, Benz 423 entered and shared the first solvation shell with Benz 65, until Benz 65 left at $t_2 = 28.3 \text{ ps}$. Therefore, the exchange process, taking place in panel **P1** in Figure 3.10c), took about 10 ps. The residence time of Benz 423 could be approximated from the widths of panel **P1** and **P2** to be about 23

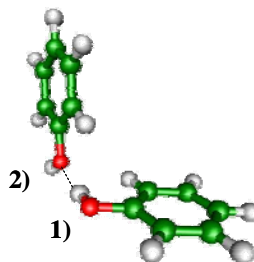
ps, compared to the residence time of water molecule in the first hydration shell of the -COO^- group of about 5 ps (Sagarik and Dokmaisrijan, 2005). The latter possesses considerably lower average potential energy barriers to water exchange. The same exchange process repeated again in panel **P3**; at $t_3 = 41.6$ ps, Benz 65 reentered and shared the first solvation shell with Benz 423 etc. Investigation of the H-bond exchange diagrams in details revealed that, Benz molecules at the O-H group of PhOH exchange through large-amplitude vibrational motions, which involve the displacement of the O-H... π H-bond as discussed in Sun and Bernstein (1996). Moreover, according to the five-exchange mechanisms proposed by Langford and Gray (1966), the exchanges seem to favor the associative-interchange (**I_a**) scheme, in which a solvent molecule enters and spends sometime in the first solvation shell before the other leaves. Analyses of the time evolutions of the cage structures in $[\text{Benz}]_{\text{liquid}}$ (Rabani, Gezelter, and Berne, 1997; Gezelter, Rabani, and Berne, 1999) showed two relaxation components, which could affect the exchange of Benz molecules constituting the solvent cage; the slow relaxing component is associated with the cage lifetime, whereas the fast relaxing component with the structural rearrangements due to molecular vibrations. Since the average cage potentials or the average potential energy wells are quite low in $[\text{PhOH}]_{\text{Benz}}$, it was reasonable and possible to investigate the fast component. Based on the assumption that, at short time, the dynamic equilibrium between the associated and dissociated forms could be studied from characteristic vibrational frequency of H-bond (Zheng et al., 2005), the lifetime of the PhOH-Benz 1 : 1 complex could be approximated. Since the O-H... π H-bond is responsible for the association in the PhOH-Benz 1 : 1 complex, FFT (Borse, 1997) was focused on the O-H... π H-bond exchange curve, from which the lifetime of

the PhOH-Benz 1 : 1 complex ($\tau_{\text{O-H}\cdot\pi}^{\text{PhOH-Benz}}$) was approximated as half of the association-dissociation dynamic equilibrium cycle time. Examples of FFT obtained from MD-[PhOH]_{Benz}^{free} are shown in Figure 3.10d), together with $\tau_{\text{O-H}\cdot\pi}^{\text{PhOH-Benz}}$. Due to lower degree of freedom, MD-[PhOH]_{Benz}^{frozen} yielded the upper limit of $\tau_{\text{O-H}\cdot\pi}^{\text{PhOH-Benz}}$ to be 9.2 ps (not shown here), whereas MD-[PhOH]_{Benz}^{free} predicted the lower limit to be 3.1 ps. The values are in reasonable agreement with the 2D-IR vibrational echo spectroscopy of 8 ps (Kwak et al., 2006).

It should be noted that, the present MD simulations estimated $\tau_{\text{O-H}\cdot\pi}^{\text{PhOH-Benz}}$ directly from the vibrational frequencies of the O-H $\cdot\pi$ H-bond, whereas the 2D-IR vibrational echo experiment (Kwak et al., 2006) compared the O-H stretching frequencies in the free PhOH with those in the PhOH-Benz 1 : 1 complex. Although efficient coupling of the O-H stretching with the low-frequency O-H $\cdot\pi$ H-bond vibrations could be presumed, the excited O-H stretching could live longer than 4 ps (Hartland et al., 1992). It should also be augmented that, MD-[PhOH]_{Benz}^{free} was based on pair-wise additive intermolecular potentials, in which many-body contributions were not taken into account. The inclusion of the cooperative effects should lead to more associated PhOH-Benz 1 : 1 complex and longer $\tau_{\text{O-H}\cdot\pi}^{\text{PhOH-Benz}}$. Therefore, the discrepancy between MD-[PhOH]_{Benz}^{free} and the 2D-IR vibrational echo experiment is reasonable and explainable.

MD-[(PhOH)₂]_{Benz}

In order to distinguish H-bonds in [(PhOH)₂]_{Benz}, the oxygen atoms were numbered as follow:



Since the O1-H..O2 H-bond was fixed in MD-[(PhOH)₂]_{Benz}^{frozen}, only the O2-H group could act as proton donor towards the π -electron cloud of Benz. Structural and energetic results obtained from MD-[(PhOH)₂]_{Benz}^{frozen} demonstrated that, the solvent cages in [(PhOH)₂]_{Benz} are stronger and more complicated than in [PhOH]_{Benz}. The π -PD maps in Figures 3.11a) to 3.11d), show well-defined solvent structures in the vicinities of (PhOH)₂, especially in Figures 3.11a) and 3.11b). The preferential solvation positions are labeled with **A** to **E**. It is obvious that, Benz molecules prefer to stay at the O2-H group, with the highest probability at **A** ($Z = -2.0 - 1.0 \text{ \AA}$) in Figure 3.11c) and $\langle \Delta E_{\text{Benz}}^{\text{PB-BB-PD}} \rangle_{\text{min}}$ in Table 3.5 of $-86.5 \text{ kJ mol}^{-1}$. It appeared that, the C-H.. π H-bonds between PhOH and Benz become stronger upon dimer formation. They are labeled with **B**, **C** and **D** on the π -PD maps. The PB-PD and PB-BB-PD maps in Figure 3.11b) show a larger and more well-defined energy channel in [(PhOH)₂]_{Benz}, compared to [PhOH]_{Benz}. Therefore, a possibility for the solvent exchange within the first solvation shell of frozen (PhOH)₂ could be anticipated at **E**, **D** and **C**. In [(PhOH)₂]_{Benz}, the preferential solvation order according to $\langle P^{\pi\text{-PD}} \rangle_{\text{max}}$

and the average interaction energy orders based on the absolute values of $\langle \Delta E_{\text{Benz}}^{\text{PB-PD}} \rangle_{\text{min}}$, $\langle \Delta E_{\text{Benz}}^{\text{BB-PD}} \rangle_{\text{min}}$ and $\langle \Delta E_{\text{Benz}}^{\text{PB-BB-PD}} \rangle_{\text{min}}$ in Table 3.5 can be written as:

$$\begin{aligned} \langle P^{\pi\text{-PD}} \rangle_{\text{max}} : & \quad \mathbf{A} > \mathbf{C} > \mathbf{D} > \mathbf{E} > \mathbf{B} \\ \langle \Delta E_{\text{Benz}}^{\text{PB-PD}} \rangle_{\text{min}} : & \quad \mathbf{D} > \mathbf{E} \geq \mathbf{B} > \mathbf{A} > \mathbf{C} \\ \langle \Delta E_{\text{Benz}}^{\text{BB-PD}} \rangle_{\text{min}} : & \quad \mathbf{C} > \mathbf{E} > \mathbf{A} > \mathbf{B} > \mathbf{D} \\ \langle \Delta E_{\text{Benz}}^{\text{PB-BB-PD}} \rangle_{\text{min}} : & \quad \mathbf{A} > \mathbf{E} > \mathbf{B} > \mathbf{D} > \mathbf{C}. \end{aligned}$$

The cross section plots in Figures 3.11e) and 3.11f) show high average potential energy barriers for solvent exchanges between the first solvation shell and the outside, up to about 138 kJ mol^{-1} at **A** in Figure 3.11e) (IV). Since the π -PD, PB-PD and PB-BB-PD maps show high-density contours in the vicinity of the O1-H..O2 H-bond, one could anticipate its easy access by Benz molecules, and due to additional entropic effects when $(\text{PhOH})_2$ are free to move, the H-bond dissociation could be expected, as in the cases of $(\text{BA})_2$ (Sagarik and Rode, 2000) and the guanidinium-formate ($\text{Gdm}^+\text{-FmO}^-$) complexes in aqueous solutions (Sagarik and Chaiyapongs, 2005).

Table 3.5 The highest probabilities at the labeled contours on the π -PD maps ($\langle P^{\pi\text{-PD}} \rangle_{\text{max}}$) in Figure 3.11, together with the corresponding lowest average interaction energies ($\langle \Delta E_{\text{Benz}}^X \rangle_{\text{min}}$) obtained from MD-[(PhOH)₂]_{Benz}^{frozen}. Energies are in kJ mol⁻¹ and X = PB-PD, BB-PD or PB-BB-PD.

	$\langle P^{\pi\text{-PD}} \rangle_{\text{max}}$	$\langle \Delta E_{\text{Benz}}^{\text{PB-PD}} \rangle_{\text{min}}$	$\langle \Delta E_{\text{Benz}}^{\text{BB-PD}} \rangle_{\text{min}}$	$\langle \Delta E_{\text{Benz}}^{\text{PB-BB-PD}} \rangle_{\text{min}}$
Z = -0.5 – 0.5 Å				
A	0.08	-15.1	-79.9	-94.1
B	0.05	-23.7	-65.4	-79.3
C	0.05	-11.7	-76.2	-79.6
E	0.02	-23.9	-71.3	-93.3
Z = 0.0 – 1.0 Å				
B	0.04	-20.3	-70.2	-89.8
C	0.05	-9.1	-80.0	-82.2
D	0.05	-11.8	-73.2	-84.7
E	0.06	-23.9	-71.4	-91.2
Y = -2.0 – -1.0 Å				
A	0.13	-22.1	-73.1	-86.5
B	0.06	-7.1	-74.9	-80.8
C	0.04	-10.9	-81.6	-81.3
D	0.04	-20.9	-70.8	-86.5
E	0.04	-8.3	-80.3	-84.3
X = -1.0 – 0.0 Å				
A	0.05	-13.7	-74.1	-85.5
B	0.04	-18.0	-74.1	-92.1
C	0.11	-9.1	-75.1	-79.6
D	0.09	-26.7	-67.9	-87.7
E	0.04	-15.2	-78.1	-91.6

Structures and dynamics in $[(\text{PhOH})_2]_{\text{Benz}}$ were examined in MD- $[(\text{PhOH})_2]_{\text{Benz}}^{\text{free}}$, in which both PhOH and all Benz molecules were free to move. Due to weak solute-solute interaction and the thermal energy fluctuation at 298 K, the O1-H..O2 H-bond was dissociated in MD- $[(\text{PhOH})_2]_{\text{Benz}}^{\text{free}}$. $g(R_{\text{O1-O2}})$ in Figure 3.12a) shows three well-defined peaks at $R_{\text{O1-O2}} = 5.7, 8.1$ and 9.4 \AA , and for $g(R_{\pi_{\text{Ph1}}-\pi_{\text{Ph2}}})$, two main peaks are seen at $R_{\pi_{\text{Ph1}}-\pi_{\text{Ph2}}} = 6.5$ and 9.2 \AA . Since the latter is more structured, with two well-defined shoulders at $R_{\pi_{\text{Ph1}}-\pi_{\text{Ph2}}} = 8.1$ and 9.8 \AA , one could conclude that, the majority of $(\text{PhOH})_2$ in MD- $[(\text{PhOH})_2]_{\text{Benz}}^{\text{free}}$ took solvent-separated structures. Comparison of $g(R_{\text{O-H}\dots\pi})$ and $g(R_{\pi_{\text{Ph}}\dots\pi})$ in Figures 3.12b) and 3.12c) with those obtained from MD- $[\text{PhOH}]_{\text{Benz}}^{\text{free}}$ in Figure 3.9a) confirms the dissociation of the O1-H..O2 H-bond and the existence of solvent-separated structures in MD- $[(\text{PhOH})_2]_{\text{Benz}}^{\text{free}}$. Investigation of structures of $(\text{PhOH})_2$ in the course of MD- $[(\text{PhOH})_2]_{\text{Benz}}^{\text{free}}$ revealed four examples of close-contact and solvent-separated structures, with $R_{\pi_{\text{Ph1}}-\pi_{\text{Ph2}}}$ comparable to the positions of the main peaks and shoulders of $g(R_{\pi_{\text{Ph1}}-\pi_{\text{Ph2}}})$. They are shown in Figure 3.12d), and will be used in the discussion of the exchange diagrams in Figures 3.12e) and 3.12f). In structure (I), both PhOH molecules are in close contact, with $R_{\pi_{\text{Ph1}}-\pi_{\text{Ph2}}} = 6.7 \text{ \AA}$. Benz 496 separates both PhOH molecules in structures (II), (III) and (IV), with $R_{\pi_{\text{Ph1}}-\pi_{\text{Ph2}}}$ of 8.1, 9.0 and 9.7 \AA , respectively. Figure 3.12e) shows the distances between the center of mass of Benz 496 ($\pi_{\text{Benz 496}}$) and those of PhOH molecules ($R_{\pi_{\text{Ph1}}-\pi_{\text{Benz 496}}}$ and $R_{\pi_{\text{Ph2}}-\pi_{\text{Benz 496}}}$) as functions of MD simulation time. Instantaneous solvent-separated structures could be

recognized in panels **P1** and **P3**, in which Benz 496 stayed between both PhOH molecules, with comparable $R_{\pi_{\text{Ph1}}-\pi_{\text{Benz496}}}$ and $R_{\pi_{\text{Ph2}}-\pi_{\text{Benz496}}}$. PhOH 2 and PhOH 1 could be temporarily separated from Benz 496 in panel **P2** and **P4**, respectively. Finally, at $t_5 = 43.6$ ps, Benz 496 moved away from PhOH 1, resulting in close-contact structures similar to structure (**I**) in Figure 3.12d). Figure 3.12f) reveals further that, Benz 502 stayed closer to PhOH 2 from $t = 15$ to 33 ps. A similar water separated structure was proposed from experiment, in which the association of $(\text{PhOH})_2$ in water saturated CCl_4 was studied (Badger and Greenough, 1961); spectroscopic evidence revealed that, the hydrogen atoms of water are not involved in H-bond and it was presumed that, the dimer owes its stability to weak interaction between the hydrogen atoms of the O-H groups of both PhOH molecules and the oxygen atom of water. The so called “hemihydrate dimer” was used to describe this dimer.

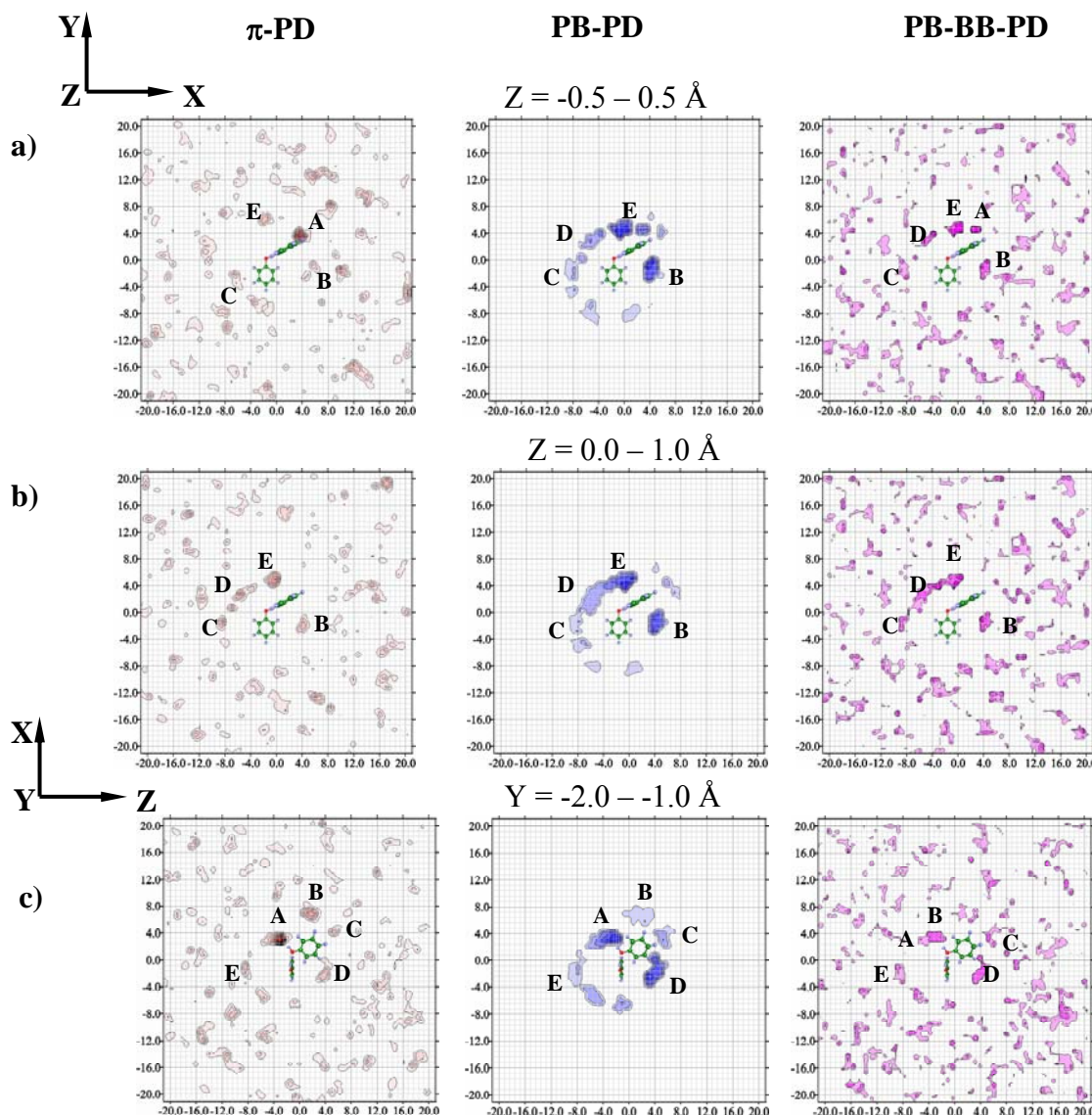


Figure 3.11 Structural and energetic results obtained from MD- $[(\text{PhOH})_2]_{\text{Benz}}^{\text{frozen}}$. X-,

Y- and Z-axes are in Å, energies in kJ mol^{-1} . a) – d) The π -PD, PB-PD and PB-BB-

PD maps. e) – f) Average potential energy landscapes and the cross section plot

computed from longitudinal and transverse profile lines. _____ PB-BB-PD cross

section plot. - - - - - PB-PD cross section plot. - - - - - BB-PD cross section plot.

π -PD contour: min = 0.0 : max = 0.13: interval = 0.01. PB-PD contour: min = -30.0:

max = -1.0: interval = 4.5. PB-BB-PD contour: min = -99.0: max = -70.0: interval =

7.2.

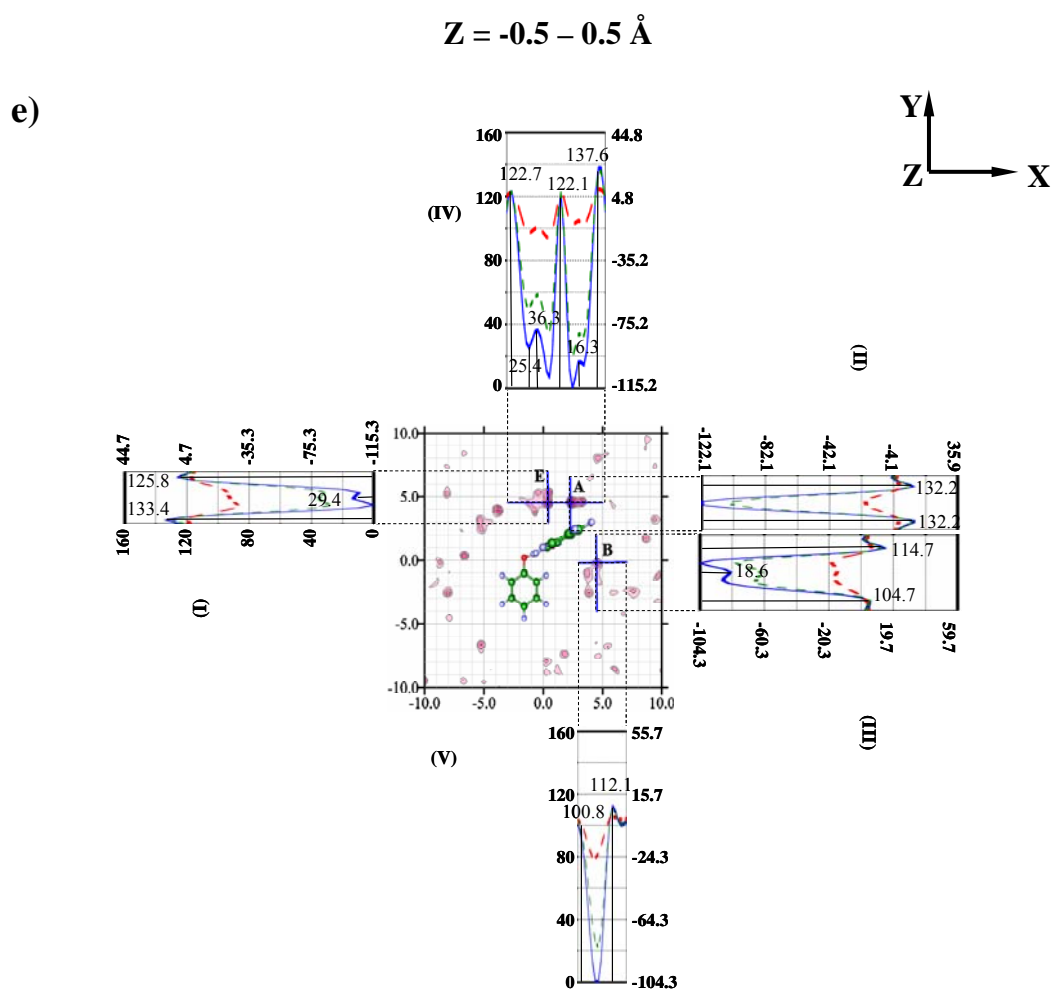
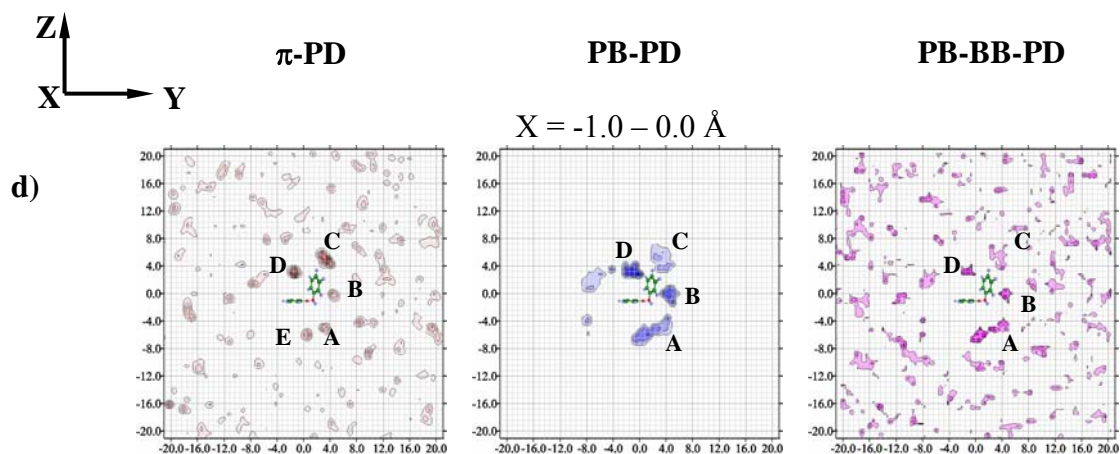


Figure 3.11 (Continued).

f)

$$Y = -2.0 \text{ -- } -1.0 \text{ \AA}$$

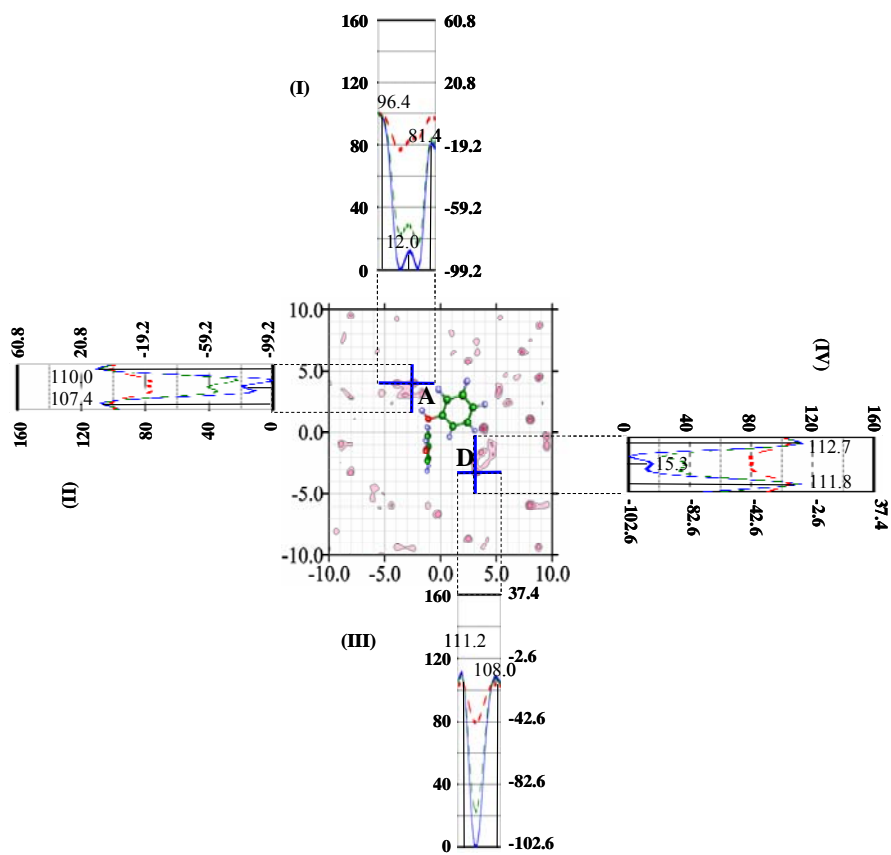


Figure 3.11 (Continued).

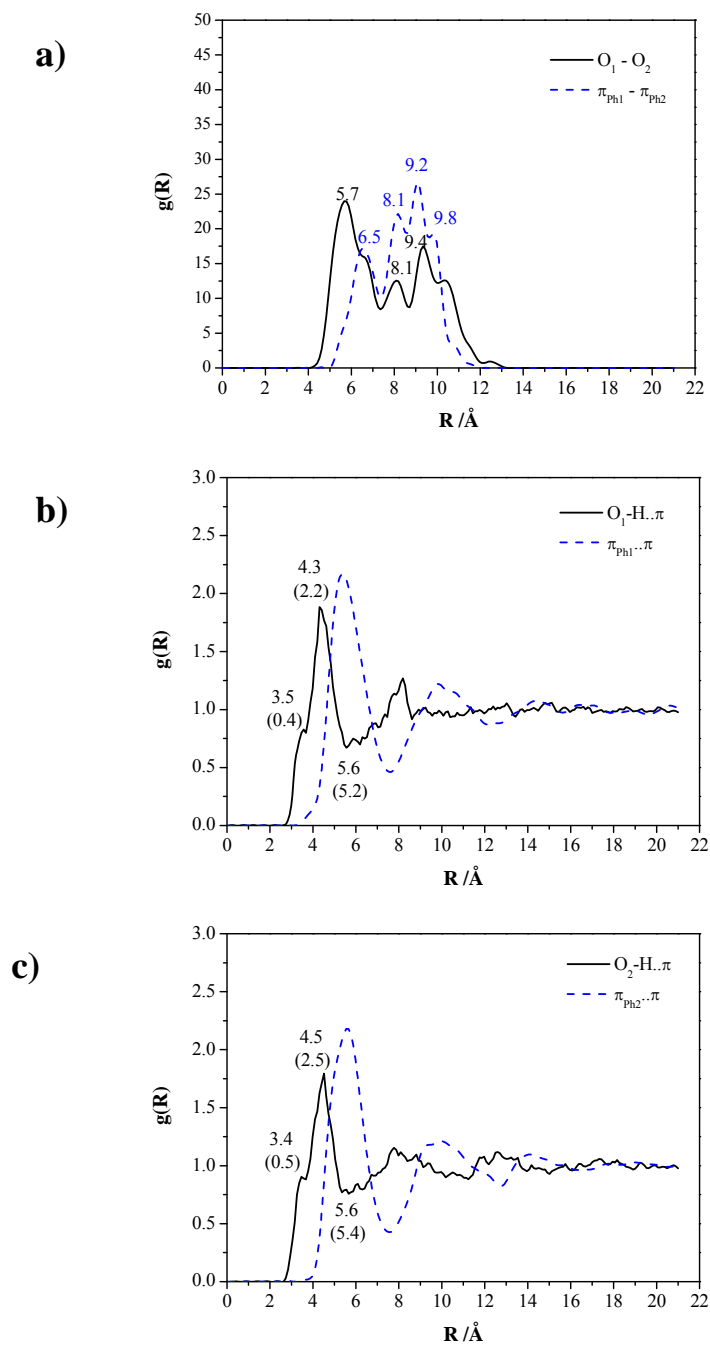


Figure 3.12 Structural and dynamic results obtained from MD- $[(\text{PhOH})_2]_{\text{Benz}}^{\text{free}}$. a) – c) $g(R)$; characteristic distances given with $n(R)$ in parentheses. d) Snapshots of the PhOH-Benz clusters in $[(\text{PhOH})_2]_{\text{Benz}}$. e) – f) Example of H-bond exchange diagram.

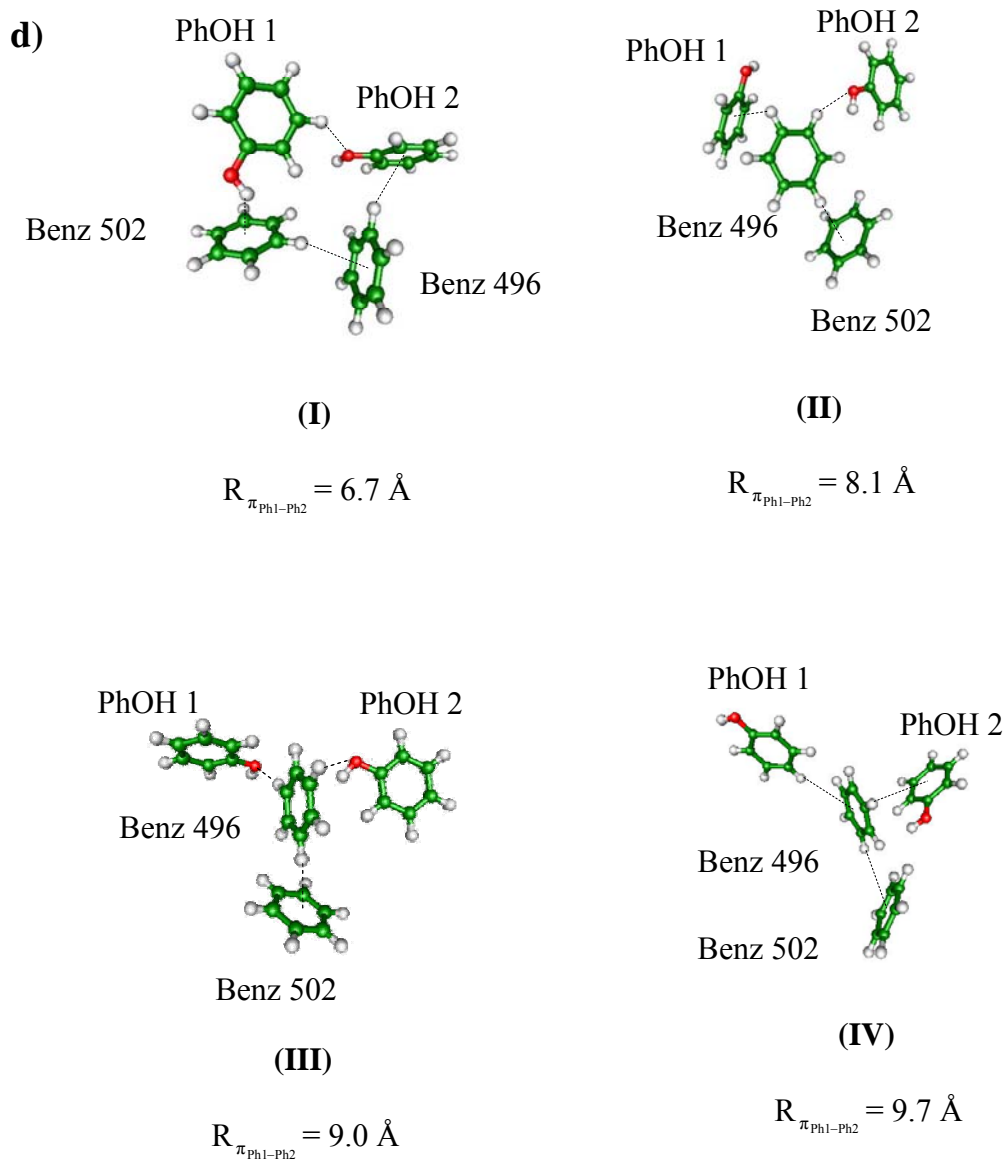


Figure 3.12 (Continued).

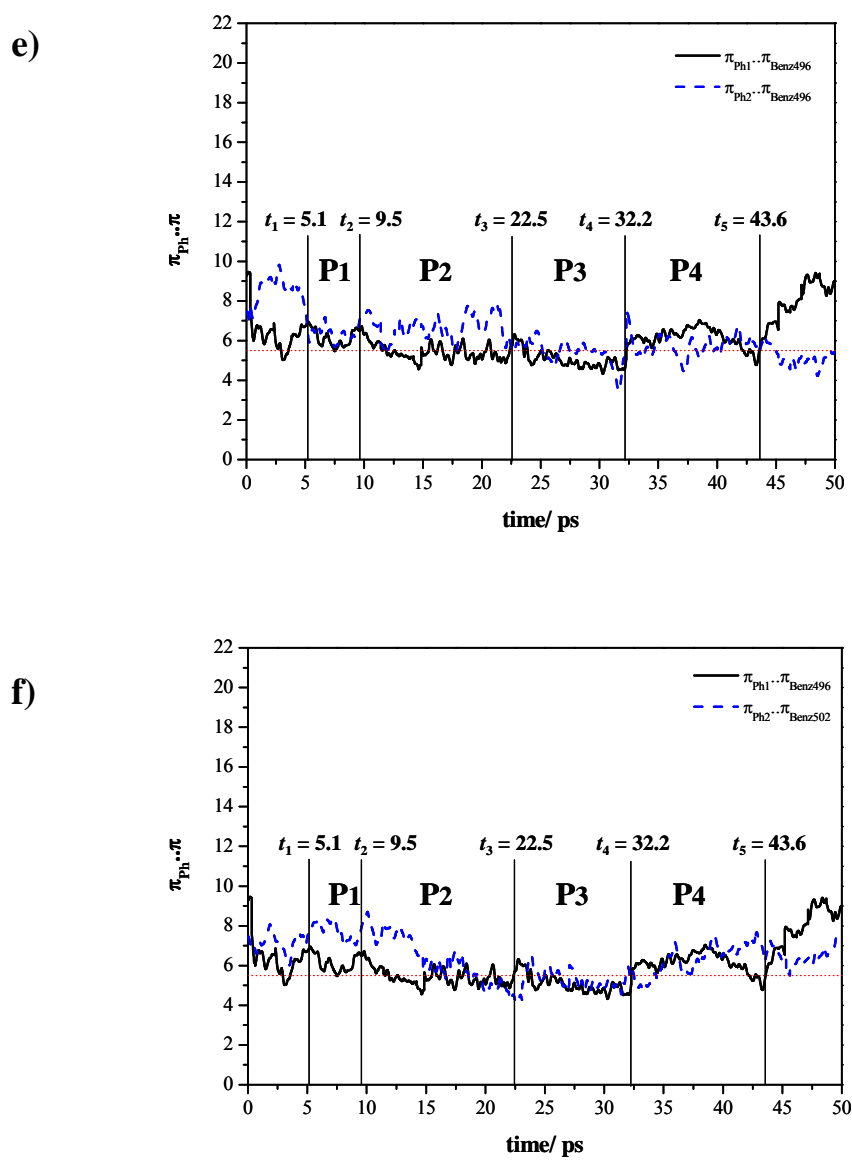
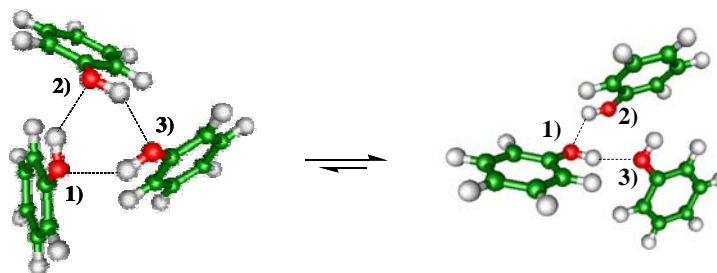


Figure 3.12 (Continued).

MD-[(PhOH)₃]_{Benz}

Structures and dynamics of (PhOH)₃ in Benz solution are discussed based on MD-[(PhOH)₃]_{Benz}^{free}. It turned out that, the cyclic O-H..O H-bonds, similar to the water trimer, could be partially opened in the course of MD-[(PhOH)₃]_{Benz}^{free}, as follow:



This is evident from $g(R_{O..O})$ in Figure 3.13a); $g(R_{O_1..O_2})$ and $g(R_{O_1..O_3})$ are quite similar, with the main peak positions at the average O-H..O H-bond distance of 2.8 Å (Sagarik and Asawakun, 1997), whereas $g(R_{O_2..O_3})$ possesses different structure, a broad peak with maximum at 4 Å. In Figures 3.13b) and 3.13c), similar trends were observed for $g(R_{O_1..π_{Ph2}})$, $g(R_{O_1..π_{Ph3}})$ and $g(R_{O_2..π_{Ph3}})$, as well as for $g(R_{π_{Ph1}..π_{Ph2}})$, $g(R_{π_{Ph1}..π_{Ph3}})$ and $g(R_{π_{Ph2}..π_{Ph3}})$, respectively. Although the average structure was not as compact as in the gas phase, one could conclude that, (PhOH)₃ formed H-bond clusters in MD-[(PhOH)₃]_{Benz}^{free}. Comparison of the solute structures in the course of MD-[(PhOH)₂]_{Benz}^{free} and MD-[(PhOH)₃]_{Benz}^{free} revealed that, the O-H..O H-bonds in (PhOH)₃ are more sterically hindered by the three PhOH molecules, therefore not easily accessible by Benz molecules. Similar steric effects were observed in our

previous MD- $[(BA)_2]_{Benz}^{free}$ in Sagarik, Chaiwongwattana, and Sisot, (2004), in which cyclic H-bonds in $(BA)_2$ were sterically hindered from Benz molecules, but could be partially opened by small polar molecule such as water.

As mentioned earlier that, molecular associations of aromatic compounds in non-aqueous solvents, such as Benz and CCl_4 , represent classical problems in the area of molecular associations, in which partition experiments and various spectroscopic methods have been generally employed in the investigations. For some H-bonded solutes, the associated forms are sufficiently stable to be detected easily in experiments. However, for PhOH, there have been disagreements as to the most important species in solutions. The majority of the partition experiments seem to point to the existence of the PhOH- $(PhOH)_3$ equilibrium in CCl_4 , whereas several spectroscopic results were interpreted in terms of the PhOH- $(PhOH)_2$ equilibrium. At infinite dilution and within ps time scale, the present MD simulations seem to favor instantaneous solvent-separated structures in $[(PhOH)_2]_{Benz}$ and H-bond clusters in $[(PhOH)_3]_{Benz}$. Since it is well accepted that, different experiments could lead to different results, and the advancement of femtosecond laser technology has allowed experiments to probe instantaneous molecular structures and dynamics in weakly associated systems in smaller time scales, it seems unrealistic to rule out possibilities of finding various forms of dimers and trimers, as well as larger clusters in Benz or CCl_4 solutions. More generally, we anticipate that, no single associated form could be representative in solutions, except in very restricted experimental conditions, such as temperature, concentration and time scale.

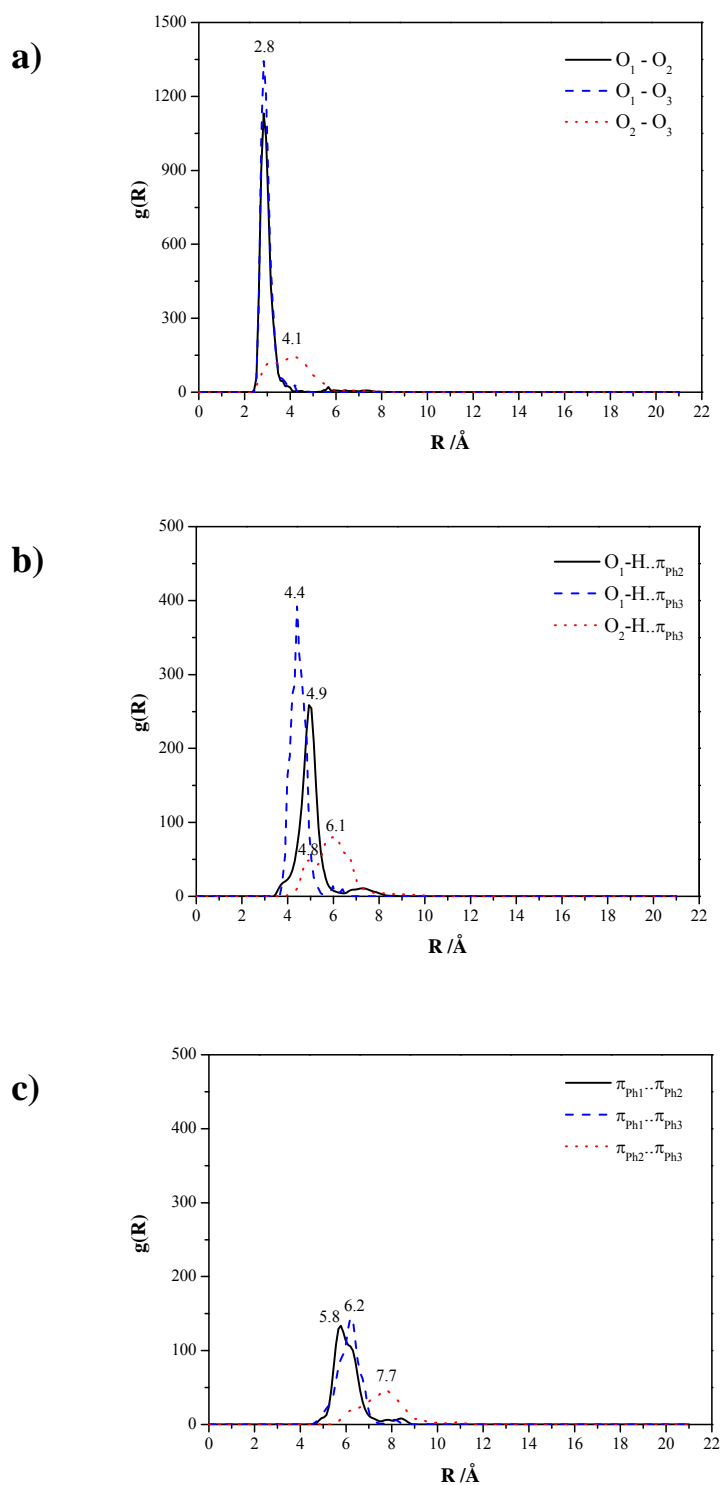


Figure 3.13 $g(R)$ obtained from MD- $[(\text{PhOH})_3]_{\text{Benz}}^{\text{free}}$, together with characteristic distances.

CHAPTER IV

CONCLUSIONS

In the present thesis, the interplay between H-bond and π - π interactions in non-aqueous environment was theoretically studied using two aromatic systems. In the first system, structures and stabilities of cyclic H-bonds in Benz solutions were examined using $(BA)_2$ and the BA-H₂O m : n complexes, m and n = 1 - 2, whereas in the second system, the effects of weak C-H.. π , O-H.. π H-bond and π .. π interactions on structures, energetic and dynamics of $(PhOH)_n$, n = 1 - 3, in Benz solutions were studied.

For BA systems, a series of MD simulations were conducted on $[(BA)_2]_{Benz}^{T=X}$, as well as $[m:n]_{Benz}^{T=X}$ with m and n = 1 - 2, and X = 280 and 298 K. Since the solute-solvent and solvent-solvent interactions are quite moderate in $[m:n]_{Benz}^{T=X}$, the solvation shells around the solute clusters are weak and mobile, especially at room temperature. This allows the thermal energy and the structure of the solvation shells to play important roles in determining the structures and stability of the BA-H₂O clusters. The MD results also revealed that, due to the solvent effects, some microhydrates not particularly associated in the gas phase appeared with long lifetime in the course of MD simulations. This reflects the impact of weak but complicated solute-solvent and solvent-solvent interactions, such as C-H.. π , O-H.. π and π - π interactions, on structures and stability of the H-bond clusters. This seems to be in accordance with

the experimental observations that, if the solute-solvent interactions are much greater than those of the solvent-solvent, then the latter may be ignored.

The MD results showed two types of the H-bond exchange in BA systems namely, the mutual and non-mutual ones. Both H-bond exchanges were detected since the dynamic behaviors were taken into account in the present theoretical models. The existence of the H-bond exchanges also implies that, equilibrium static structures obtained from Molecular Mechanics (MM) or *ab initio* geometry optimizations with continuum model are not complete enough to investigate the systems with complicated solute-solvent and solvent-solvent interactions, such as in $[m : n]_{\text{Benz}}^{\text{T-X}}$. The approach adopted in the present thesis is, therefore, appropriate, since the structures of the BA-H₂O complexes were derived in the presence of Benz molecules, and their stability was discussed in terms of probabilities obtained based on the dynamic behaviors of all interacting molecules in the systems.

For PhOH systems, in order to acquire some basic information on equilibrium structures and interaction energies in the gas phase, the PhOH-Benz $m : n$ complexes, m and $n = 1 - 2$, were investigated using the T-model potentials. It appeared that, the H-bond structure, in which the O-H group of PhOH acts as proton donor towards the π -electrons of Benz, represents the absolute minimum energy geometry of the PhOH-Benz 1 : 1 complex. Although the C-H group is not an effective proton donor, various possibilities for the C-H..O and C-H.. π H-bond formations were observed from the T-model results on large PhOH-Benz complexes.

Based on the T-model potentials, a series of NVE-MD simulations was performed on $[(\text{PhOH})_n]_{\text{Benz}}$, $n = 1 - 3$, at 298 K. Insights on the solvent cage structures and energetic were obtained from $[\text{PhOH}]_{\text{Benz}}$ and $[(\text{PhOH})_2]_{\text{Benz}}$. It was

observed from the average three-dimensional structures in $[\text{PhOH}]_{\text{Benz}}$ that, at least three Benz molecules solvate at the O-H group, and PhOH could act both as proton donor and acceptor towards Benz molecules. The average potential energy landscapes and cross section plots obtained from MD simulations indicated that, the size and shape of the average potential energy wells are determined nearly exclusively by the average solvent-solvent interactions, and the average potential energy barriers to solvent exchanges at the O-H group are quite high. Therefore, Benz molecules at the O-H group could form part of quite strong local solvent cage. The interpretation of dynamics of solvent molecules in connection to the average potential energy landscapes is similar to Rabani, Gezelter, and Berne (1997), by which molecular translation in liquid was proposed to occur through jumps between potential energy wells, separated by high-energy barriers.

Investigation on the H-bond exchange diagrams revealed that, Benz molecules at the O-H group could exchange through large-amplitude nuclear motions. These involve the displacement of the O-H... π H-bond and the solvent exchanges seem to favor the associative-interchange scheme; a solvent molecule enters and spends sometime in the first solvation shell before the other leaves. Since the large-amplitude nuclear motions were pointed out to be one of the main reasons for the non-rigidity in aromatic van der Waal clusters and, based on the assumption that, at short time the dynamic equilibrium between the associated and dissociated forms could be studied from characteristic vibrational frequency of H-bond, the lifetimes of the PhOH-Benz 1 : 1 complex were approximated and in reasonable agreement with 2D-IR vibrational echo experiment.

Due to weak interaction and the thermal energy fluctuation at 298 K, the O-H...O H-bond in $(\text{PhOH})_2$ was disrupted in MD simulations. Instantaneous solvent-separated structures, in which a Benz molecule separates both PhOH molecules, were observed in $[(\text{PhOH})_2]_{\text{Benz}}$, whereas cyclic H-bonds in $(\text{PhOH})_3$ were only opened in $[(\text{PhOH})_3]_{\text{Benz}}$. A similar water separated dimer was suggested from experiment, in which spectroscopic evidence revealed that the hemihydrated $(\text{PhOH})_2$ owes its stability to weak interaction between the hydrogen atoms of the O-H groups of both PhOH molecules and the oxygen atom of water. Comparisons of the π -PD maps and the dimer and trimer structures in the course of MD simulations revealed that, the O-H...O H-bonds in $(\text{PhOH})_3$ were quite well protected by the three PhOH molecules, therefore not easily accessible by Benz molecules as in the case of $(\text{PhOH})_2$. This suggested that, the competition between solute-solute and solute-solvent interactions could be studied only when explicit solvent molecules are taken into account in the model calculations.

It should be noted finally that, the MD results reported here were based on pair-wise additive scheme, in which many-body effects were not taken into account. Since the interactions among aromatic compounds are not particularly strong, the inclusion of the cooperative effects in the model calculations should not lead to significant change in structures and stability of the complexes considered here; only slightly more associated complexes with longer association times could be anticipated. For organic and biological systems, weak intermolecular interactions could produce complexes that are short-lived. Although short-lived and cannot be detected easily by conventional experimental techniques, the dissociation and association of such complexes can influence chemical processes, especially reactivity

and mechanisms in biochemical reactions. The author wishes that the MD results reported here could provide additional piece of important information and can attract more attention from theoretician and experimentalist to further investigate these complicated non-aqueous interacting systems, using more advanced theoretical and spectroscopic techniques.

REFERENCES

REFERENCES

- Ahlich, R., Böhm, H. J., Ehrhardt, C., Scharf, P., Schiffer, H., Lischka, H., and Schindler, M. (1985). Implementation of an electronic structure program system on the CYBER 205. **Journal of Computational Chemistry**. 6: 200-208.
- Allen, G., Watkinson, J. G., and Webb, K. H. (1966). An infra-red study of the association of benzoic acid in the vapour phase, and in dilute solution in non-polar solvents. **Spectrochimica Acta**. 22: 807-814.
- Badger, R. M., and Greenough, R. C. (1961). The association of phenol in water saturated carbon tetrachloride solutions. **Journal of Physical Chemistry**. 65: 2088-2090.
- Bartell, L. S., and Dulles, F. J. (1995). Monte carlo study of small benzene clusters. 2. transition from rigid to fluxional forms. **Journal of Physical Chemistry**. 99: 17107-17112.
- Böhm, H. J., and Ahlich, R. (1982). A study of short-range repulsions. **Journal of Chemical Physics**. 77: 2028-2034.
- Böhm, H. J., Ahlich, R., Scharf, P., and Schiffer, H. (1984). Intermolecular potentials for CH₄, CH₃F, CHF₃, CH₃Cl, CH₂Cl₂, CH₃CN and CO₂. **Journal of Chemical Physics**. 81: 1389-1395.
- Borse, G. J. (1997). **Numerical methods with MATLAB: A resources for scientists and engineers**. Boston: PWS Publishing.

- Brutschy, B. (2000). The structure of microsolvated benzene derivatives and the role of aromatic substituents. **Chemical Review**. 100: 3891-3920.
- Case, D. A., Pearlman, D. A., Caldwell, J. W., Cheatham III, T. E., Ross, W. S., Simmerling, C., Darden, T., Merz, K. M., Stanton, R. V., Cheng, A., Vincent, J. J., Crowley, M., Tsui, V., Radmer, R., Duan, Y., Pitera, J., Massova, I., Seibel, G. L., Singh, U. C., Weiner, P., Kollman, P. A. **AMBER 6** (University of California, San Francisco, 1999).
- Chelli, R., Cardini, G., Procacci, P., Righini, R., Califano, S., and Albrecht, A. (2000). Simulated structure, dynamics, and vibrational spectra of liquid benzene. **Journal of Chemical Physics**. 113: 6851-6863.
- Chocholoušová, J., Vacek, J., and Hobza, P. (2003). Acetic acid dimer in the gas phase, nonpolar solvent, microhydrated environment, and dilute and concentrated acetic acid: Ab Initio quantum chemical and molecular dynamics simulations. **Journal of Physical Chemistry A**. 107: 3086-3092.
- Christian, S. D., Affsprung, H. E., and Taylor, S. A. (1963). The role of dissolved water in partition equilibria of carboxylic acids. **Journal of Physical Chemistry**. 67: 187-189.
- Cieplak, P., Pawlowski, W., and Wieckowska, E. (1992). Hydration of benzoic acid in benzene solution. III. Interaction-energy calculations. **Zeitschrift Fur Physikalische Chemie Neue Folge**. 177: 63-74.
- Deeying, N., and Sagarik, K. (2006). Effects of metal ion and solute conformation change on hydration of small amino acid. **Biophysical Chemistry**. 125: 14-33.

- Dymond, J. H., and Smith, E. B. (1980). **The virial coefficients of pure gases and mixtures**, Oxford: Clarendon Press.
- Endo, K. (1926). The molecular association of phenol in benzene and water. **Bulletin of the Chemical Society of Japan**. 1: 25-29.
- Frisch, M. J., Trucks, G. W., Schlegel, H. B., Scuseria, G. E., Robb, M. A., Cheeseman, J. R., Zakrzewski, V. G., Montgomery, J. A., Stratmann, R. E., Burant, J. C., Dapprich, S., Millam, J. M., Daniels, A. D., Kudin, K. N., Strain, M. C., Farkas, O., Tomasi, J., Barone, V., Cossi, M., Cammi, R., Mennucci, B., Pomelli, C., Adamo, C., Clifford, S., Ochterski, J., Petersson, G. A., Ayala, P. Y., Cui, Q., Morokuma, K., Malick, D. K., Rabuck, A. D., Raghavachari, K., Foresman, J. B., Cioslowski, J., Ortiz, J. V., Baboul, A. G., Stefanov, B. B., Lui, G., Liashenko, A., Piskorz, P., Komaromi, I., Gomperts, R., Martin, R. L., Fox, D. J., Keith, T., Al-Laham, M. A., Peng, C. Y., Nanayakkara, A., Gonzalez, C., Challacombe, M., Gill, P. M. W., Johnson, B. G., Chen, W., Wong, M. W., Andres, J. L., Head-Gordon, M., Replogle, E. S., and People, J. A. (2005). **Gaussian 03** package (revision D.1) [Computer software]. Wallingford, CT, USA: Gaussian.
- Finkelstein, I. J., Zheng, J., Ishikawa, H., Kim, S., Kwak, K., and Fayer, M. D. (2007). Probing dynamics of complex molecular systems with ultrafast 2D IR vibrational echo spectroscopy. **Physical Chemistry Chemical Physics**. 9: 1533-1549.
- Fujii, Y., Yamada, H., and Mizuta, M. (1988). Self-association of acetic acid in some organic solvents. **Journal of Physical Chemistry**. 92: 6768-6772.

- Gezelter, J. D., Rabani, E., and Berne, B. J. (1999). Calculation the hopping rate for diffusion in molecular liquids: CS₂. **Journal of Chemical Physics**. 110: 3444-3452.
- Grover, J. R., Walters, E. A., and Hui, E. T. (1987). Dissociation energies of the benzene dimer and dimer cation. **Journal of Physical Chemistry**. 91: 3233-3237.
- Gruenloh, C. J., Florio, G. M., Carney, J. R., Hagemester, F. C., and Zwier, T. S. (1999). C-H stretch modes as a probe of H-bonding in methanol-containing clusters. **Journal of Physical Chemistry A**. 103: 496-502.
- Gruenloh, C. J., Hagemester, F. C., Carney, J. R., and Zwier, T. S. (1999). Resonant ion-dip infrared spectroscopy of ternary benzene-(water)_n(methanol)_m hydrogen-bonded clusters. **Journal of Physical Chemistry A**. 103: 503-513.
- Guedes, R. C., Coutinho, K., Costa Cabral, B. J., Canuto, S., Correia, C. F., Borges dos Santos R. M., and Martinho Simões, J. A. (2003). Solvent effects on the energetics of the phenol O-H bond: differential solvation of phenol and phenoxy radical in benzene and acetonitrile. **Journal of Physical Chemistry A**. 107: 9197-9207.
- Hartland, G. V., Henson, B. F., Venturo, V. A., and Felker, P. M. (1992). Ionization-loss stimulated raman spectroscopy of jet-cooled hydrogen-bonded complexes containing phenols. **Journal of Physical Chemistry**. 96: 1164-1173.

- Hunter, C. A., Singh, J., and Thornton, J. M. (1991). π - π interactions: the geometry and energetics of phenylalanine-phenylalanine interaction in proteins. **Journal of Molecular Biology**. 218: 837-846.
- Jacoby, Ch., Roth, W., Schmitt, M., Janzen, Ch., Spangenberg, D., and Kleinermanns, K. (1998). Intermolecular vibrations of phenol(H₂O)₂₋₅ and phenol(D₂O)₂₋₅ - d₁ studied by UV double-resonance spectroscopy and ab initio theory. **Journal of Physical Chemistry A**. 102: 4471-4480.
- Kearley, G. J., Johnson, M. R., and Tomkinson, J. (2006). Intermolecular interactions in solid benzene. **Journal of Chemical Physics**. 124: 044514-044519.
- Knee, J. L., Khundkar, L. R., and Zewail, A. H. (1987). Picosecond photofragment spectroscopy. III. vibrational predissociation of van der Waals' clusters. **Journal of Chemical Physics**. 87: 115-127.
- Kwac, K., Lee, C., Jung, Y., Han, J., Kwak, K., Zheng, J., Fayer, M. D., and Cho, M. (2006). Phenol-benzene complexation dynamics: quantum chemistry calculation, molecular dynamics simulations, and two dimensional IR spectroscopy. **Journal of Chemical Physics**. 125: 244508-244516.
- Kwak, K., Zheng, J., Cang, H., and Fayer, M. D. (2006). Ultrafast two-dimensional infrared vibrational echo chemical exchange experiments and theory. **Journal of Physical Chemistry B**. 110: 19998-20013.
- Langford, C. H., and Gray, H. B. (1996). **Ligand Substitution Processes**. New York: W. A. Benjamin.
- Lassette, E. N., and Dickinson, R. G. (1939). A comparative method of measuring vapor pressure lowering with application to solution of phenol in benzene. **Journal of the American Chemical Society**. 61: 54-57.

- Lipert, R. J., and Colson, S. D. (1988). Study of phenol-water complexes using frequency- and time-resolved pump-probe photoionization. **Journal of Chemical Physics**. 89: 4579-4585.
- Magro, A., Frezzato, D., Polimeno, A., Moro, G. J., Chelli, R., and Righini, R. (2005). Dynamics of liquid benzene: a cage analysis. **Journal of Chemical Physics**. 123: 124511-124517.
- Meijer, G., de Vries, M. S., Hunziker, H. E., and Wendt, H. R. (1990). Laser desorption jet-cooling spectroscopy of para-amino benzoic acid monomer, dimer, and clusters. **Journal of Chemical Physics**. 92: 7625-7635.
- Meyer, E. A., Castellano, R. K., and Diederich, F. (2003). Interactions with aromatic rings in chemical and biological recognition. **Angewandte Chemie. International edition in English**. 42: 1210-1250.
- Mikami, N. (1995). Spectroscopic study of intracuster proton transfer in small size hydrogen-bonding clusters of phenol. **Bulletin of the Chemical Society of Japan**. 68: 683-695.
- Neumann, M., Brougham, D. F., McGloin, C. J., Johnson, M. R., Horsewill, A. J., Trommsdorff, H. P. (1998). Proton tunneling in benzoic acid crystals at intermediate temperatures: nuclear magnetic resonance and neutron scattering studies. **Journal of Chemical Physics**. 109: 7300-7311.
- Ohashi, K., Inokuchi, Y., and Nishi, N. (1996). Photodissociation spectroscopy of phenol dimer ion. lack of resonance interaction between the aromatic rings. **Chemical Physics Letters**. 257: 137-142.

- Olkawa, A., Abe, H., Mikami, N., and Ito, M. (1983). Solvated phenol studied by supersonic jet spectroscopy. **Journal of Physical Chemistry.** 87: 5083-5090.
- Parthasarathi, R., Subramanian, V., and Sathyamurthy, N. (2005). Hydrogen bonding in phenol, water, and phenol-water clusters. **Journal of Physical Chemistry A.** 109: 843-850.
- Perutz, M. F. (1993). The role of aromatic rings as hydrogen-bond acceptors in molecular recognition. **Philosophical Transactions of the Royal Society: Physical and Engineering Sciences.** 345: 105-112.
- Philbrick, F. A. (1934). The association of phenol in different solvents. **Journal of the American Chemical Society.** 56: 2581-2585.
- Rabani, E., Gezelter, J. D., and Berne, B. J. (1997). Calculating the hopping rate for self-diffusion on rough potential energy surfaces: cage correlations. **Journal of Chemical Physics.** 107: 6867-6876.
- Refson, K. (1996). **Moldy** (revision 2.20 for release 2.14) [Computer software]. Oxford UK: Department of Earth Science, Oxford University.
- Ricci, M., Bartolini, P., Chelli, R., Cardini, G., Califano, S., and Righini, R. (2001). The fast dynamics of benzene in the liquid phase part I. optical kerr effect experimental investigation. **Physical Chemistry Chemical Physics.** 3: 2795-2802.
- Rode, B. M., Schwenk, C. F., Hofer, T. S., and Randolph, B. R. (2005). Coordination and ligand exchange dynamics of solvated metal ions. **Coordination Chemistry Reviews.** 249: 2993-3006.

- Roth, W., Schmitt, M., Jacoby, Ch., Spangenberg, D., Janzen, Ch., and Kleinermanns, K., (1998). Double resonance spectroscopy of phenol(H_2O)₁₋₁₂: evidence for ice-like structures in aromate-water clusters?. **Chemical Physics**. 239: 1-9.
- Sagarik, K. P., Pongpituk, V., Chaiyapongs, S., and Sisot, P. (1991). Test-particle model potentials for hydrogen-bonded complexes: complexes formed from HCN, HF, H_2O , NH_3 , HCONH_2 , HCONHCH_3 , guanine and cytosine. **Chemical Physics**. 156: 439-456.
- Sagarik, K. P., and Spohr, E. (1995). Statistical mechanical simulations on properties of liquid pyridine. **Chemical Physic**. 199: 73-82.
- Sagarik, K., and Asawakun, P. (1997). Intermolecular potential for phenol based on the test particle model. **Chemical Physics**. 219: 173-191.
- Sagarik, K., and Chaiyapongs, S. (2005). Structures and stability of salt-bridge in aqueous solution. **Biophysical Chemistry**. 117: 18-39.
- Sagarik, K., and Dokmaisrijan, S. (2005). A theoretical study on hydration of alanine zwitterions. **Journal of Molecular Structure (THEOCHEM)**. 718: 31-47.
- Sagarik, K., and Rode, B. M. (2000). Intermolecular potential for benzoic acid-water based on the test-particle model and statistical mechanical simulations of benzoic acid in aqueous solutions. **Chemical Physics**. 260: 159-182.
- Sagarik, K., Chaiwongwattana, S., and Sisot, P. (2004). A theoretical study of benzoic acid-water in benzene solutions. **Chemical Physics**. 306: 1-12.
- Saunders, M., and Hyne, J. B. (1958). Study of hydrogen bonding in systems of hydroxylic compounds in carbon tetrachloride through the use of NMR. **Journal of Chemical Physics**. 29: 1319-1323.

- Sawamura, T., Fujii, A., Sato, S., Ebata, T., and Mikami, N. (1996). Characterization of the hydrogen-bonded cluster ions [phenol-(H₂O)_n]⁺ ($n = 1-4$), (Phenol)₂⁺, and (Phenol-Methanol)⁺ as studied by trapped ion infrared multiphoton dissociation spectroscopy of their OH stretching vibrations. **Journal of Physical Chemistry**. 100: 8131-8138.
- Schlegel, H. B. (1982). Optimization of equilibrium geometries and transition structures. **Journal of Computational Chemistry**. 3: 214-218.
- Shamsul Huq, A. K. M., and Lodhi, S. A. K. (1966). Distribution of benzoic acid between benzene and water and dimerization of benzoic acid in benzene. **Journal of Physical Chemistry**. 70: 1354-1358.
- Sinnokrot, M. O., Valeev, E. F., and Sherrill, C. D. (2002). Estimates of the ab initio limit for π - π interactions: The benzene dimer. **Journal of the American Chemical Society**. 124: 10887- 10893.
- Sinnokrot, M. O., and Sherrill, C. D. (2004). Substituent effects in π - π interactions: sandwich and T-shaped configurations. **Journal of the American Chemical Society**. 126: 7690-7697.
- Sun, S., and Bernstein, E. R. (1996). Aromatic van der Waals cluster: structure and nonrigidity. **Journal of Physical Chemistry**. 100: 13348-13366.
- SURFER** for windows (version. 6.04) [Computer software]. (1997). USA: Golden Software.
- Van Duyne, R., Taylor, S. A., Christian, S. D., and Affsprung, H. E. (1967). Self-association and hydration of benzoic acid in benzene. **Journal of Physical Chemistry**. 71: 3427-3430.

- Van Holde, K. E., Johnson, W. C., and Ho, P. S. (1998). **Principles of Physical Biochemistry**. New Jersey: Prentice Hall.
- Wall, F. T. (1942). Distribution of benzoic acid between water and benzene. **Journal of the American Chemical Society**. 64: 472-473.
- Wall, F. T., and Rouse Jr., P. E. (1941). Association of benzoic acid in benzene. **Journal of the American Chemical Society**. 63: 3002-3005.
- Young, D. C. (2001). **Computational Chemistry: A practical guide for applying techniques to real-world problems**. New York: Wiley Interscience.
- Zaugg, N. S., Steed, S. P., and Woolley, E. M. (1972). Intermolecular hydrogen bonding of acetic acid in carbon tetrachloride and benzene. **Thermochimica Acta**. 3: 349-354.
- Zheng, J., Kwak, K., Asbury, J., Chen, X., Piletic, I. R., and Fayer, M. D. (2005). Ultrafast dynamics of solute-solvent complexation observed at thermal equilibrium in real time. **Science**. 309: 1338-1343.
- Zheng, J., Kwak, K., Chen, X., Asbury, J. B., and Fayer, M. D. (2006). Formation and dissociation of intra-intermolecular hydrogen-bonded solute-solvent complexes: chemical exchange two-dimensional infrared vibrational echo spectroscopy. **Journal of the American Chemical Society**. 128: 2977-2987.
- Zheng, J., Kwak, K., and Fayer, M. D. (2007). Ultrafast 2D IR vibrational echo spectroscopy. **Accounts of Chemical Research**. 40: 75-83.

APPENDICES

APPENDIX A
THE T-MODEL PARAMETERS

Table A.1 T-model parameters for Benzene (Sagarik, Chaiwongwattana, and Sisot, 2004) and Benzoic acid (Sagarik and Rode, 2000). Values are in atomic units.

Molecule	Atom	σ_i	ρ_i	q_i
Benz				
	C	1.170780	0.291419	-0.092300
	H	0.166423	0.251114	0.092300
BA				
	O1	1.138607	0.236810	-0.548532
	O2	1.129559	0.245188	-0.465275
	C1	0.529477	0.396220	0.519581
	C2	1.342103	0.214636	0.100950
	C3	1.120595	0.307058	-0.180925
	C4	1.245962	0.261224	-0.017924
	C5	0.929315	0.367166	-0.124305
	C6	1.329701	0.234160	-0.038697
	C7	1.028291	0.337961	-0.164809
	H1	-0.243465	0.288071	0.409564
	H2	0.029207	0.270760	0.118136
	H3	0.081551	0.269920	0.083979
	H4	0.179658	0.228821	0.097361
	H5	0.048919	0.283433	0.086936
	H6	0.029352	0.265465	0.123960

Table A.2 T-model parameters for PhOH (Sagarik and Asawakun , 1997) and water (Sagarik and Rode, 2000). Values are in atomic units.

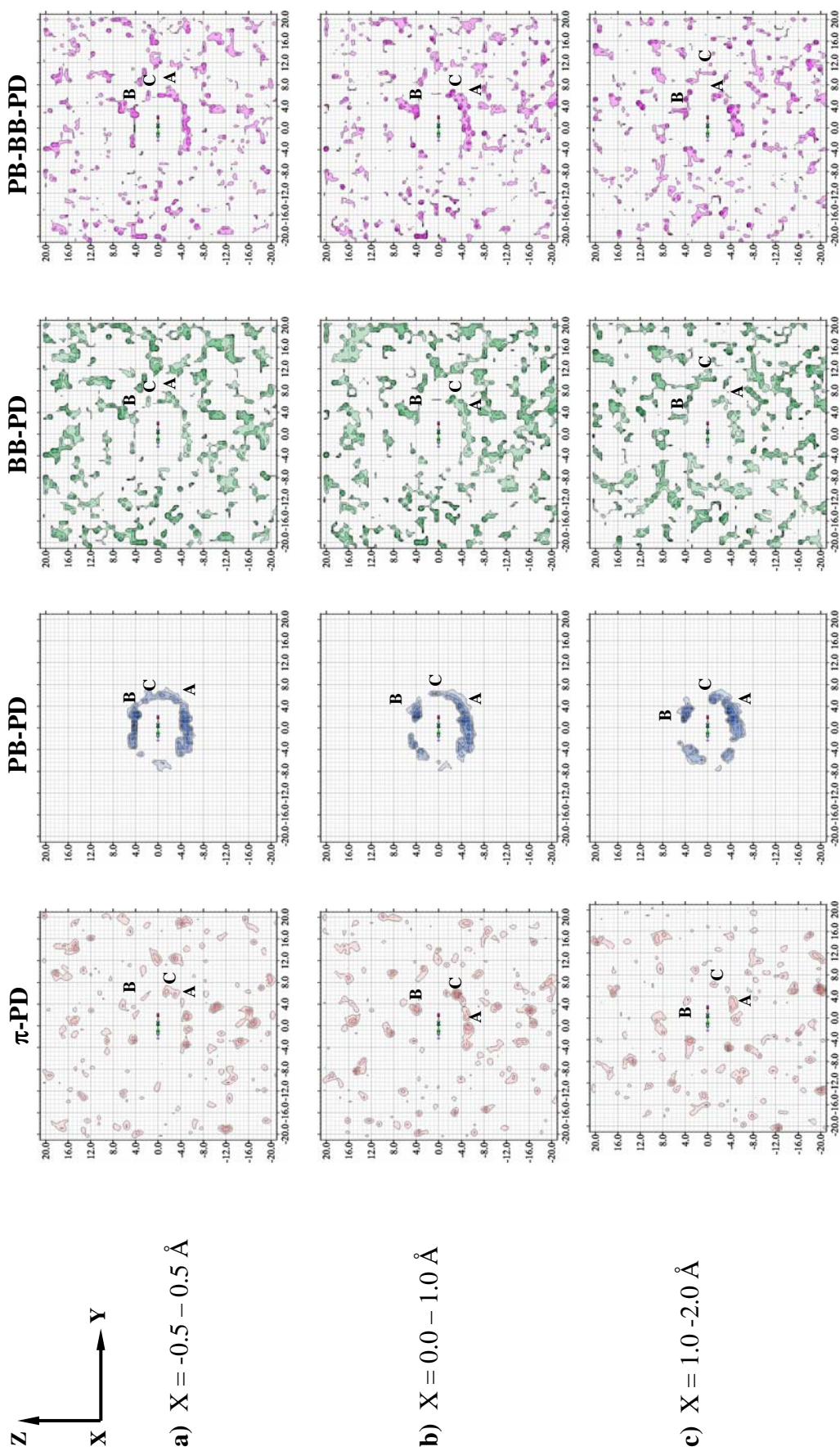
Molecule	Atom	σ_i	ρ_i	q_i
PhOH				
	O	1.122591	0.234594	-0.667863
	C1	1.201071	0.277213	-0.202844
	C2	1.276142	0.236488	-0.053883
	C3	1.091620	0.358983	-0.504382
	C4	1.278229	0.172507	0.602824
	C5	1.189580	0.295535	-0.352276
	C6	1.053884	0.339821	-0.171089
	H1	-0.067537	0.331718	0.138852
	H2	-0.013779	0.303927	0.165180
	H3	0.040251	0.262547	0.199031
	H4	-0.177958	0.267606	0.452293
	H5	0.017042	0.278423	0.205855
	H6	-0.004693	0.284322	0.188302
H₂O				
	O	1.284091	0.200370	-0.451660
	H	-0.318644	0.311849	0.514110
	D			-0.576560

Note D is a dummy charge on the C2 axis of H₂O, 0.26 Å from oxygen and in the opposite direction of the lone pair.

APPENDIX B

SUPPLEMENTARY RESULTS

FOR MD SIMULATIONS OF [PhOH]_{Benz}



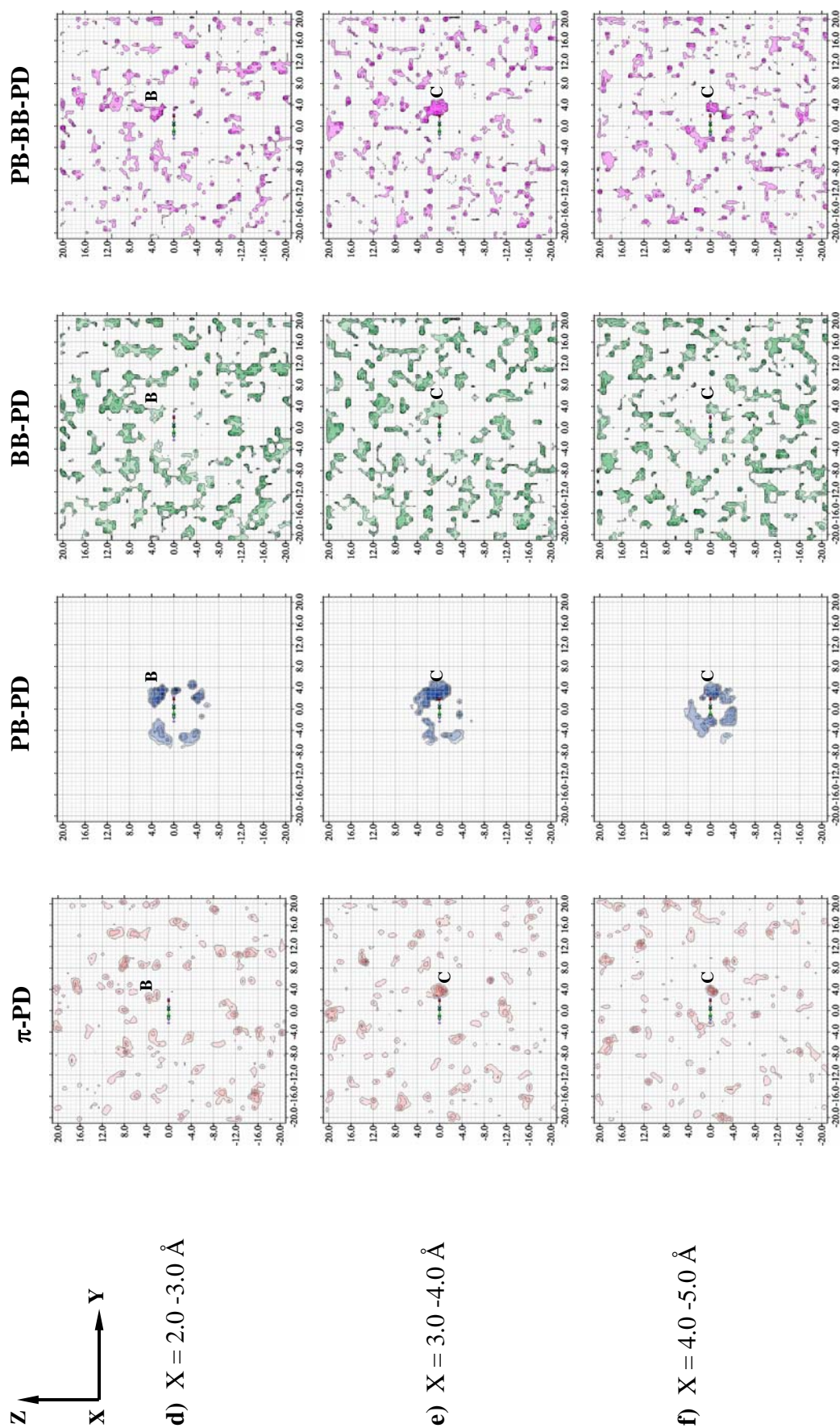


Figure B.1 (Continued).

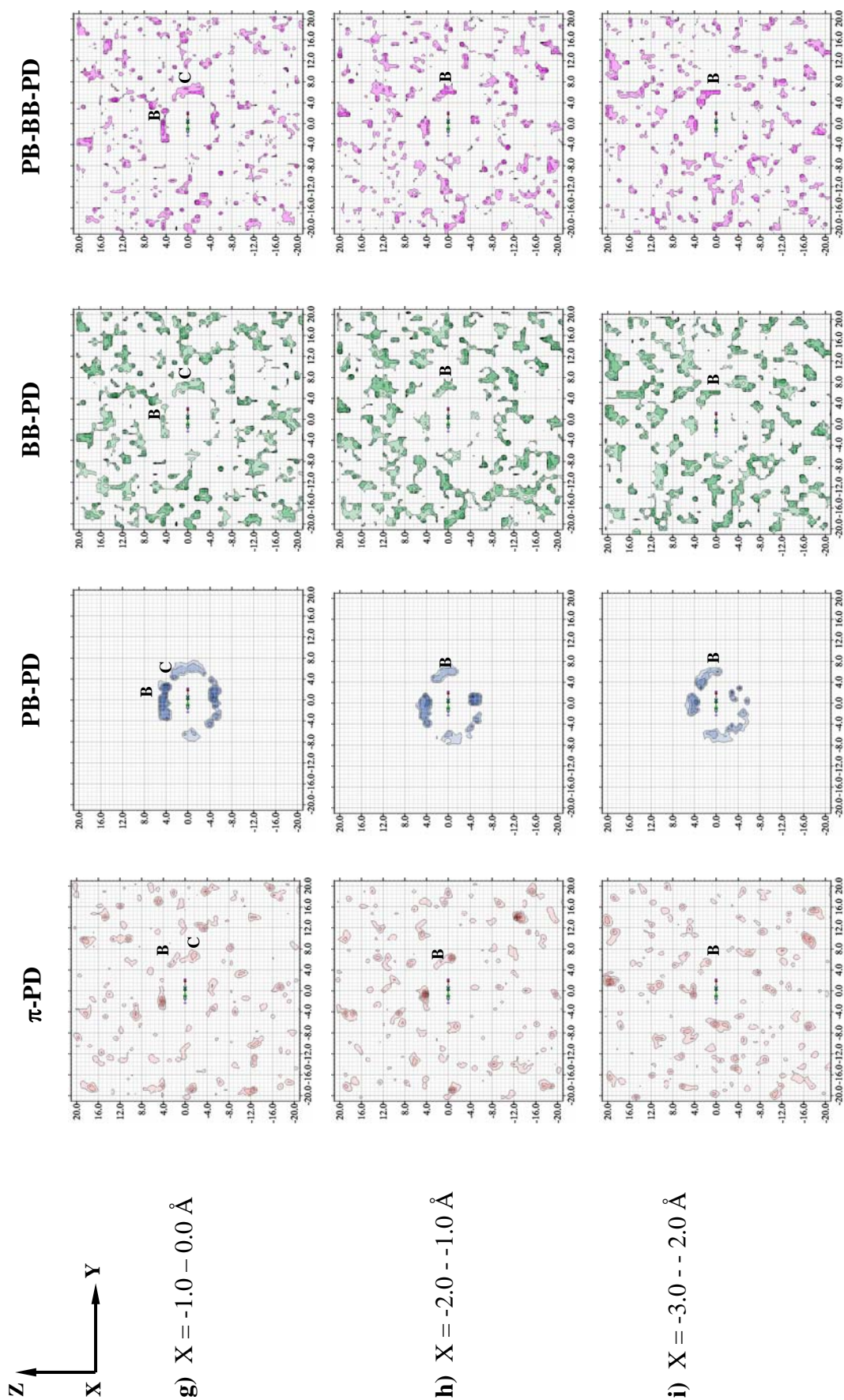
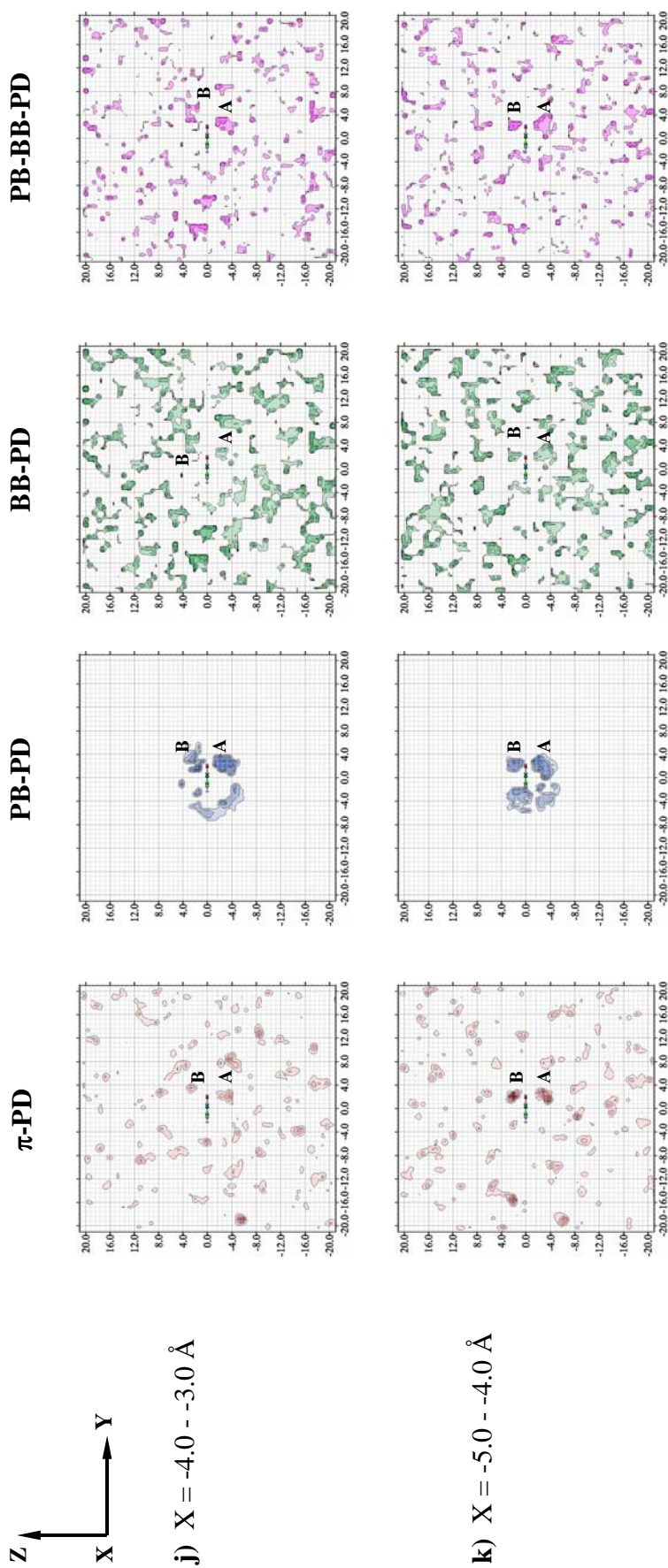


Figure B.1 (Continued).


Figure B.1 (Continued).

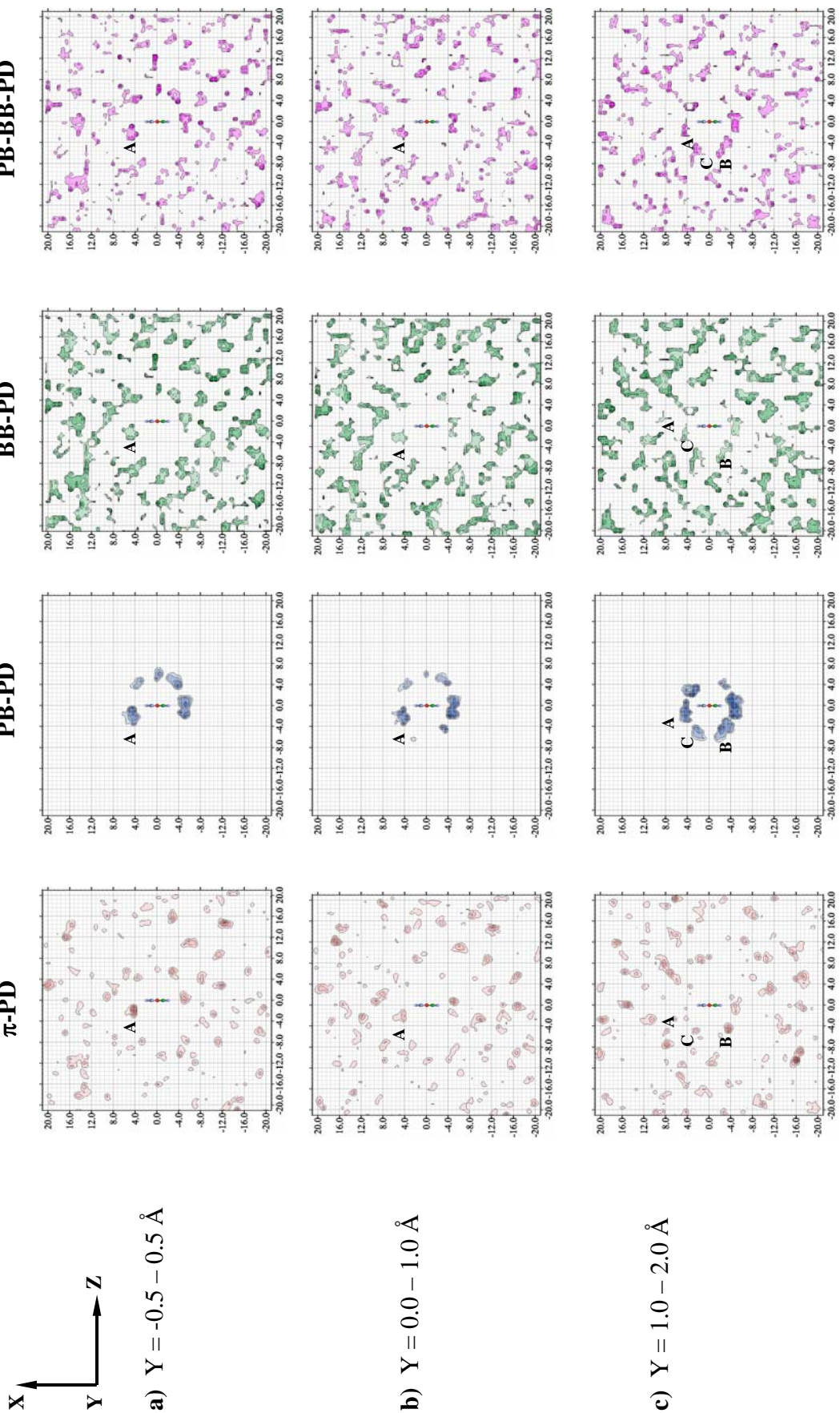


Figure B.2 The π -PD, PB-PD, BB-PD and PB-BB-PD maps with respect to reference plane **III** obtained from MD-[PhOH]_{Benz}.

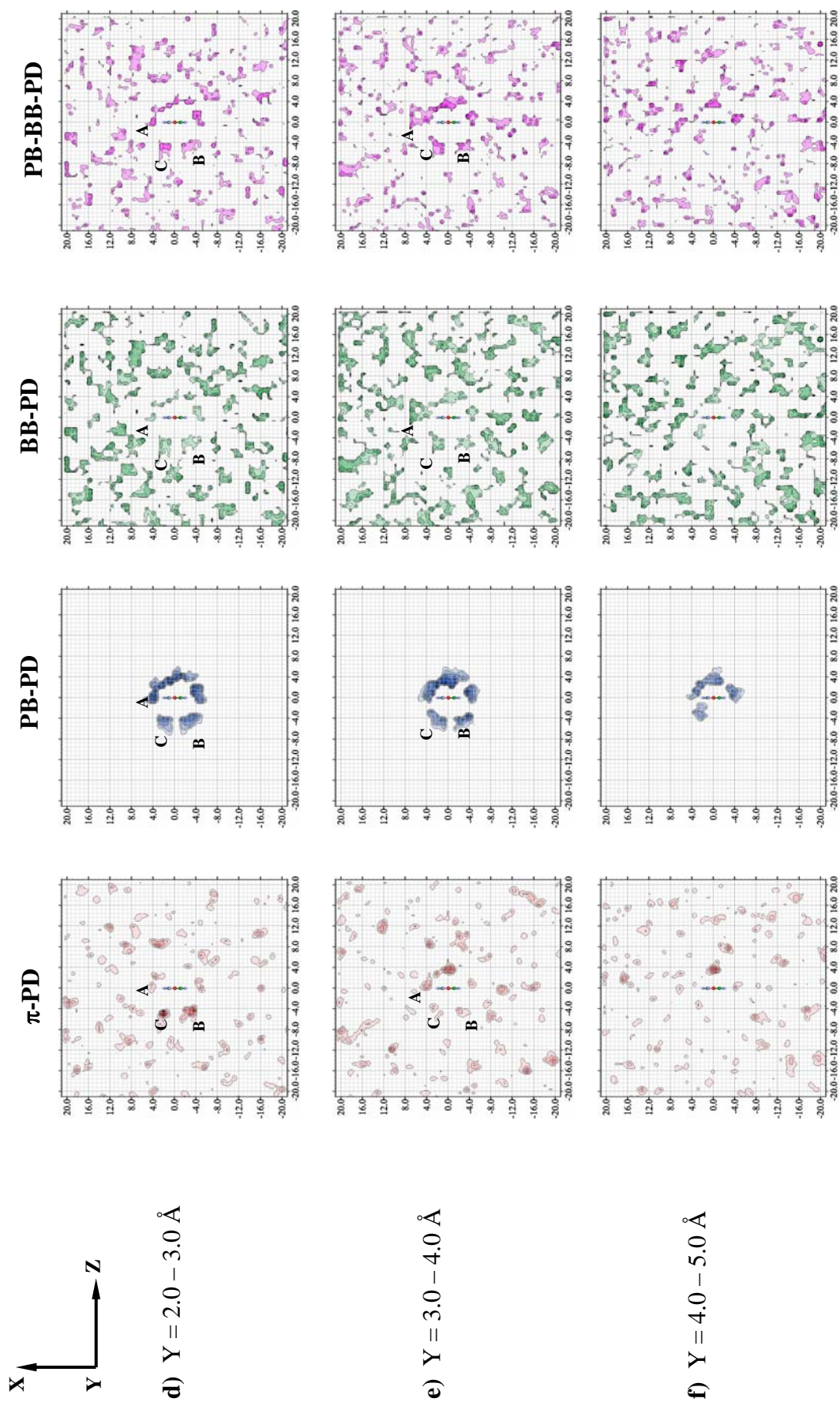


Figure B.2 (Continued).

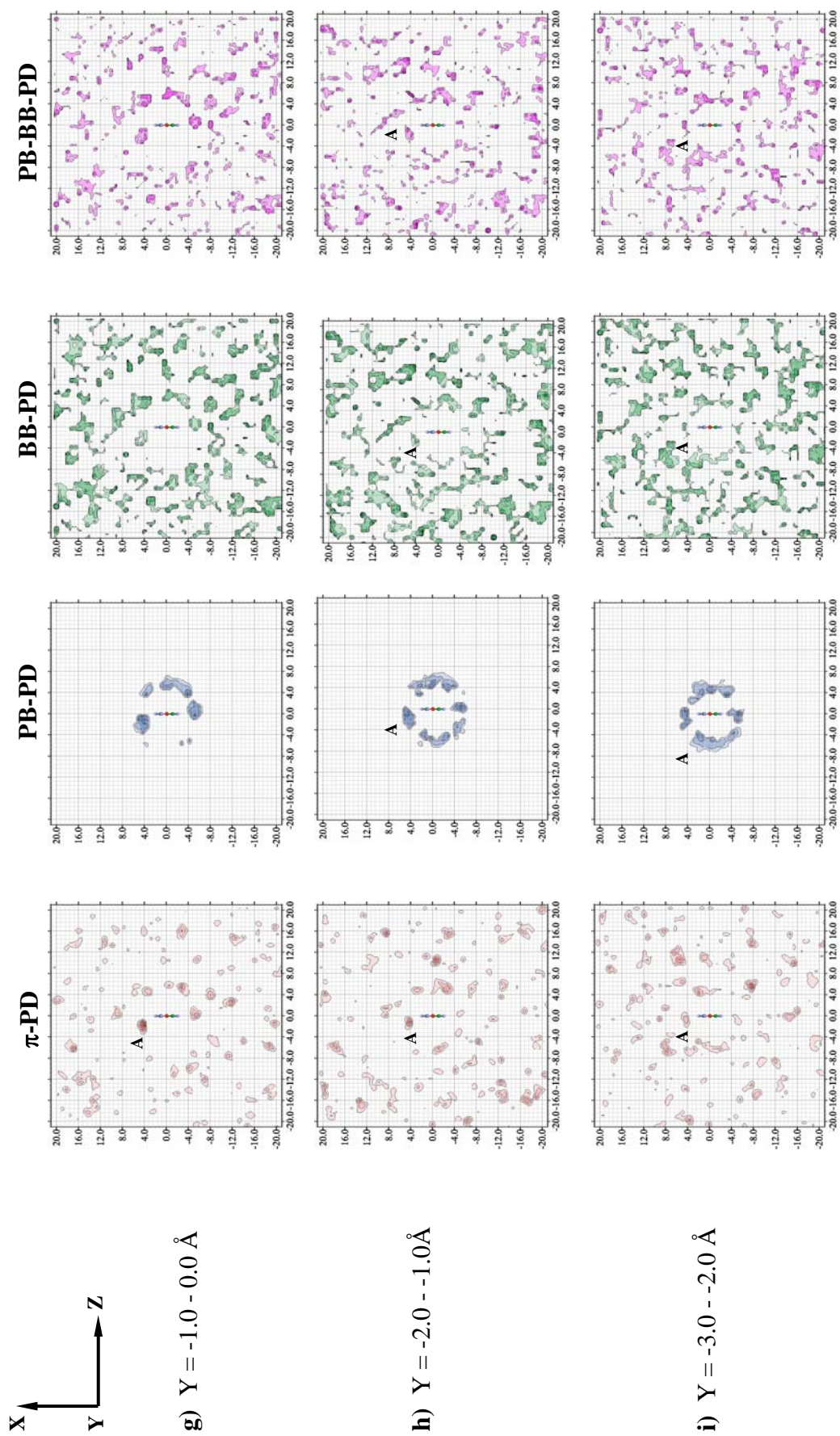


Figure B.2 (Continued).

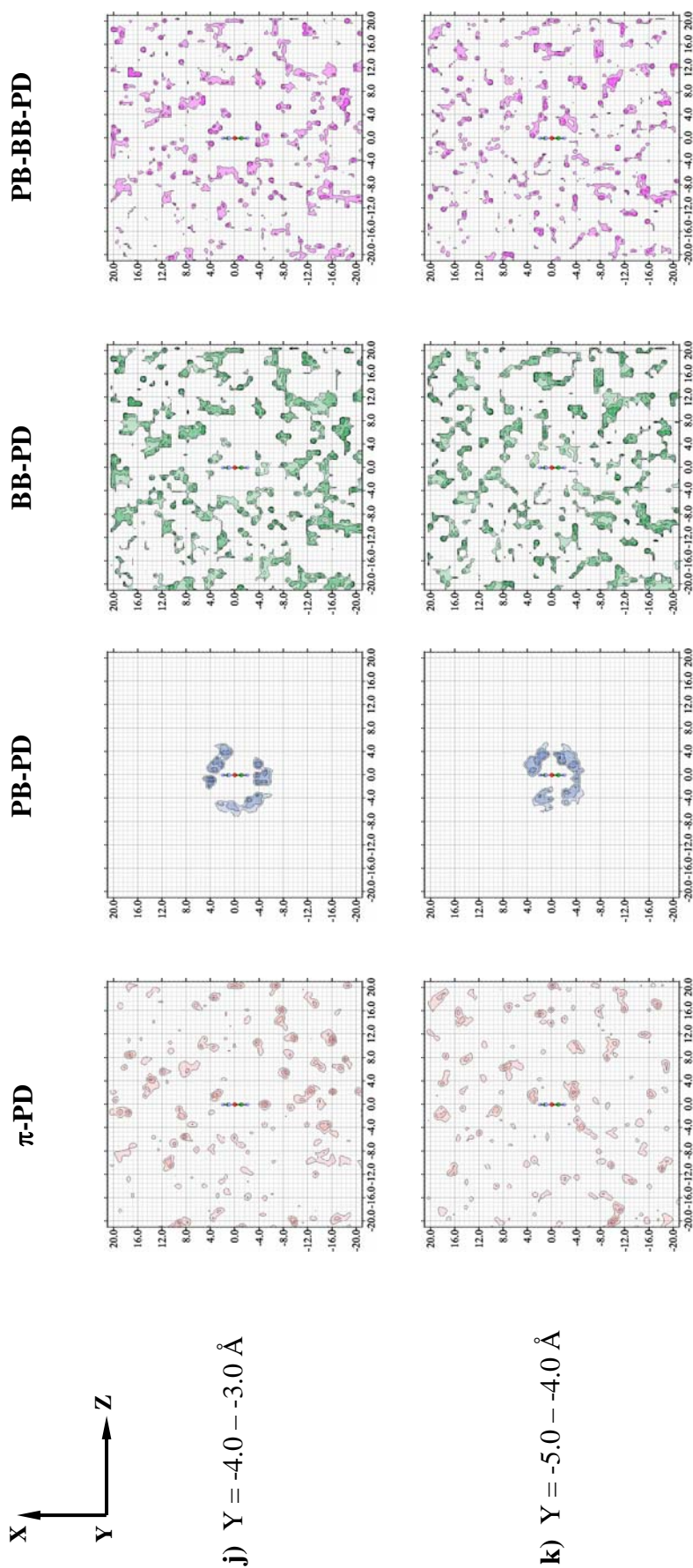
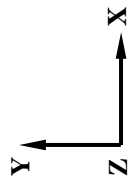


Figure B.2 (Continued).



d) $Z = 2.0 - 3.0 \text{ \AA}$

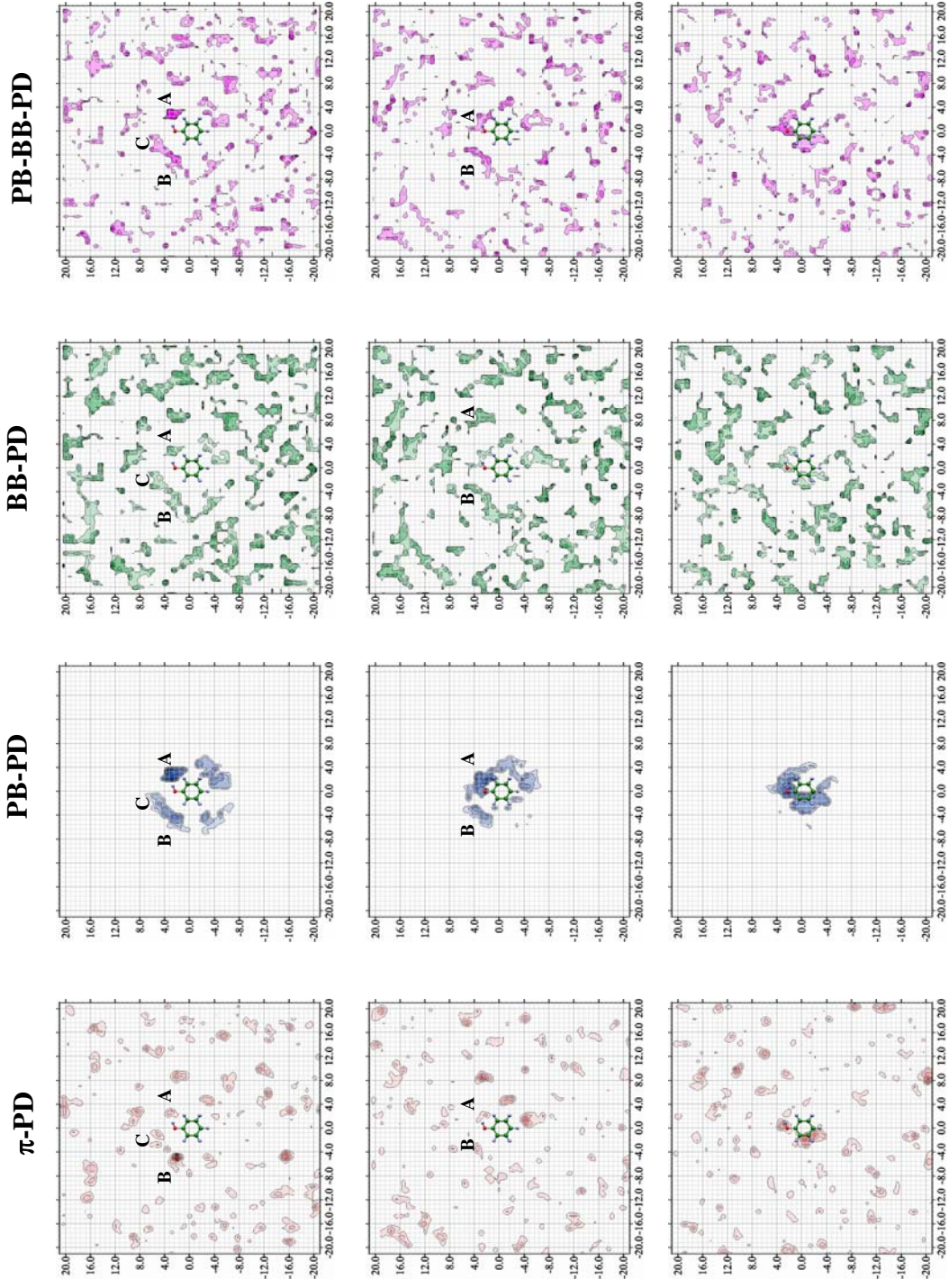


Figure B.3 (Continued).

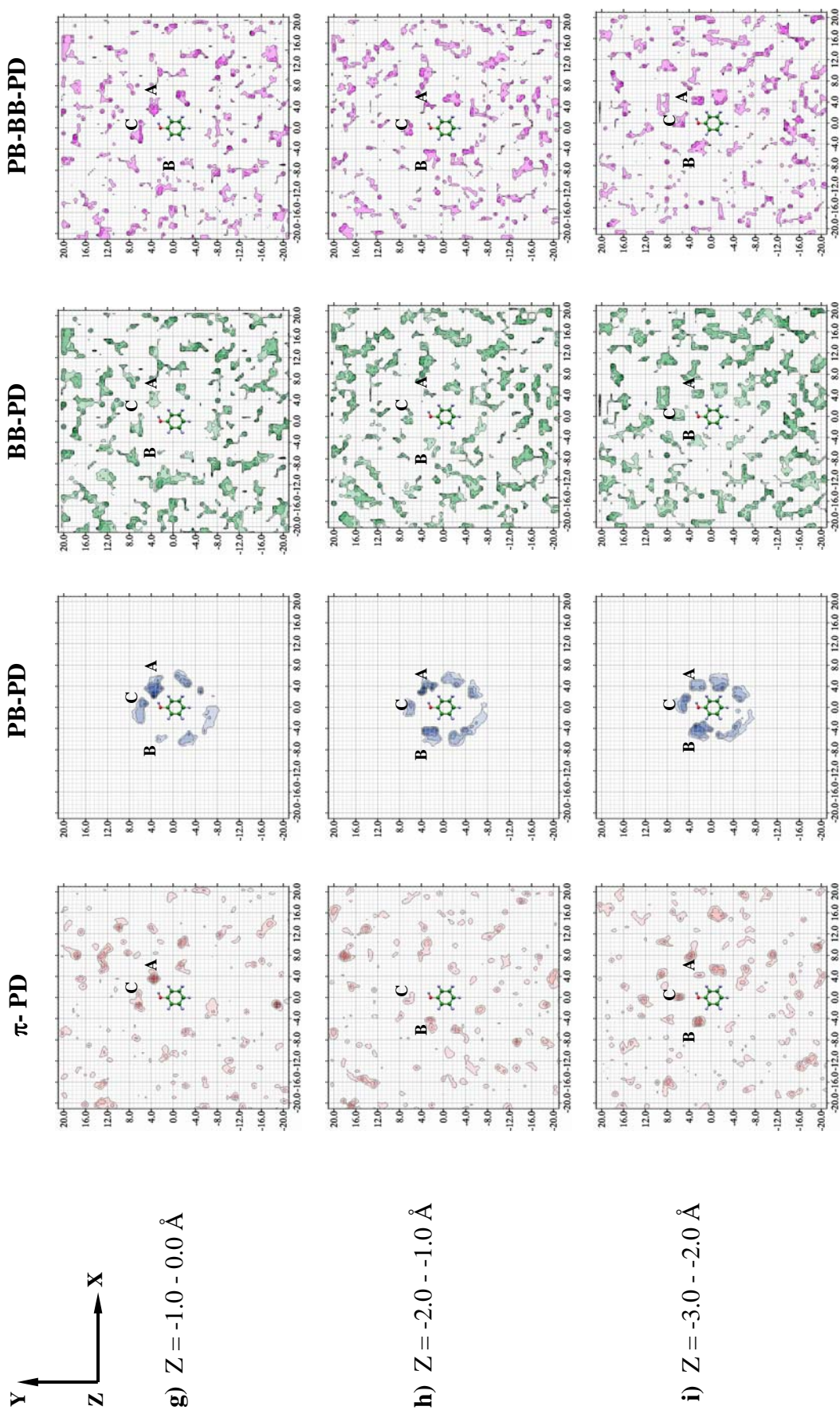


Figure B.3 (Continued).

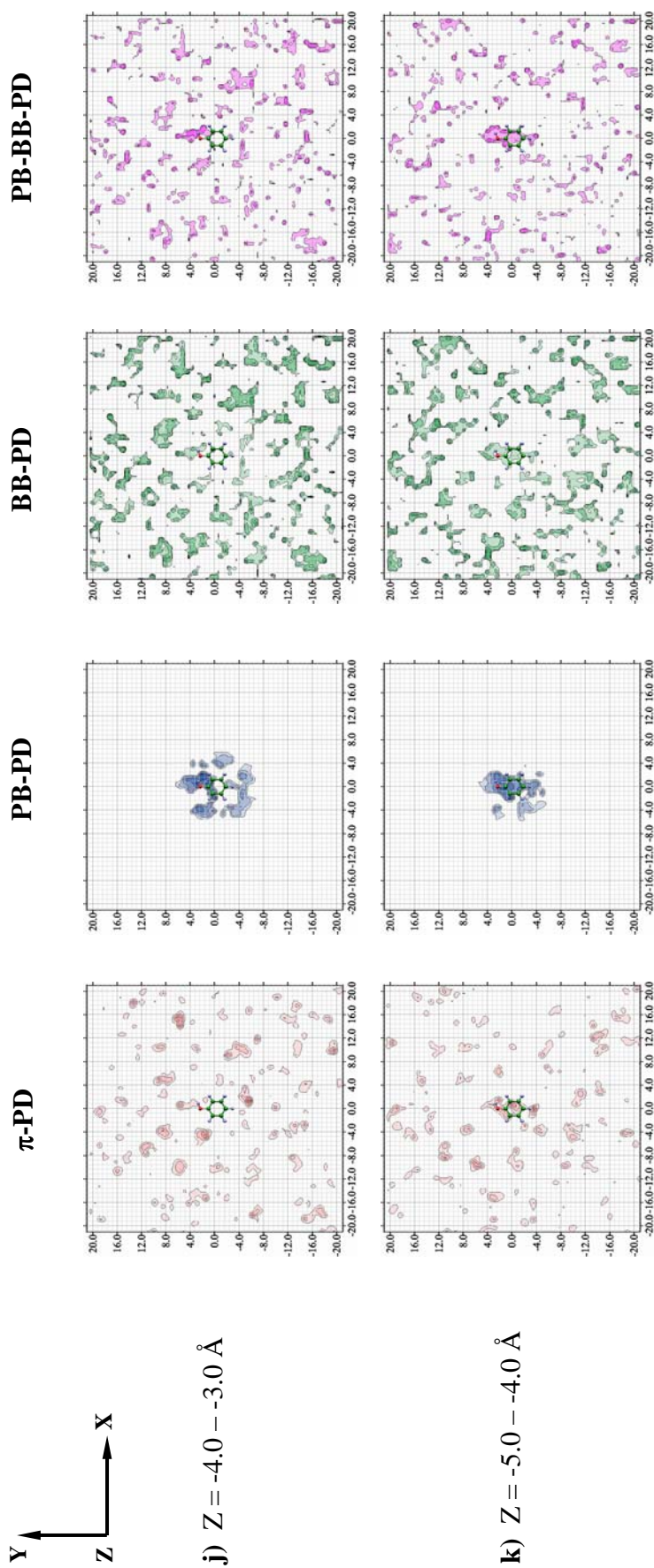


Figure B.3 (Continued).

APPENDIX C

SUPPLEMENTARY RESULTS

FOR MD SIMULATIONS OF $[(\text{PhOH})_2]_{\text{Benz}}$

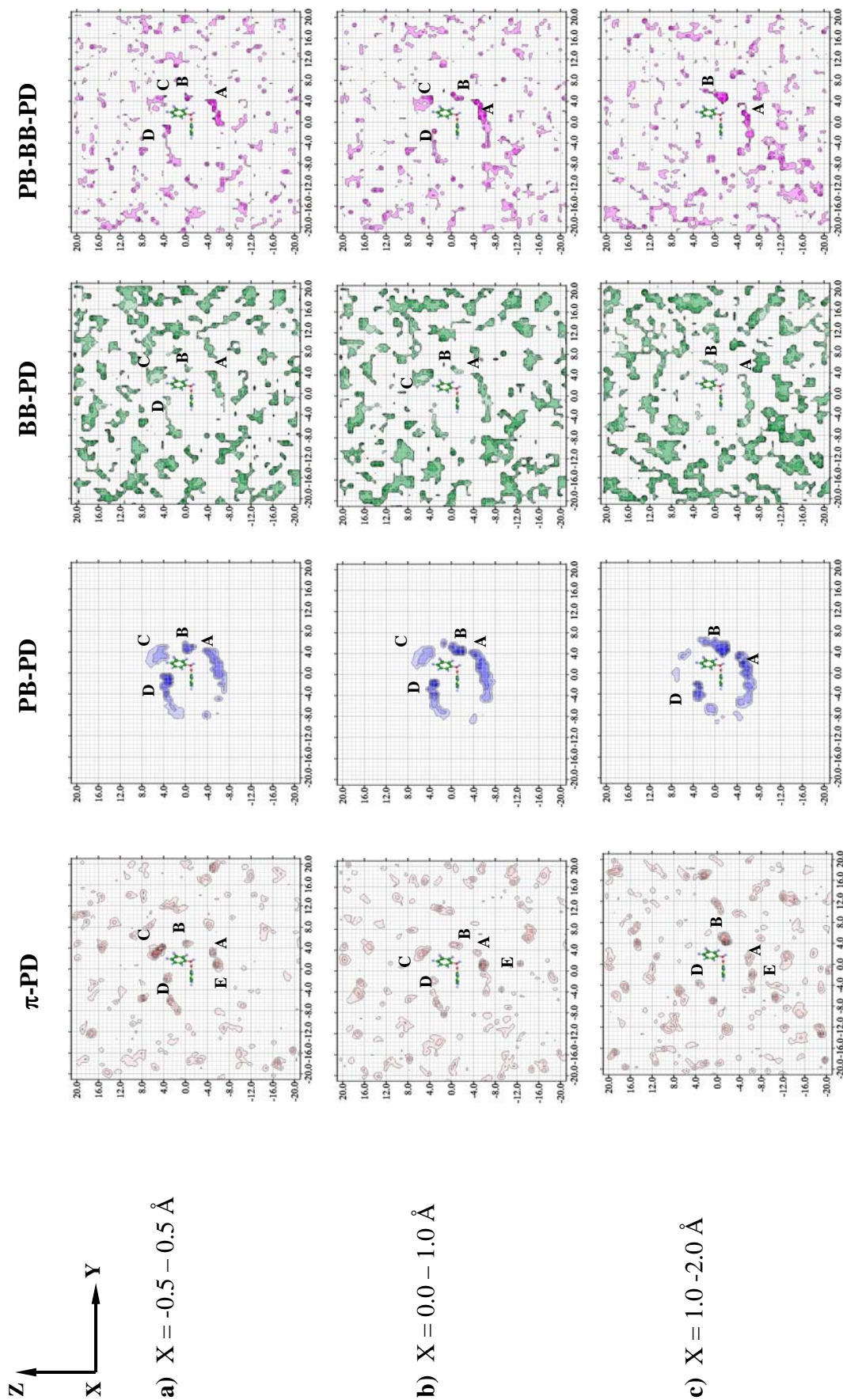


Figure C.1 The π -PD, PB-PD, BB-PD and PB-BB-PD maps with respect to reference plane **II** obtained from MD-[(PhOH)₂]_{Benz}

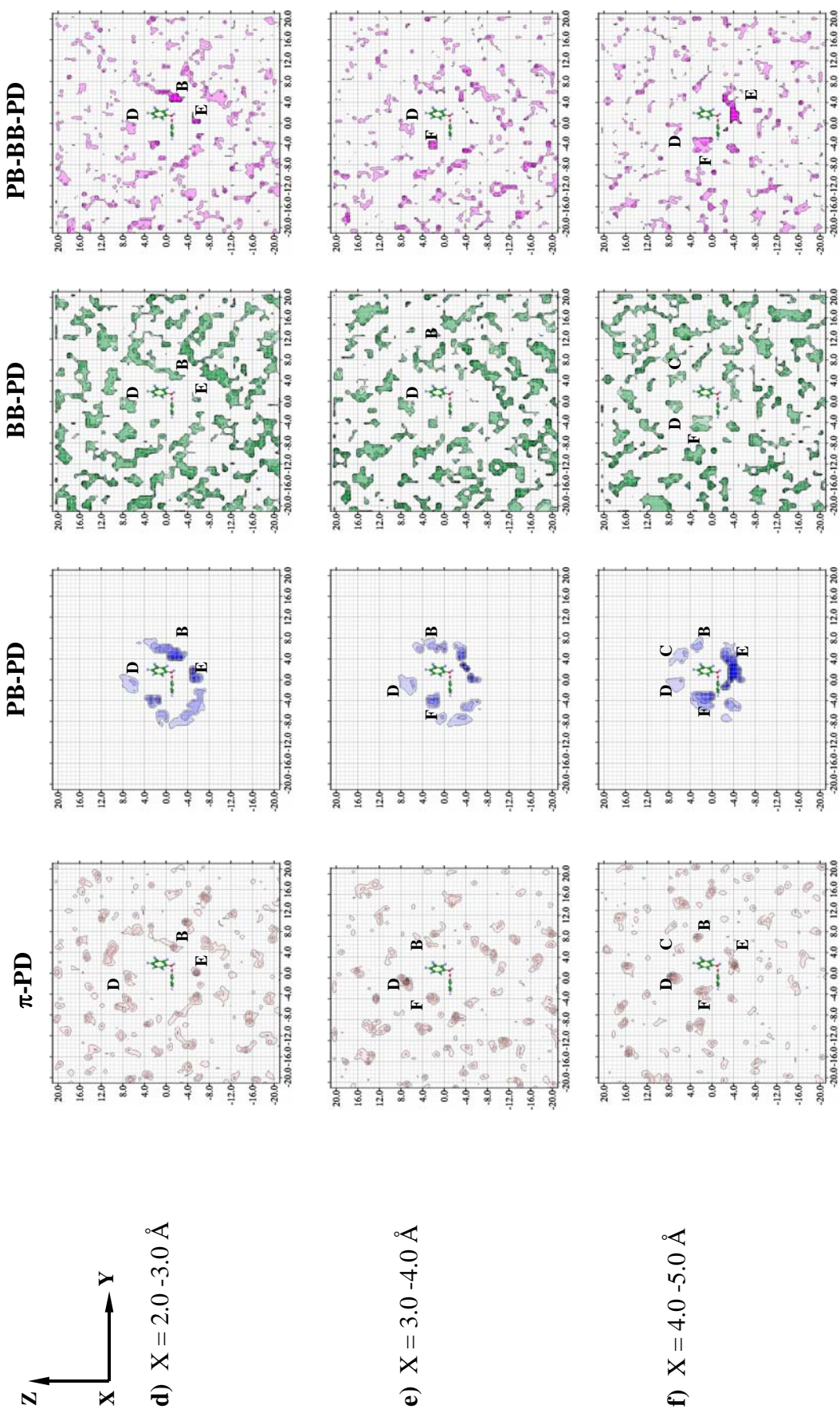


Figure C.1 (Continued).

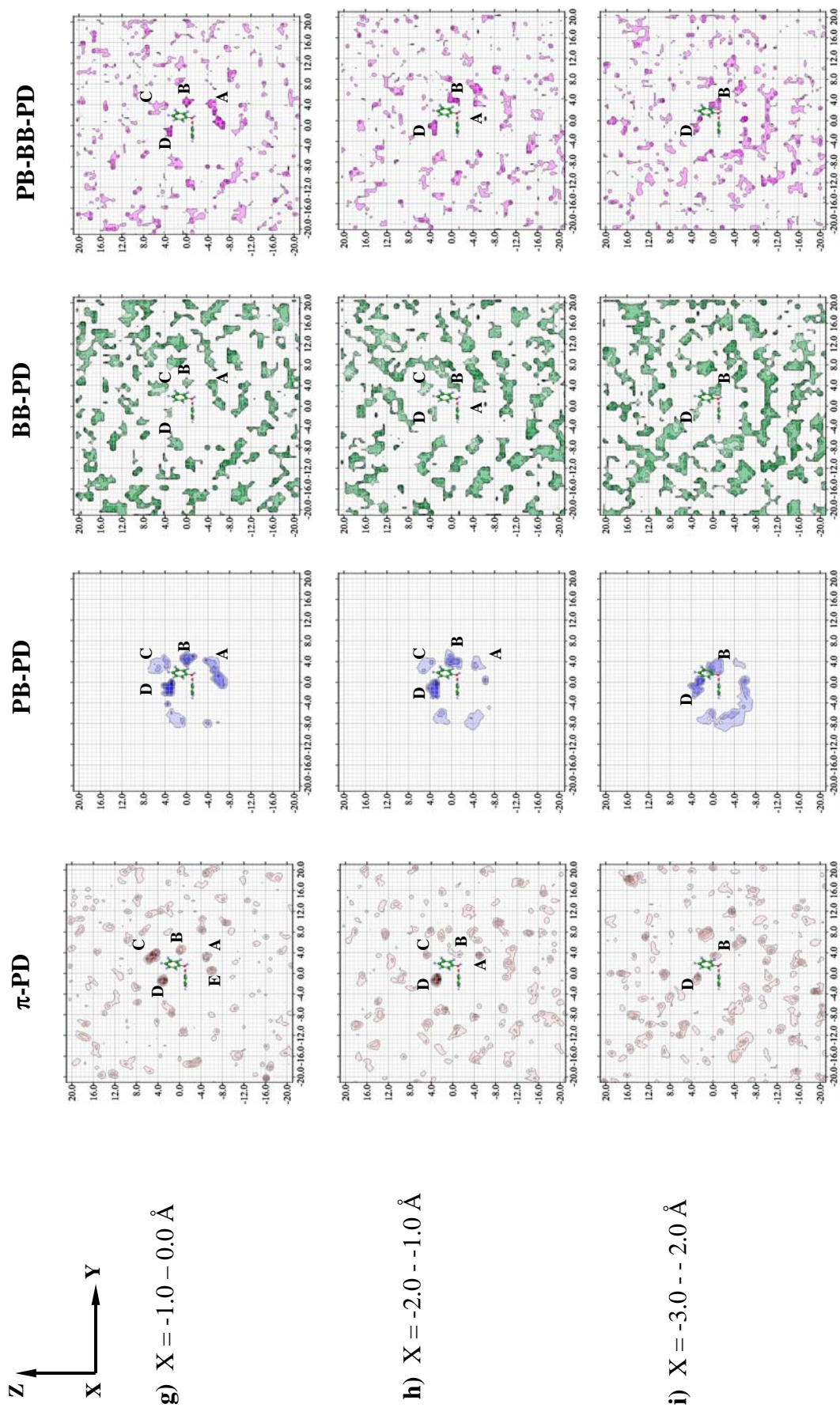


Figure C.1 (Continued)

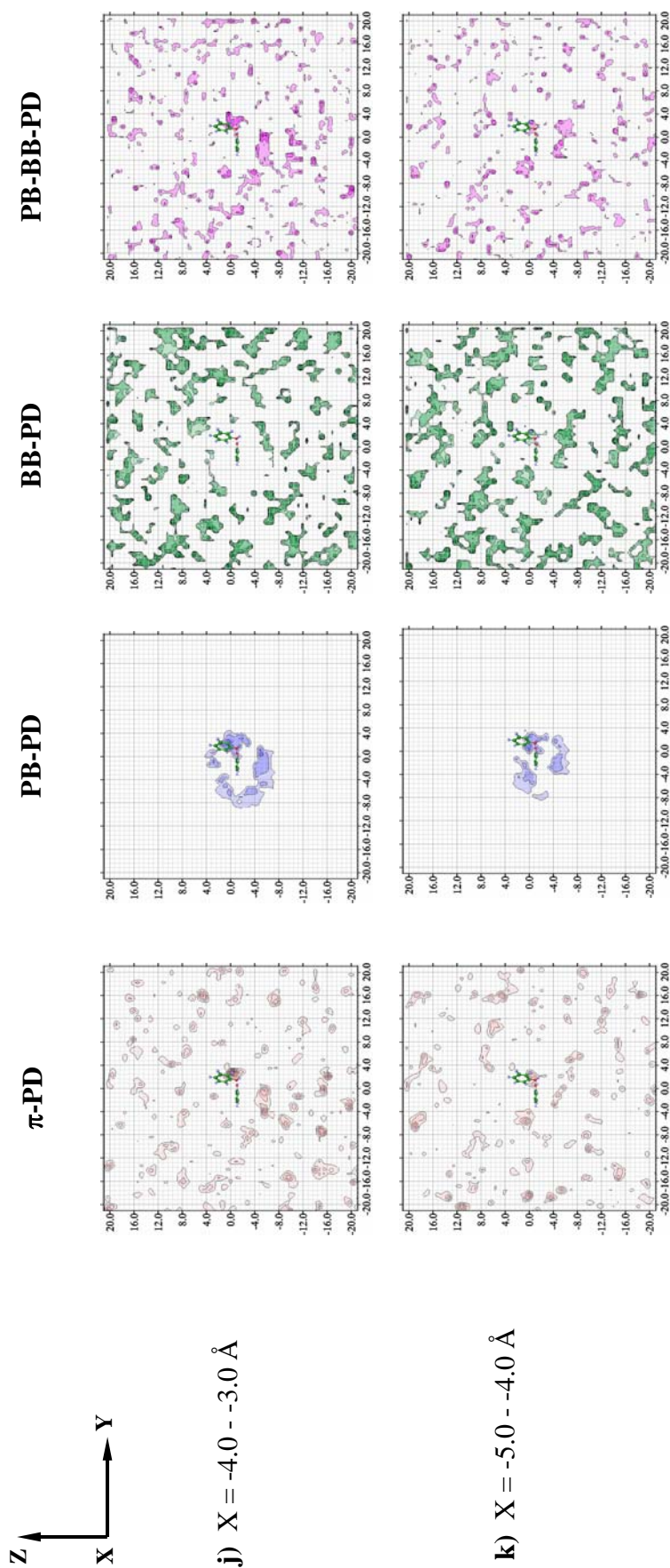


Figure C.1 (Continued).

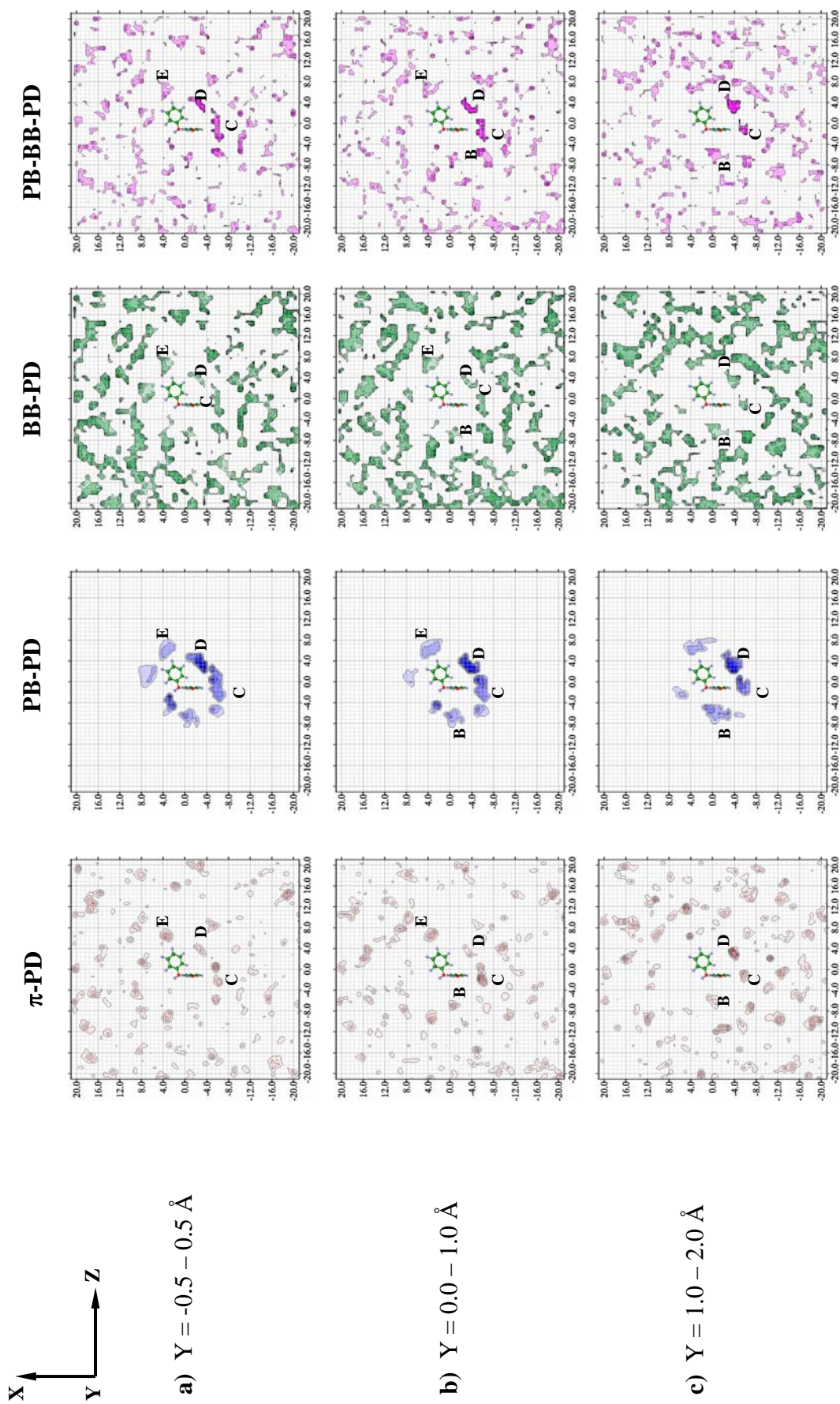


Figure C.2 The π -PD, PB-PD, BB-PD and PB-BB-PD maps with respect to reference plane **III** obtained from MD-[(PhOH)₂]Benz

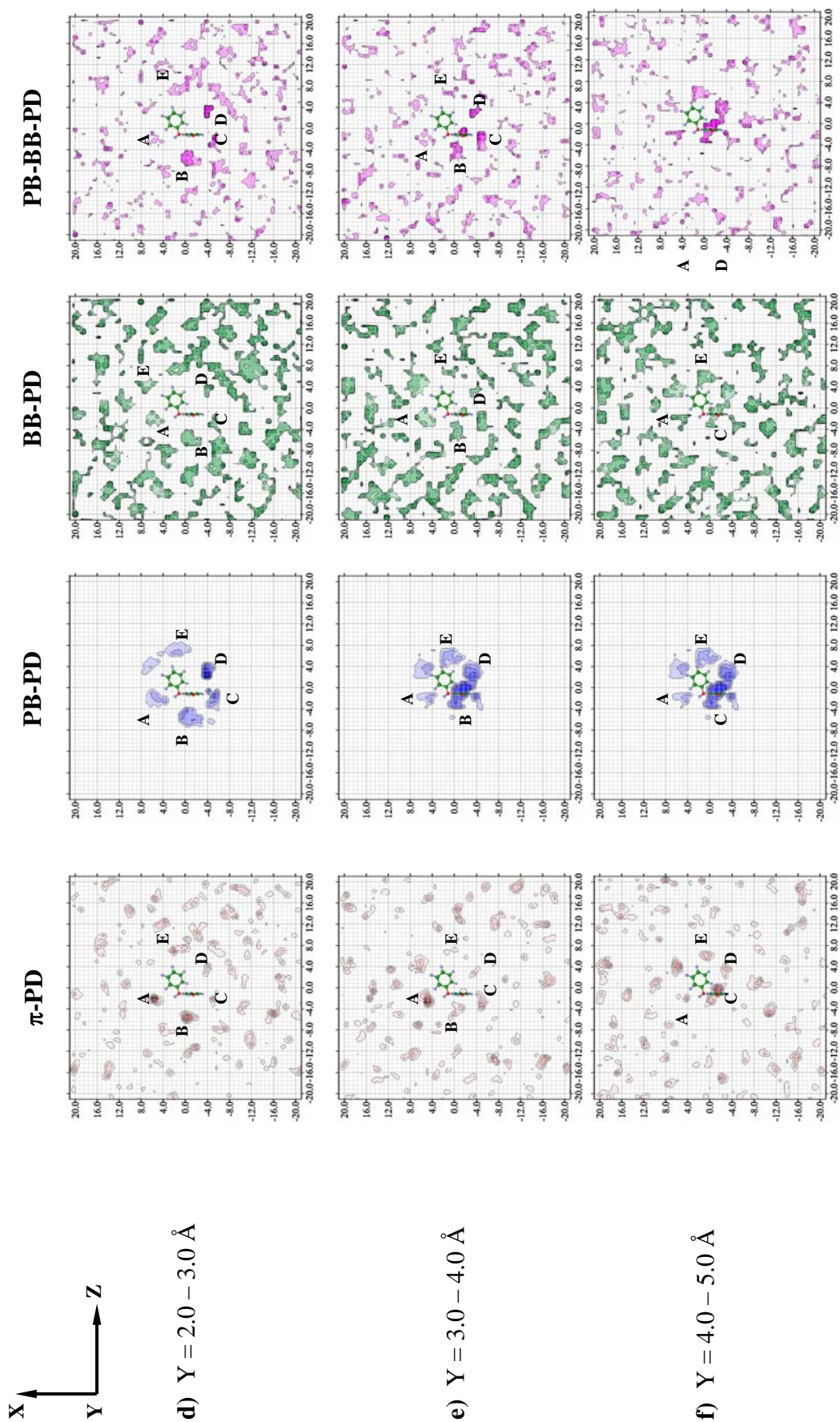
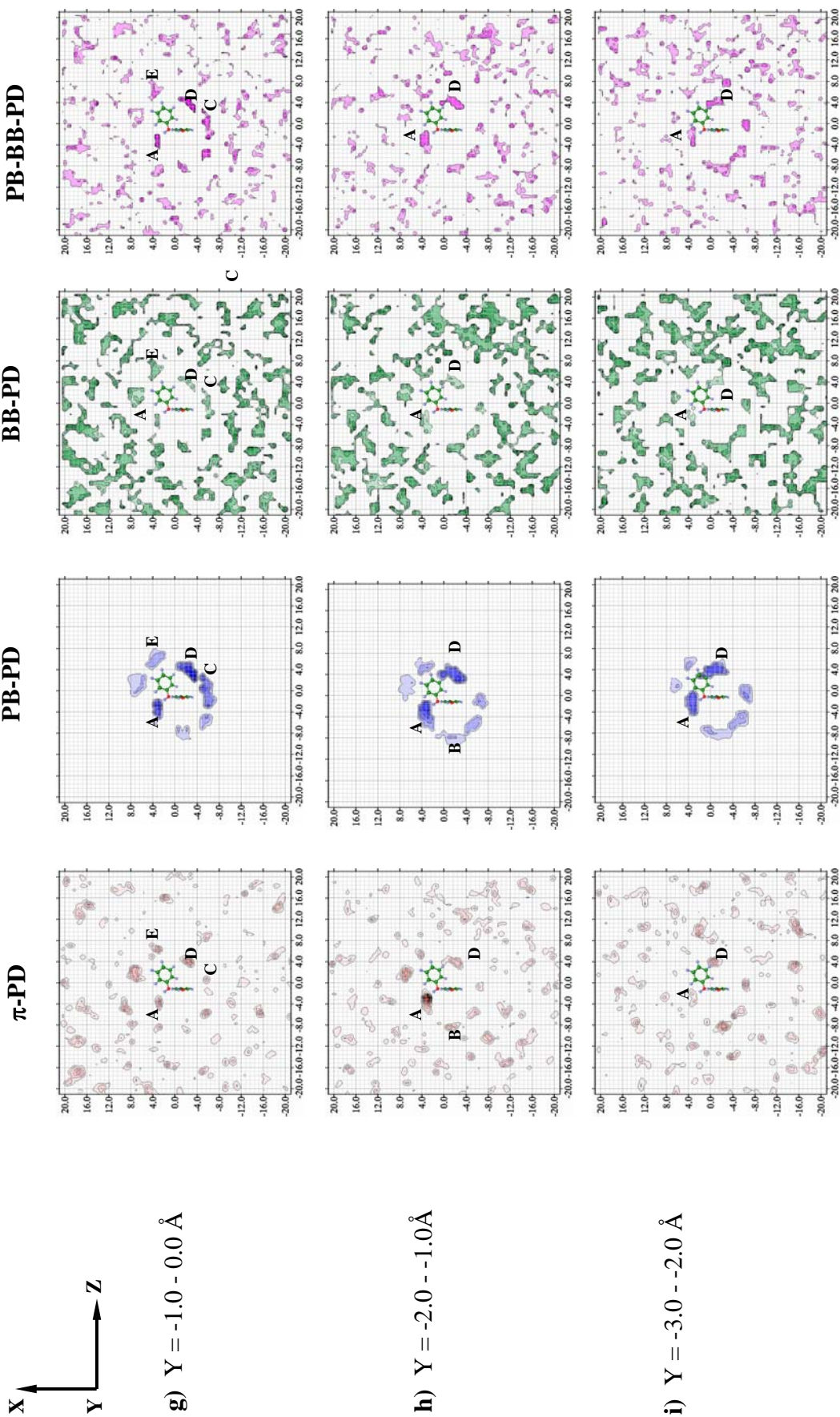


Figure C.2 (Continued).



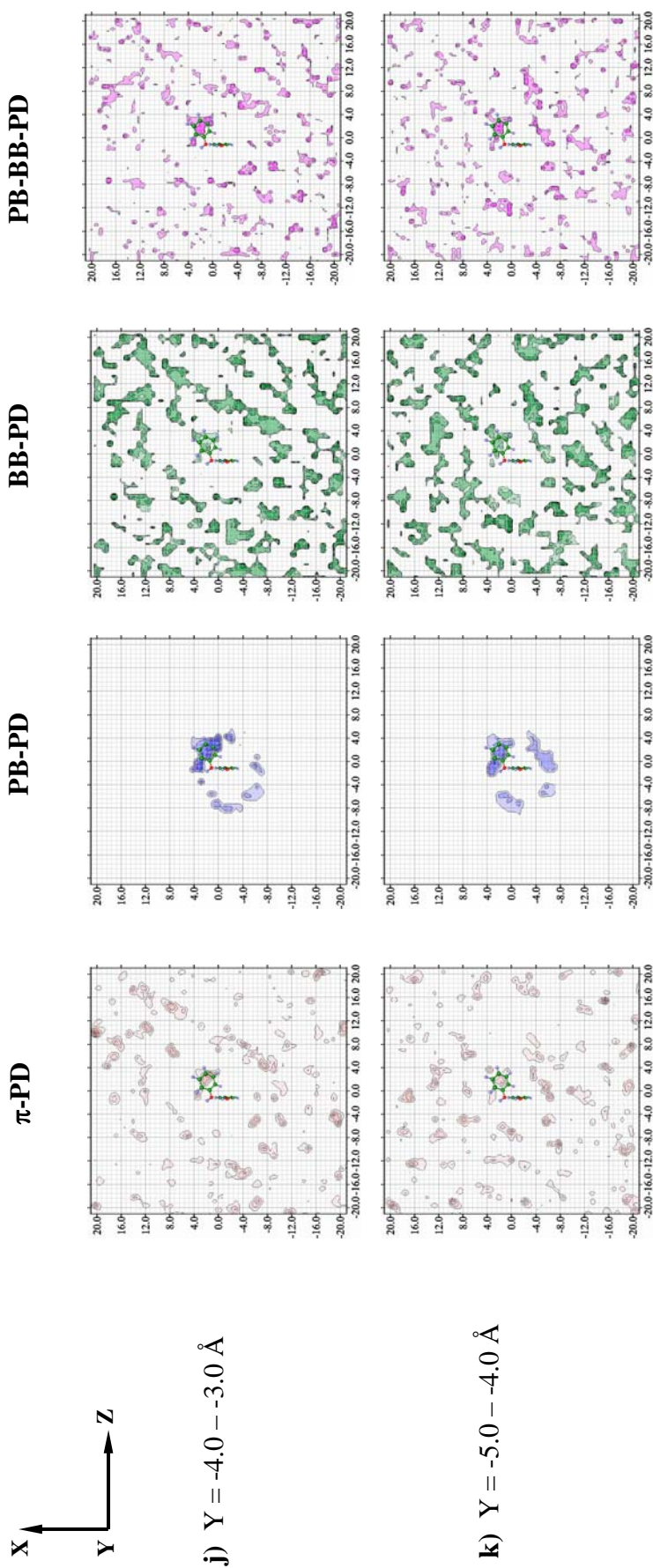


Figure C.2 (Continued).

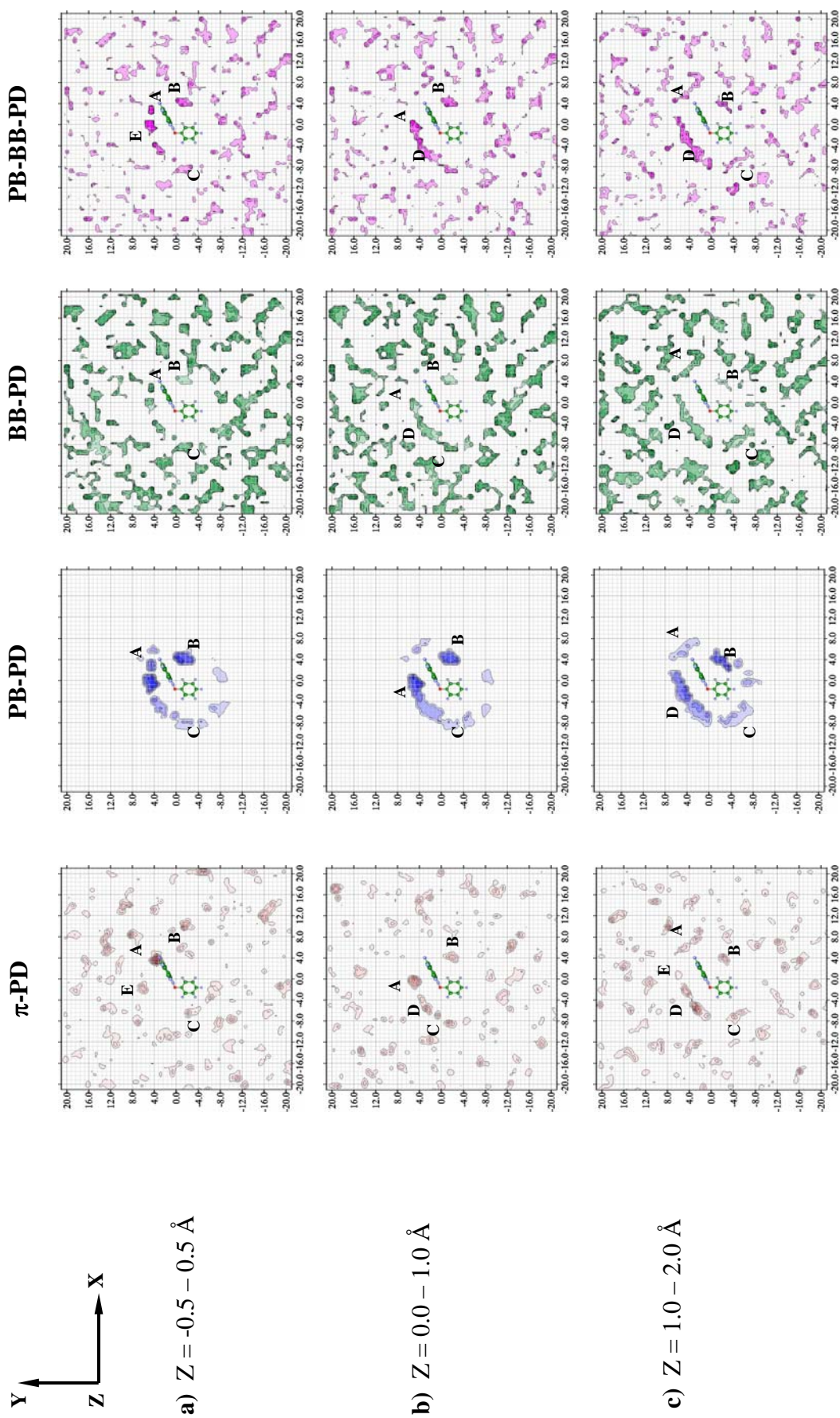


Figure C.3 The π -PD, PB-PD, BB-PD and PB-BB-PD maps with respect to reference plane I obtained from MD-[(PhOH)₂]_{Benz}

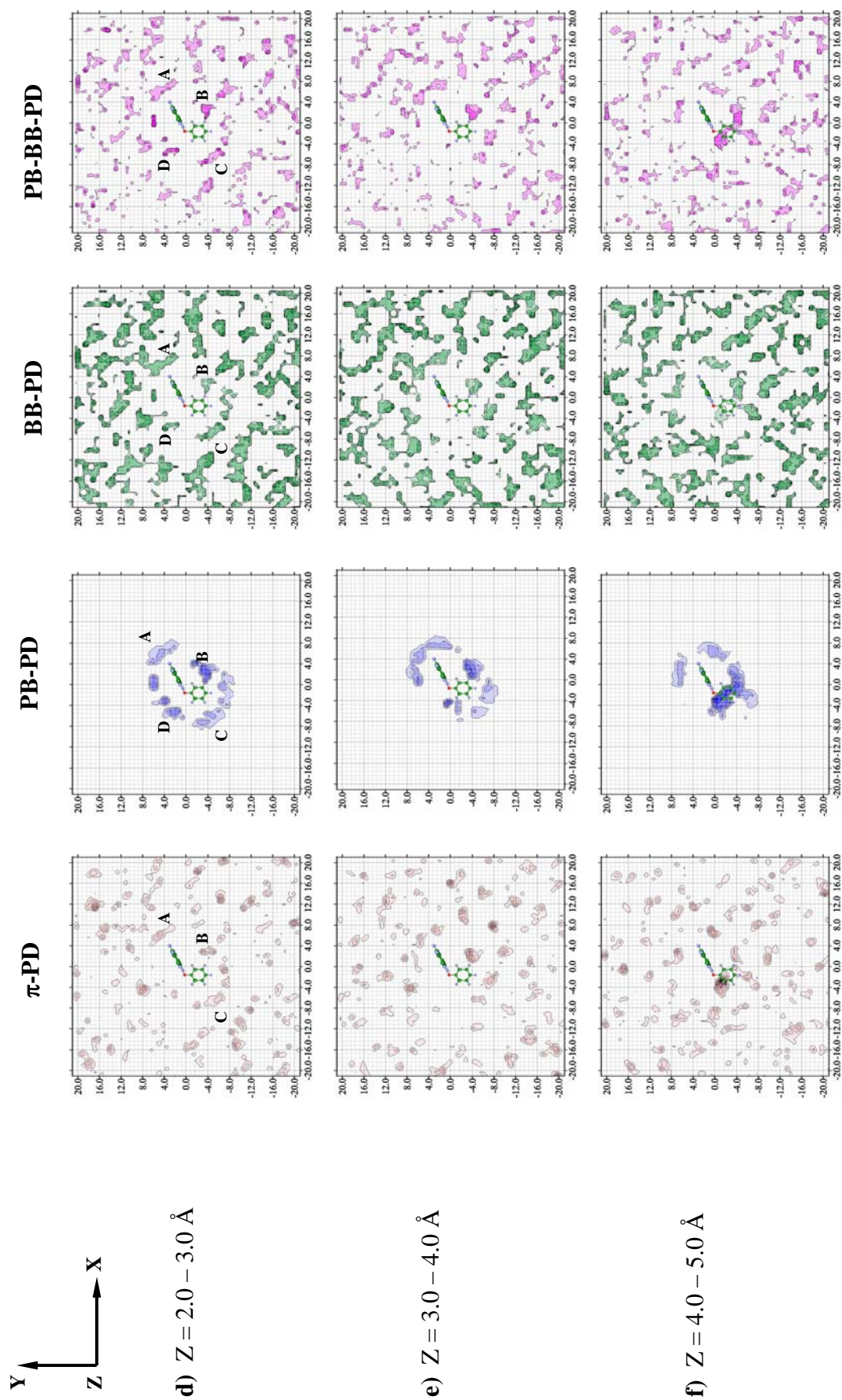


Figure C.3 (Continued).

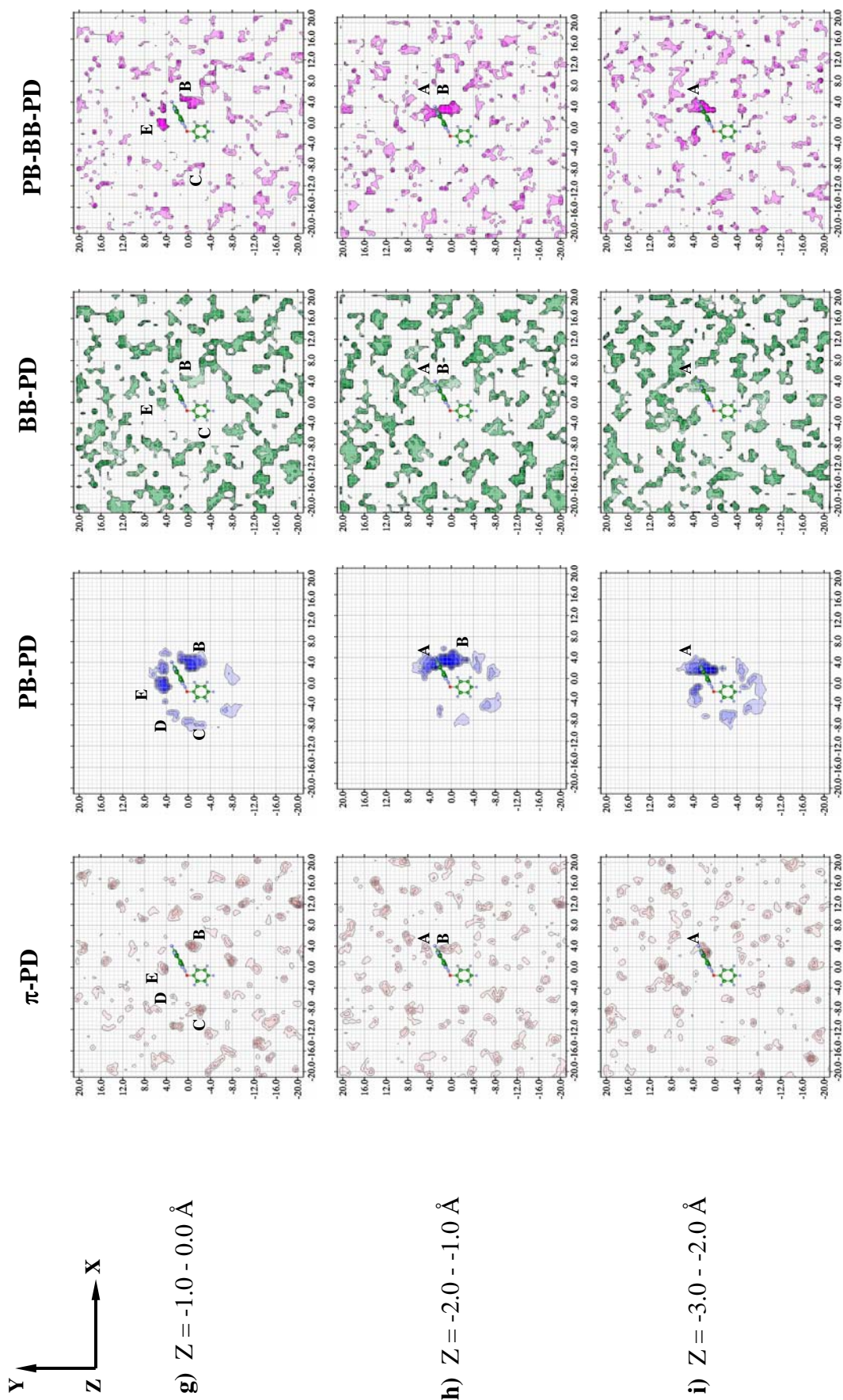


Figure C.3 (Continued).

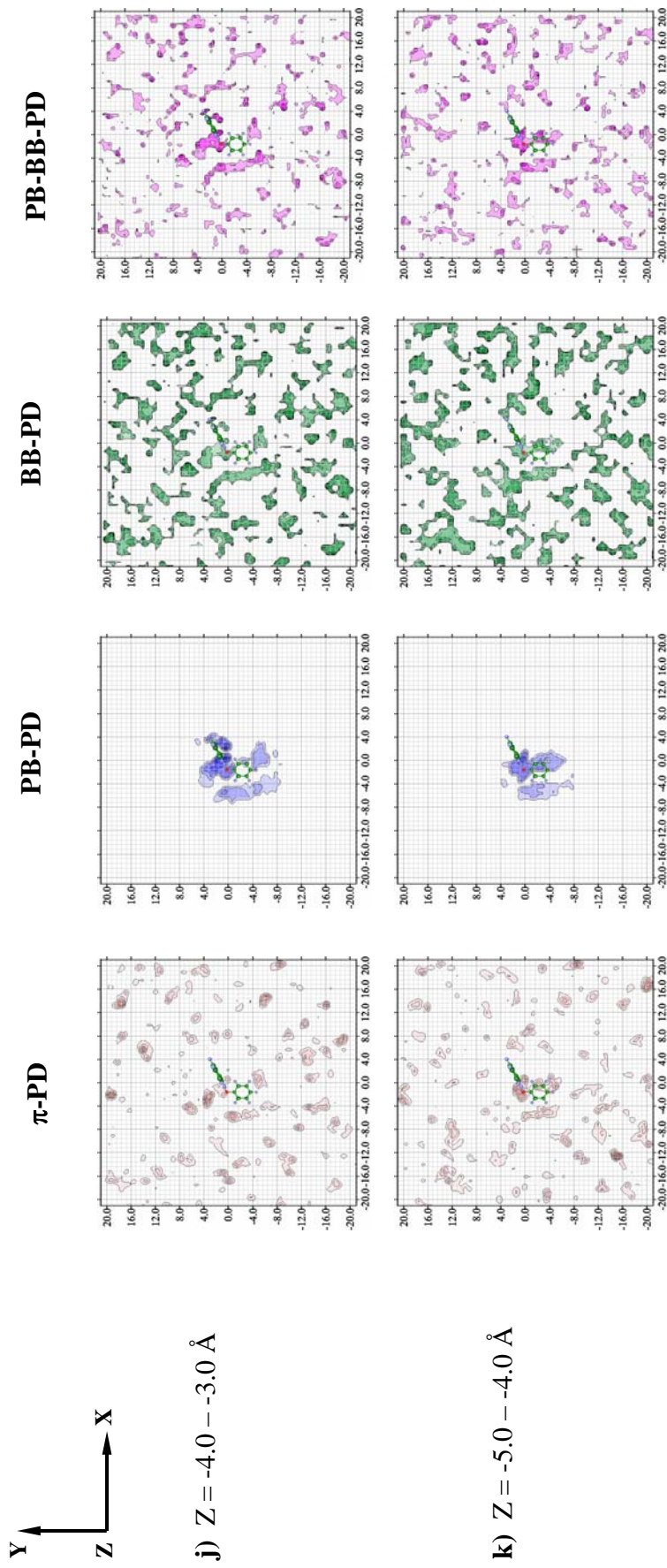


Figure C.3 (Continued).

APPENDIX D
LISTS OF PRESENTATIONS

1. Sermsiri Chaiwongwattana and Kritsana Sagarik. (October 20-22, 2003). Hydration structures and free energy profiles for methanol dimer in aqueous solutions. **29th Congress on Science and Technology of Thailand (STT29th)**. Khon Kaen University, Khon Kaen, Thailand.
2. Sermsiri Chaiwongwattana and Kritsana Sagarik. (October 18-10, 2005). Structures and stability of phenol and phenol dimer in aqueous solutions. **31th Congress on Science and Technology of Thailand (STT31th)**. Suranaree University of Technology, Nakhon Ratchasima, Thailand.
3. Sermsiri Chaiwongwattana, Kritsana Sagarik and Fu Ming Tao. (January 22-25, 2006). Molecular structure and proton transfer in small clusters of trifluoromethanesulfonic acid with water molecules. **40th Western Regional Meeting American Chemical Society (ACS)**. Anaheim/ Orange, California, United States.
4. Sermsiri Chaiwongwattana and Kritsana Sagarik. (January 22-25, 2006). Hydration structures and stability of Phenol dimer in aqueous solutions. **40th Western Regional Meeting American Chemical Society (ACS)**. Anaheim/ Orange, California, United States.
5. Sermsiri Chaiwongwattana and Kritsana Sagarik. (March 22-24, 2006). Structures and stability of phenol and phenol dimer in benzene solutions. **The 10th Annual National Symposium on Computational Science and Engineering (ANSCSE10)**. Chang Mai University, Chang Mai, Thailand.

APPENDIX E
LISTS OF PUBLICATIONS

1. Sagarik, K., Chaiwongwattana, S. and Sisot. P. (2004). A theoretical study on clusters of benzoic acid in benzene solutions. **Chemical Physics**. 306: 1-12.
2. Chaiwongwattana, S. and Sagarik, K. (2008). Structures and dynamics of phenol clusters in benzene solutions. **Chemical Physics**. Submitted.

Available online at www.sciencedirect.com

SCIENCE @ DIRECT®

Chemical Physics 306 (2004) 1–12

Chemical
Physicswww.elsevier.com/locate/chemphys

A theoretical study on clusters of benzoic acid–water in benzene solutions

Kritsana Sagarik^{a,*}, Sermsiri Chaiwongwattana^a, Phittaya Sisot^b^a School of Chemistry, Institute of Science, Suranaree University of Technology, Nakhon Ratchasima 30000, Thailand^b Department of Chemistry, Faculty of Science, Ramkhamhaeng University, Bangkok 10240, Thailand

Received 8 January 2004; accepted 2 April 2004

Available online 21 August 2004

Abstract

Structures and stability of benzoic acid dimer ((BA)₂) and benzoic acid–water (BA–H₂O) *m:n* complexes, with *m* and *n* = 1, 2, were studied in benzene solutions, using molecular dynamics (MD) simulations. It appeared that nearly all hydrogen bond (H-bond) complexes suggested from different partition experiments existed in MD simulations, with the probability depending on their size and temperature. The MD results revealed the probability of finding H-bonds between water molecules, as well as the non-self-association of water molecules in benzene solutions. Although the H-bonds in (BA)₂ are quite strong in the gas phase and pure benzene, they can be opened by water molecules, forming microhydrates in benzene solutions. It was shown that, in order to provide insights into the structures and stability of the BA–H₂O complexes in benzene solution, solvent molecules as well as dynamic and temperature effects have to be included in theoretical investigation.

© 2004 Elsevier B.V. All rights reserved.

Keywords: Benzoic acid dimer; Benzene solution; T-model; Molecular dynamics simulation

1. Introduction

Association of organic acids in organic solvents has been frequently and extensively studied in the past two decades, using various theoretical and experimental techniques [1–19]. The self-association and hydration constants of organic acids in non-polar solvents can be obtained by distribution of an organic acid between two immiscible solvents, such as water and benzene (BEN). For small carboxylic acids such as acetic acid (AA), cyclic hydrogen-bond (H-bond) dimers were reported to be very stable in the gas phase, as well as in chloroform [4], benzene [5] and carbon tetrachloride [5,13]. It was concluded in [6] that the more inactive the solvent, the more pronounced is the tendency of the acid to react with itself. The magnitudes of the en-

thalpy changes for the dimerization of benzoic acid (BA) evaluated from IR vary with solvent in the order: benzene < carbon tetrachloride < cyclohexane < vapor [7]. Distribution experiments also suggested the formation of microhydrates of the organic acid monomer [11] and dimer [9–12] in organic solvents.

Distribution of benzoic acid between the benzene and water phases, as well as the number of water molecules H-bonded to BA in the benzene phase, represents one of the classical problems in the area of molecular association in solutions [9–12,14–19]. It was shown that BA [9,11] exists as monomer in aqueous solution. The distribution data in [11] revealed that the important associated species in benzene solution at 298 K are (BA)₂, the BA–H₂O 1:1, 1:2 and 2:1 complexes. In order to obtain a satisfactory correlation of the results, they must be taken into account in the analysis of the distribution data. However, based on the assumption that the hydrated (BA)₂ can be ignored, it was proposed in [14] that

* Corresponding author. Tel./fax: +66 44 224 635.
E-mail address: kritsana@ccs.sut.ac.th (K. Sagarik).

a single BA molecule is hydrated by a water molecule in the benzene phase. These opposite to the assumption made in [12], in which the probability of finding microhydrates of BA and $(BA)_2$ in the benzene phase was completely neglected in the analysis.

In our previous work [20], structures and stability of the cyclic H-bond planar (CHP) and side-on type (SOT) dimers of BA in the water phase were studied based on the intermolecular potentials derived from the test-particle model (T-model) and molecular dynamics (MD) simulations. It was recognized that, in the gas phase and dilute aqueous solution, the cyclic H-bonds in the CHP and SOT dimers can be disrupted by H-bonding with water, as well as thermal energy fluctuation. The theoretical results agree well with the previous reports [9,11], and the experimental finding that the concentration of $(BA)_2$ is less than 3% of the concentration of the unionized BA [21,22]. The situations in $(BA)_2$ are quite similar to $(AA)_2$, in which water-separated dimer structures were suggested to dominate in the gas phase and aqueous solution [13].

In the present work, the theoretical investigation [20] was extended into the benzene phase. The study of H-bonds in $(BA)_2$ in dilute benzene solution ($((BA)_2)_{BEN}$) began with the construction of the T-model potential for benzene. MD simulations on the CHP dimer in benzene were conducted at 298 K, using the T-model potential. In order to examine the structures and stability of $(BA)_2$ and microhydrates of BA, the $BA-H_2O$ $m:n$ complexes (with m and $n = 1, 2$) in benzene were studied by performing a series of MD simulations at 280 and 298 K. The structures and stability of the H-bond complexes in benzene solutions were discussed based on the average H-bond distances ($\langle R_{A-H \cdots B} \rangle$) and angles ($\langle \theta_{A-H \cdots B} \rangle$), as well as the H-bond lifetimes ($\langle \tau_{A-H \cdots B} \rangle$). The stability of $(BA)_2$ and the microhydrates of BA was also analyzed and discussed using the average solute–solute interaction energies ($\langle E_{BEN}^{sol} \rangle$) and the average potential energies of benzene solutions ($\langle E_{BEN}^{pot} \rangle$) derived from MD simulations.

2. Methods

Although in principle ab initio calculations such as the self-consistent reaction field (SCRF) method could help provide insight into molecular association in continuum solvent, they seem to be appropriate for the system, in which solvent acts only as a perturbation on the gas-phase property of the system. The neglect of specific short-range solute–solvent interactions as well as temperature effects in the ab initio SCRF calculations makes it inappropriate for the systems with highly anisotropic environment. Since the systems considered in the present study involve various types of solute–solvent interactions e.g., the $O-H \cdots \pi$, $C-H \cdots \pi$ and $\pi-\pi$ interactions,

and it was the main objective to demonstrate how aromatic non-polar solvent effects the structures and stability of H-bond solute clusters, the solvent molecules were modeled explicitly using the T-model.

2.1. T-model potential

The geometries of benzoic acid, benzene and water were taken from [20,23] and kept constant throughout the calculations. In our previous work [20,24–30] H-bonds between various types of molecule have been investigated successfully using the intermolecular potentials derived from T-model. The applicability of the T-model potentials on aromatic systems [20,26,29,30] has been studied systematically, using pyridine [29], phenol [30] and BA [20]. The derivation of T-model has been presented in detail elsewhere [31–33]. Here only some important aspects will be briefly summarized.

Within the framework of T-model, the interaction energy (ΔE) of the $A \cdots B$ system is written as a sum of the first-order interaction energy (ΔE_{SCF}^1) and a higher-order energy term ($\Delta E'$)

$$\Delta E_{T\text{-model}} = \Delta E_{SCF}^1 + \Delta E', \quad (1)$$

where ΔE_{SCF}^1 accounts for the exchange repulsion and electrostatic energy contributions. It is computed from ab initio SCF calculations [31] and takes the following analytical form:

$$\Delta E_{SCF}^1 = \sum_{i \in A} \sum_{j \in B} \left[\exp \left[\frac{-R_{ij} + \sigma_i + \sigma_j}{\rho_i + \rho_j} \right] + \frac{q_i q_j}{R_{ij}} \right], \quad (2)$$

where i and j in Eq. (2) label the sites of molecules and σ_i , ρ_i and q_i are site parameters. R_{ij} is the site–site distance. The exponential term in Eq. (2) represents the size and shape of the interacting molecules A and B. The point charges q_i and q_j are obtained from the requirement that a point-charge model reproduces the electrostatic potentials of molecules of interest. In our previous study [27,29,30], we showed that the potential derived [34] and CHelpG charges [35] are also applicable. In the present study, q_i and q_j for benzene were determined by a fit of the electrostatic potentials at points selected according to the CHelpG scheme. The electrostatic potentials used in the fit were computed from ab initio calculations at the MP2/6-311G(d,p) level of theory. About 9000 electrostatic energy values were employed in the fit of the atomic charges. The charges on the carbon and hydrogen atoms of benzene are -0.0923 and 0.0923 , respectively.

The higher-order energy contribution, $\Delta E'$ in Eq. (1), could be determined from theoretical or experimental data. A calibration of the incomplete potential to the properties related to intermolecular interaction energies, such as the second virial coefficients $B(T)$, dimerization energies or potential energy of liquid etc., has been

proved to be applicable. ΔE^r represents the dispersion and polarization contributions of the intermolecular potential. It takes the following form:

$$\Delta E^r = - \sum_{i \in A} \sum_{j \in B} C_{ij}^6 F_{ij}(R_{ij}) R_{ij}^{-6}, \quad (3)$$

where

$$F_{ij}(R_{ij}) = \exp \left[- (1.28R_{ij}^0/R_{ij} - 1)^2 \right], \quad R_{ij} < 1.28R_{ij}^0 \\ = 1, \quad \text{elsewhere}, \quad (4)$$

and

$$C_{ij}^6 = C_6 \frac{3}{2} \frac{\alpha_i \alpha_j}{(\alpha_i/N_i)^{1/2} + (\alpha_j/N_j)^{1/2}}, \quad (5)$$

where R_{ij}^0 in Eq. (4) is the sum of the van der Waals radii of the interacting atoms. Eq. (5) is the Slater–Kirkwood relation, in which α_i and N_i denote the atomic polarizability and the number of valence electrons of the corresponding atom, respectively. $F_{ij}(R_{ij})$ in Eq. (4) is a damping function, introduced to correct the behavior of R_{ij}^{-6} at short R_{ij} distance. Only C_6 in Eq. (5) is unknown.

For benzene, the experimental $B(T)$ are available in the temperature range between 290 and 600 K [36]. Thus, C_6 was determined in the present study by calibration of the incomplete T-model potential with the experimental $B(T)$. The agreement between the experimental and the theoretical $B(T)$ is shown in Fig. 1(a). The value of C_6 for benzene–benzene interaction is 1.43.

A four-site model similar to the MCY potential [37] was used in the construction of the T-model parameters of water [26]. Only the C_6 parameter must be determined for BEN–H₂O interaction. In this case, the so-called second virial cross-coefficients ($B_{12}(T)$) are available in the temperature range between 363 and 433 K [38]. Based on the experimental $B_{12}(T)$, the C_6 parameter for the BEN–H₂O interaction was determined to be 1.40. The correlation between the experimental and the theoretical $B_{12}(T)$ is shown graphically in Fig. 1(b). The parameters for the T-model potentials of benzene, water and benzoic acid are listed in Table 1. The T-model parameters have been examined and applied successfully in the investigation of the structures and energetic of molecular cluster, both in the gas phase and in aqueous solutions. Some results were discussed in details in [20,26,30].

2.2. MD simulations

In order to get insight into the structure and stability of H-bonds in $[(BA)_2]_{\text{BEN}}$, as well as in the microhydrates of BA and $(BA)_2$ in benzene solution, a series of NVE-MD simulations were conducted using the T-model parameters in Table 1. The investigations included MD simulations of $[(BA)_2]_{\text{BEN}}$, $[1:1]_{\text{BEN}}$,

$[1:2]_{\text{BEN}}$, $[2:1]_{\text{BEN}}$ and $[2:2]_{\text{BEN}}$ at 298 K. These correspond to MD-0, MD-1, MD-2, MD-3 and MD-4 in Table 2, respectively. The CHP dimer was chosen in the present study since it was reported to represent the most stable structure in the gas phase [4,20]. In MD simulations of $[(BA)_2]_{\text{BEN}}$, the CHP dimer and 124 benzene molecules were put in a cubic box subject to periodic boundary conditions. The density of $[(BA)_2]_{\text{BEN}}$ was maintained at the liquid density of 0.874 g/cm³ [39]. The cutoff radius was half of the box length. The Ewald summation was employed to account for the long-range Coulomb interactions. The time step applied in solving the equations of motion was 0.5 fs. In order to systematically follow the changes in structures and stability of H-bonds in $(BA)_2$, two consecutive sets of equilibration were made before property calculations took place. In the first equilibration, the CHP dimer was treated as a supermolecule, in which both BA molecules were not allowed to move in the course of MD simulations. After the solvent molecules were well equilibrated, the second equilibration was made. All molecules, including both BA in the CHP dimer, were allowed to move in the second equilibration. Twenty thousand MD steps were devoted to each equilibration and another 20,000 steps to property calculations.

It was recognized that the cyclic H-bonds in the CHP dimer were considerably strong in pure benzene. After the second equilibration, the structures of the CHP dimer did not change substantially in the course of MD simulations. Since in the present case, the atom pair correlation functions ($g(R)$) between H-bond donor and acceptor showed only sharp peaks, it seems more informative and meaningful to analyze the structure and stability of the H-bond dimer based on the average H-bond distances ($\langle R_{\text{A-H}\cdots\text{B}} \rangle$) and angles ($\langle \theta_{\text{A-H}\cdots\text{B}} \rangle$), as well as the H-bond lifetimes ($\langle t_{\text{A-H}\cdots\text{B}} \rangle$). $\theta_{\text{A-H}\cdots\text{B}}$ is defined as the angle between the A–H bond and the line connecting atoms A and B. H-bond is considered to be strictly linear when $\langle \theta_{\text{A-H}\cdots\text{B}} \rangle$ is 0°. $\langle t_{\text{A-H}\cdots\text{B}} \rangle$ is defined as the percentage of simulation step during which H-bond donor and acceptor are coming close enough to engage in H-bond formation. Therefore, $\langle t_{\text{A-H}\cdots\text{B}} \rangle$ could be regarded as the probability of finding A–H \cdots B H-bond in the course of MD simulations. Since the H-bond lifetime depends upon the degree of association as well as the dynamic behavior of the interacting molecules, it can be used to measure the stability of H-bond complex. In the present work, H-bond donor and acceptor are considered to engage H-bond formation when the donor–acceptor distance is shorter than 4 Å. With this H-bond cutoff, the standard deviation (SD) of $\langle R_{\text{A-H}\cdots\text{B}} \rangle$ was found in the present work to be 0.36 Å at most.

The parameters employed in the present MD simulations are summarized in Table 2. MD simulations were made using the Moldy program written and maintained by Refson [40]. $\langle R_{\text{A-H}\cdots\text{B}} \rangle$ and $\langle \theta_{\text{A-H}\cdots\text{B}} \rangle$ with $\langle t_{\text{A-H}\cdots\text{B}} \rangle$

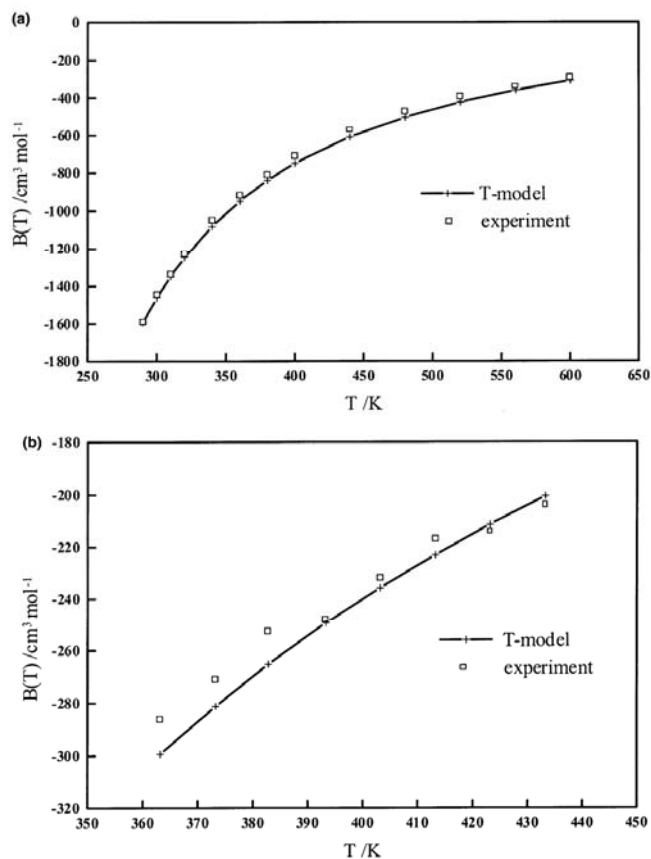


Fig. 1. (a) Second virial coefficients for benzene. (b) Second virial cross-coefficients for BEN-H₂O complex.

above 10% are presented in Table 3, together with snapshots of the most probable solute clusters extracted from the MD trajectory files. Molecules in the snapshot were numbered to simplify the discussion. For example, $\langle R_{A-H \dots B} \rangle(1-2)$ represents the average distance between the H-bond donor A-H in molecule (1) and the H-bond acceptor B in molecule (2). The energetic results of the benzene solutions were discussed based on the average solute-solute interaction energies $\langle (E_{\text{BEN}}^{\text{sol}}) \rangle$ and the average potential energies of benzene solutions $\langle (E_{\text{BEN}}^{\text{pot}}) \rangle$. They are included in Table 2. $\langle (E_{\text{BEN}}^{\text{sol}}) \rangle$ could be used to measure the deviation from the gas-phase structure. They were the results of the average over

MD steps. $\langle (E_{\text{BEN}}^{\text{pot}}) \rangle$ were the results of the average over MD steps as well as the number of solvent molecules.

Structures and stability of the BA-H₂O $m:n$ complexes, with m and $n = 1, 2$, in benzene solution were investigated and analyzed using the same approach. In the case of the BA-H₂O complexes, the gas-phase equilibrium structures reported in the previous work [20] were used as the starting configurations in MD simulations. In order to obtain information at lower temperature, additional MD simulations were performed on $[m:n]_{\text{BEN}}$ at 280 K. The temperature is slightly higher than the freezing point of pure benzene. They were represented by MD- χT in Tables 2 and 3.

Table 1
Parameters for the T-model potentials of benzene, benzoic acid and water

Atom	σ_i	ρ_i	q_i
BEN			
C	1.170780	0.291419	-0.092300
H	0.166423	0.251114	0.092300
BA^a			
O1	1.138607	0.236810	-0.548532
O2	1.129559	0.245188	-0.465275
C1	0.529477	0.396220	0.519581
C2	1.342103	0.214636	0.100950
C3	1.120595	0.307058	-0.180925
C4	1.245962	0.261224	-0.017924
C5	0.929315	0.367166	-0.124305
C6	1.329701	0.234160	-0.038697
C7	1.028291	0.337961	-0.164809
H1	-0.243465	0.288071	0.409564
H2	0.029207	0.270760	0.118136
H3	0.081551	0.269920	0.083979
H4	0.179658	0.228821	0.097361
H5	0.048919	0.283433	0.086936
H6	0.029352	0.265465	0.123960
H₂O^a			
O	1.284091	0.200370	-0.451660
H	-0.318644	0.331849	0.514110
D			-0.576560

D, a dummy charge on the C₂ axis of H₂O, 0.26 Å from oxygen and in the opposite direction of the lone pair.

^a Values taken from [20]

3. Results and discussions

In this section, structures and stability as well as some dynamic behaviors of the H-bond clusters in benzene solutions derived from MD simulations are discussed first. Then, comments are made on the results obtained from distribution experiments, especially the situation in benzene solutions.

Table 2
The MD results on (BA)₂ and BA H₂O complexes in benzene solutions

MD	System	T (K)	L (Å)	$\langle E_{\text{BEN}}^{\text{pot}} \rangle$ (kJ/mol)	$\langle E_{\text{BEN}}^{\text{sol-sol}} \rangle$ (kJ/mol)
MD-0	[(BA) ₂] _{BEN}	298	26.61	-36.73	-39.92
MD-1	[1:1] _{BEN}	298	26.52	-37.24	-21.03
MD-1T	[1:1] _{BEN}	280	26.52	-37.53	-22.85
MD-2	[1:2] _{BEN}	298	26.53	-37.33	-23.09
MD-2T	[1:2] _{BEN}	280	26.53	-37.90	-41.02
MD-3	[2:1] _{BEN}	298	26.50	-37.51	-50.78
MD-3T	[2:1] _{BEN}	280	26.50	-37.79	-56.22
MD-4	[2:2] _{BEN}	298	26.50	-37.76	-54.06
MD-4T	[2:2] _{BEN}	280	26.50	-38.37	-51.07

The number of benzene molecules in [(BA)₂]_{BEN}, [1:1]_{BEN} and [1:2]_{BEN} are 124 and those in [2:1]_{BEN} and [2:2]_{BEN} are 122. [(BA)₂]_{BEN}, benzoic acid in benzene solution; [1:1]_{BEN}, BA H₂O 1:1 complex in benzene solution; [1:2]_{BEN}, BA H₂O 1:2 complex in benzene solution; [2:1]_{BEN}, BA H₂O 2:1 complex in benzene solution; [2:2]_{BEN}, BA H₂O 2:2 complex in benzene solution; L, simulation box length; $\langle E_{\text{BEN}}^{\text{pot}} \rangle$, average potential energy of benzene solution; $\langle E_{\text{BEN}}^{\text{sol-sol}} \rangle$, average solute-solute interaction energy.

3.1. [(BA)₂]_{BEN}

The results of MD-0 suggest that the cyclic H-bonds in (BA)₂ are very associated in pure benzene, with $\langle t_{\text{O1-H}\cdots\text{O2}} \rangle(1-2)$ and $\langle t_{(2-1)} \rangle$ about 100%. The CHP structure changed only slightly in the course of MD simulations. $\langle R_{\text{O1-H}\cdots\text{O2}} \rangle(1-2)$ and $\langle E_{\text{BEN}}^{\text{sol-sol}} \rangle$ derived from MD-0 are 2.93 Å and -39.92 kJ/mol, respectively. The average H-bond distance is only 0.05 Å longer than the gas-phase structure [20]. $\langle E_{\text{BEN}}^{\text{sol-sol}} \rangle$ is about 7 kJ/mol higher than the interaction energy of the CHP dimer in the gas phase [20], and comparable with the enthalpy of dimerization in benzene derived from experiment, 37.6 kJ/mol [12].

3.2. [1:1]_{BEN}

The gas phase structure of the BA-H₂O 1:1 complex [20], in which the O1-H1 group of BA acts as proton donor toward oxygen of water, did not change much in the course of MD simulations. The results of MD-1 reveal that the O1-H1...O_w H-bond is quite strong in benzene. The H-bond interaction energy ($\langle E_{\text{BEN}}^{\text{sol-sol}} \rangle$) of [1:1]_{BEN} at 298 K is -21.03 kJ/mol, compared with the gas phase of -32.33 kJ/mol [20]. The statistical analysis of H-bond in Table 3(b) shows that water spends most of the time at the hydroxyl group of BA, with the H-bond lifetime ($\langle t_{\text{O1-H1}\cdots\text{Ow}} \rangle(2-1)$) of about 100%. $\langle R_{\text{O1-H1}\cdots\text{Ow}} \rangle(2-1)$ and $\langle \theta_{\text{O1-H1}\cdots\text{Ow}} \rangle(2-1)$ derived from MD-1 are 2.88 Å and 21.43°, respectively. For the BA-H₂O 1:1 complex, the probability of finding the cyclic H-bond structure could be inferred from $\langle t_{\text{Ow-Hw}\cdots\text{O2}} \rangle(1-2)$. In [1:1]_{BEN} at 298 K, $\langle t_{\text{Ow-Hw}\cdots\text{O2}} \rangle(1-2)$ is about 22%.

The MD results on [1:1]_{BEN} at 298 and 280 K are virtually the same. At lower temperature, the degree of H-bond association is slightly higher as expected. The probability of finding the cyclic H-bond structure ($\langle t_{\text{Ow-Hw}\cdots\text{O2}} \rangle(1-2)$) increases to 35%. $\langle E_{\text{BEN}}^{\text{sol-sol}} \rangle$ of [1:1]_{BEN} at 280 K is -22.85 kJ/mol, with $\langle R_{\text{O1-H1}\cdots\text{Ow}} \rangle$

Table 3
Some average H-bond distances ($\langle R_{A-H \cdots B} \rangle$) and angles ($\langle \theta_{A-H \cdots B} \rangle$), as well as the H-bond lifetimes ($\langle t_{A-H \cdots B} \rangle$), derived from MD simulations

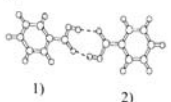
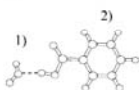
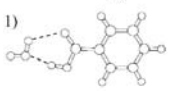
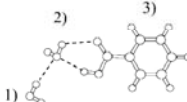
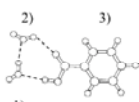
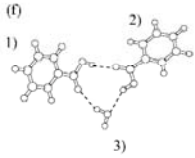
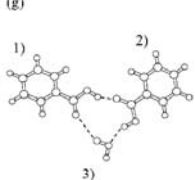
	MD-0:[(BA)] _{BEN}	298 K	SD
(a) 	O1 H1...O2(1 2) and (2 1)	$\langle R_{O1-H1 \cdots O2} \rangle$	2.93
		$\langle \theta_{O1-H1 \cdots O2} \rangle$	17.98
		$\langle t_{O1-H1 \cdots O2} \rangle$	100.0
(b) 	O1 H1...Ow(2 1)	$\langle R_{O1-H1 \cdots Ow} \rangle$	2.88
		$\langle \theta_{O1-H1 \cdots Ow} \rangle$	21.43
		$\langle t_{O1-H1 \cdots Ow} \rangle$	100.0
Ow Hw...O2(1 2)	$\langle R_{Ow-Hw \cdots O2} \rangle$	2.91	0.20
	$\langle \theta_{Ow-Hw \cdots O2} \rangle$	44.05	7.59
	$\langle t_{Ow-Hw \cdots O2} \rangle$	21.5	
(c) 	O1 H1...Ow(2 1)	$\langle R_{O1-H1 \cdots Ow} \rangle$	2.88
		$\langle \theta_{O1-H1 \cdots Ow} \rangle$	20.81
		$\langle t_{O1-H1 \cdots Ow} \rangle$	98.7
Ow Hw...O2(1 2)	$\langle R_{Ow-Hw \cdots O2} \rangle$	2.94	0.20
	$\langle \theta_{Ow-Hw \cdots O2} \rangle$	44.44	7.51
	$\langle t_{Ow-Hw \cdots O2} \rangle$	34.8	
(d) 	O1 H1...Ow(3 2)	$\langle R_{O1-H1 \cdots Ow} \rangle$	2.95
		$\langle \theta_{O1-H1 \cdots Ow} \rangle$	24.11
		$\langle t_{O1-H1 \cdots Ow} \rangle$	77.2
Ow Hw...O2(2 3)	$\langle R_{Ow-Hw \cdots O2} \rangle$	3.07	0.30
	$\langle \theta_{Ow-Hw \cdots O2} \rangle$	38.90	11.92
	$\langle t_{Ow-Hw \cdots O2} \rangle$	26.4	
Ow Hw...Ow(2 1)	$\langle R_{Ow-Hw \cdots Ow} \rangle$	3.08	0.24
	$\langle \theta_{Ow-Hw \cdots Ow} \rangle$	28.44	14.82
	$\langle t_{Ow-Hw \cdots Ow} \rangle$	28.2	
Ow Hw...Ow(1 2)	$\langle R_{Ow-Hw \cdots Ow} \rangle$	3.11	0.21
	$\langle \theta_{Ow-Hw \cdots Ow} \rangle$	31.07	15.43
	$\langle t_{Ow-Hw \cdots Ow} \rangle$	12.6	
(e) 	O1 H1...Ow(3 1)	$\langle R_{O1-H1 \cdots Ow} \rangle$	2.94
		$\langle \theta_{O1-H1 \cdots Ow} \rangle$	17.39
		$\langle t_{O1-H1 \cdots Ow} \rangle$	100.0
Ow Hw...O2(2 3)	$\langle R_{Ow-Hw \cdots O2} \rangle$	3.09	0.27
	$\langle \theta_{Ow-Hw \cdots O2} \rangle$	31.40	12.79
	$\langle t_{Ow-Hw \cdots O2} \rangle$	50.7	
Ow Hw...O2(2 3)	$\langle R_{Ow-Hw \cdots O2} \rangle$	3.14	0.30
	$\langle \theta_{Ow-Hw \cdots O2} \rangle$	29.58	13.09
	$\langle t_{Ow-Hw \cdots O2} \rangle$	39.6	
Ow Hw...O2(1 3)	$\langle R_{Ow-Hw \cdots O2} \rangle$	3.03	0.26
	$\langle \theta_{Ow-Hw \cdots O2} \rangle$	47.79	6.87
	$\langle t_{Ow-Hw \cdots O2} \rangle$	11.0	
Ow Hw...O2(1 3)	$\langle R_{Ow-Hw \cdots O2} \rangle$	3.05	0.19
	$\langle \theta_{Ow-Hw \cdots O2} \rangle$	47.37	8.23
	$\langle t_{Ow-Hw \cdots O2} \rangle$	11.1	

Table 3 (continued)

	Ow Hw...Ow(1 2)	$\langle R_{Ow-Hw...Ow} \rangle$ $\langle \beta_{Ow-Hw...Ow} \rangle$ $\langle t_{Ow-Hw...Ow} \rangle$	3.19 28.90 39.5	0.28 13.51
	Ow Hw...Ow(1 2)	$\langle R_{Ow-Hw...Ow} \rangle$ $\langle \beta_{Ow-Hw...Ow} \rangle$ $\langle t_{Ow-Hw...Ow} \rangle$	3.25 26.24 33.8	0.29 13.75
(f)	MD-3:[2:1] _{BEN}	298 K		SD
	O1 H1...O1(1 2)	$\langle R_{O1-H1...O1} \rangle$ $\langle \beta_{O1-H1...O1} \rangle$ $\langle t_{O1-H1...O1} \rangle$	3.57 39.14 29.7	0.25 9.50
	O1 H1...O1(2 1)	$\langle R_{O1-H1...O1} \rangle$ $\langle \beta_{O1-H1...O1} \rangle$ $\langle t_{O1-H1...O1} \rangle$	3.65 47.00 12.2	0.26 5.96
	O1 H1...O2(1 2)	$\langle R_{O1-H1...O2} \rangle$ $\langle \beta_{O1-H1...O2} \rangle$ $\langle t_{O1-H1...O2} \rangle$	3.07 24.87 80.1	0.32 15.10
	O1 H1...Ow(1 3)	$\langle R_{O1-H1...Ow} \rangle$ $\langle \beta_{O1-H1...Ow} \rangle$ $\langle t_{O1-H1...Ow} \rangle$	3.15 27.17 61.4	0.36 16.23
	O1 H1...Ow(2 3)	$\langle R_{O1-H1...Ow} \rangle$ $\langle \beta_{O1-H1...Ow} \rangle$ $\langle t_{O1-H1...Ow} \rangle$	2.92 18.07 100.0	0.23 9.23
	Ow Hw...O2(3 2)	$\langle R_{Ow-Hw...O2} \rangle$ $\langle \beta_{Ow-Hw...O2} \rangle$ $\langle t_{Ow-Hw...O2} \rangle$	2.94 45.41 18.3	0.24 8.96
	Ow Hw...O2(3 1)	$\langle R_{Ow-Hw...O2} \rangle$ $\langle \beta_{Ow-Hw...O2} \rangle$ $\langle t_{Ow-Hw...O2} \rangle$	3.01 25.95 27.8	0.25 13.54
	Ow Hw...O2(3 1)	$\langle R_{Ow-Hw...O2} \rangle$ $\langle \beta_{Ow-Hw...O2} \rangle$ $\langle t_{Ow-Hw...O2} \rangle$	3.11 36.59 39.6	0.31 12.87
(g)	MD-3T:[2:1] _{BEN}	280 K		SD
	O1 H1...O2(1 2)	$\langle R_{O1-H1...O2} \rangle$ $\langle \beta_{O1-H1...O2} \rangle$ $\langle t_{O1-H1...O2} \rangle$	2.89 18.50 100.0	0.16 10.51
	O1 H1...Ow(2 3)	$\langle R_{O1-H1...Ow} \rangle$ $\langle \beta_{O1-H1...Ow} \rangle$ $\langle t_{O1-H1...Ow} \rangle$	2.92 13.50 100.0	0.19 7.45
	Ow Hw...O2(3 2)	$\langle R_{Ow-Hw...O2} \rangle$ $\langle \beta_{Ow-Hw...O2} \rangle$ $\langle t_{Ow-Hw...O2} \rangle$	3.13 48.13 18.2	0.23 6.76
	Ow Hw...O2(3 2)	$\langle R_{Ow-Hw...O2} \rangle$ $\langle \beta_{Ow-Hw...O2} \rangle$ $\langle t_{Ow-Hw...O2} \rangle$	3.04 48.85 13.0	0.17 5.99
	Ow Hw...O2(3 1)	$\langle R_{Ow-Hw...O2} \rangle$ $\langle \beta_{Ow-Hw...O2} \rangle$ $\langle t_{Ow-Hw...O2} \rangle$	3.27 20.99 59.6	0.30 10.93

(continued on next page)

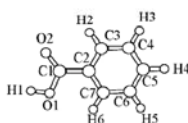
Table 3 (continued)

	$O_w H_w \cdots O_2(3\ 1)$	$\langle R_{O_w-H_w \cdots O_2} \rangle$	3.43	0.26	
		$\langle \beta_{O_w-H_w \cdots O_2} \rangle$	20.01	11.56	
		$\langle t_{O_w-H_w \cdots O_2} \rangle$	31.4		
	MD-4:[2:2] _{BEN}	298 K		SD	
(h)		O1 H1...O1(1 2)	$\langle R_{O1-H1 \cdots O1} \rangle$	3.24	0.30
			$\langle \beta_{O1-H1 \cdots O1} \rangle$	17.75	11.57
			$\langle t_{O1-H1 \cdots O1} \rangle$	29.0	
		O1 H1...O2(1 2)	$\langle R_{O1-H1 \cdots O2} \rangle$	2.98	0.28
			$\langle \beta_{O1-H1 \cdots O2} \rangle$	22.83	12.34
			$\langle t_{O1-H1 \cdots O2} \rangle$	69.4	
		O1 H1...Ow(2 4)	$\langle R_{O1-H1 \cdots O_w} \rangle$	2.93	0.21
			$\langle \beta_{O1-H1 \cdots O_w} \rangle$	22.03	11.43
			$\langle t_{O1-H1 \cdots O_w} \rangle$	93.6	
		Ow Hw...O2(4 2)	$\langle R_{O_w-H_w \cdots O_2} \rangle$	2.94	0.21
	$\langle \beta_{O_w-H_w \cdots O_2} \rangle$	44.40	7.48		
	$\langle t_{O_w-H_w \cdots O_2} \rangle$	29.4			
Ow Hw...O2(4 2)	$\langle R_{O_w-H_w \cdots O_2} \rangle$	3.01	0.23		
	$\langle \beta_{O_w-H_w \cdots O_2} \rangle$	45.63	7.50		
	$\langle t_{O_w-H_w \cdots O_2} \rangle$	11.2			
Ow Hw...O2(3 1)	$\langle R_{O_w-H_w \cdots O_2} \rangle$	3.18	0.30		
	$\langle \beta_{O_w-H_w \cdots O_2} \rangle$	27.34	13.85		
	$\langle t_{O_w-H_w \cdots O_2} \rangle$	49.3			
Ow Hw...O2(3 1)	$\langle R_{O_w-H_w \cdots O_2} \rangle$	3.14	0.30		
	$\langle \beta_{O_w-H_w \cdots O_2} \rangle$	29.04	14.20		
	$\langle t_{O_w-H_w \cdots O_2} \rangle$	39.9			
	MD-4T:[2:2] _{BEN}	280 K		SD	
(i)		O1 H1...O1(1 2)	$\langle R_{O1-H1 \cdots O1} \rangle$	3.02	0.24
			$\langle \beta_{O1-H1 \cdots O1} \rangle$	24.74	11.16
			$\langle t_{O1-H1 \cdots O1} \rangle$	50.4	
		O1 H1...Ow(2 3)	$\langle R_{O1-H1 \cdots O_w} \rangle$	2.89	0.18
			$\langle \beta_{O1-H1 \cdots O_w} \rangle$	16.62	8.89
			$\langle t_{O1-H1 \cdots O_w} \rangle$	100.0	
		O1 H1...Ow(2 4)	$\langle R_{O1-H1 \cdots O_w} \rangle$	3.54	0.34
			$\langle \beta_{O1-H1 \cdots O_w} \rangle$	39.58	10.36
			$\langle t_{O1-H1 \cdots O_w} \rangle$	14.6	
		Ow Hw...O2(3 1)	$\langle R_{O_w-H_w \cdots O_2} \rangle$	3.15	0.30
	$\langle \beta_{O_w-H_w \cdots O_2} \rangle$	35.20	11.96		
	$\langle t_{O_w-H_w \cdots O_2} \rangle$	16.9			
Ow Hw...O2(3 2)	$\langle R_{O_w-H_w \cdots O_2} \rangle$	2.99	0.25		
	$\langle \beta_{O_w-H_w \cdots O_2} \rangle$	43.71	9.32		
	$\langle t_{O_w-H_w \cdots O_2} \rangle$	14.0			
Ow Hw...O2(4 2)	$\langle R_{O_w-H_w \cdots O_2} \rangle$	3.03	0.21		
	$\langle \beta_{O_w-H_w \cdots O_2} \rangle$	28.78	13.91		
	$\langle t_{O_w-H_w \cdots O_2} \rangle$	17.8			
Ow Hw...O2(4 2)	$\langle R_{O_w-H_w \cdots O_2} \rangle$	3.10	0.29		
	$\langle \beta_{O_w-H_w \cdots O_2} \rangle$	32.88	14.05		
	$\langle t_{O_w-H_w \cdots O_2} \rangle$	12.8			

Table 3 (continued)

Ow Hw...Ow(3 4)	$\langle R_{Ow-Hw...Ow} \rangle$	3.16	0.22
	$\langle \theta_{Ow-Hw...Ow} \rangle$	29.20	13.83
	$\langle t_{Ow-Hw...Ow} \rangle$	39.3	
Ow Hw...Ow(3 4)	$\langle R_{Ow-Hw...Ow} \rangle$	3.17	0.30
	$\langle \theta_{Ow-Hw...Ow} \rangle$	29.97	14.14
	$\langle t_{Ow-Hw...Ow} \rangle$	45.7	

Only solute clusters are shown in the table. The numbering system for the carboxylic acid is



SD, standard deviation; (A H...B), H-bond donor-acceptor pair between molecules A and B, distance and angle are in Å and °, respectively.

(2-1) and $\langle \theta_{O1-H1...Ow} \rangle(2-1)$ of 2.88 Å and 20.81°, respectively.

3.3. [1:2]_{BEN}

For [1:2]_{BEN}, the MD results at 280 and 298 K are quite different. Two forms of the BA-H₂O complex dominate in benzene solutions. In the course of MD simulations at 298 K, the gas phase cyclic structure [20], employed as the starting geometry, was converted into a partially open H-bond structure, resembling in [1:1]_{BEN}. The probability of finding the cyclic BA-H₂O 1:1 like structure ($\langle t_{Ow-Hw...O2} \rangle(2-3)$) is about 26%. The H-bond lifetime ($\langle t_{O1-H1...Ow} \rangle(3-2)$) in Table 3(d) indicates that the O1-H1...Ow H-bond in [1:2]_{BEN} is less associated compared to [1:1]_{BEN}, with a slightly longer $\langle R_{O1-H1...Ow} \rangle(3-2)$. The presence of $\langle t_{Ow-Hw...Ow} \rangle(1-2)$ and $\langle t_{Ow-Hw...Ow} \rangle(2-1)$ reflects the possibility for the H-bond donor-acceptor pair exchange between water molecules in [1:2]_{BEN}. This dynamic process could be regarded as non-mutual H-bond exchange as in NMR spectroscopy. The non-mutual H-bond exchange leads in this case to the total probability of the Ow-Hw...Ow H-bond formation of about 41%. $\langle E_{BEN}^{sol} \rangle$ for [1:2]_{BEN} at 298 K is -23.09 kJ/mol, slightly lower than [1:1]_{BEN}. In the gas phase, a similar BA-H₂O 1:2 complex was reported to possess the interaction energy of -50.55 kJ/mol, structure c in [20].

The gas phase cyclic structure did not change appreciably in the course of MD simulations at 280 K. The values of $\langle E_{BEN}^{sol} \rangle$ in Table 2 and $\langle t_{A-H...B} \rangle$ in Table 3(e) reveal that H-bonds in the BA-H₂O 1:2 complex become more associated and the molecular motions are rather restricted at lower temperature. Consequently,

the probability of the non-mutual H-bond exchange is disappeared at 280 K. At this temperature, however, there exist another type of H-bond exchange process, in which a water molecule executes rotation leading to the H-bond donor exchange within the same water molecule. This dynamics exchange is regarded as mutual H-bond exchange in NMR spectroscopy. In this case, the total probability of the Ow-Hw...Ow H-bond formation ($\langle t_{Ow-Hw...Ow} \rangle(1-2)$) increases to about 73%. The mutual H-bond exchange also leads to an increase in the total probability of the cyclic H-bond formation ($\langle t_{Ow-Hw...O2} \rangle(2-3)$) to about 90%. $\langle E_{BEN}^{sol} \rangle$ for [1:2]_{BEN} at 280 K is -41.02 kJ/mol, compared with -60.30 kJ/mol in the gas phase [20]. The probability of finding the cyclic BA-H₂O 1:1 like structure in [1:2]_{BEN} seems to be decreased. The total probability of the Ow-Hw...O2 H-bond formation ($\langle t_{Ow-Hw...O2} \rangle(1-3)$) in [1:2]_{BEN} at 280 K is only about 22%.

3.4. [2:1]_{BEN}

In benzene solution, the probability of breaking H-bonds in the CHP dimer by water is evident from the MD-3 and MD-3T simulations. On average, the gas phase structure applied as the starting configuration, did not change substantially in the course of MD simulations of [2:1]_{BEN}. The O1-H1...Ow, O1-H1...O2 and Ow-Hw...O2 H-bonds are still responsible for the molecular associations as in the gas phase. However, dynamic H-bond exchanges take place in [2:1]_{BEN} at both temperatures.

At 298 K, the O1-H1...O2 and O1-H1...Ow H-bonds are the two major contributors for the cluster association. $\langle t_{O1-H1...O2} \rangle(1-2)$ and $\langle t_{O1-H1...Ow} \rangle(2-3)$ are

about 80% and 100%, respectively. Besides, there exists the possibility for the non-mutual H-bond exchange between BA molecules. The total probability of the O1–H1...O1 H-bond formation ($\langle t_{O1-H1...O1}(1-2) \rangle$ and $\langle t_{O1-H1...O1}(2-1) \rangle$) is about 42%. Similarly, due to the mutual H-bond exchange, the total probability of the O_w–H_w...O2 H-bond formation ($\langle t_{O_w-H_w...O_2}(3-1) \rangle$) increase to about 67% at 298 K. Since water molecule could form the cyclic BA–H₂O 1:1 like complex with both BA molecules, the corresponding probabilities could be estimated using $\langle t_{O_w-H_w...O_2}(3-2) \rangle$ and $\langle t_{O1-H1...O_w}(1-3) \rangle$. At 298 K, they are about 18% and 61%, respectively.

Due to the restriction in molecular motions at lower temperature, the probability of the non-mutual H-bond exchange is disappeared at 280 K. The O1–H1...O2 and O1–H1...O_w H-bonds become very associated, with $\langle t_{O1-H1...O_2}(1-2) \rangle$ and $\langle t_{O1-H1...O_w}(2-3) \rangle$ of approximately 100%. The cyclic H-bond structure in Table 3(g) seems to occupy about 91% of the simulation time, as can be seen from the values of $\langle t_{O_w-H_w...O_2}(3-1) \rangle$. At 280 K, water tends to form the cyclic BA–H₂O 1:1 like complex with only one BA molecule. The total probability of the O_w–H_w...O2 H-bond formation ($\langle t_{O_w-H_w...O_2}(3-2) \rangle$) in this case is about 31%. $\langle E_{BEN}^{sol} \rangle$ in [2:1]_{BEN} at 280 and 298 K are –56.22 and –50.78 kJ/mol, respectively, compared with the interaction energy in the gas phase of –66.87 kJ/mol [20].

3.5. [2:2]_{BEN}

Due to the increase in the H-bond cluster size, the situation in [2:2]_{BEN} are quite different from [2:1]_{BEN}. In the course of MD-4 simulations, the gas phase structure of the BA–H₂O 2:2 complex [20] was weakened and transformed into the structure shown in Table 3(h). At 298 K, water molecule tends to H-bond directly to each BA. No direct evidence shows the existence of the O_w–H_w...O_w H-bond in [2:2]_{BEN} at 298 K. The MD-4 results in Table 3(h) also indicate that, on average, both BA molecules link together through the O1–H1...O2 H-bond, with $\langle t_{O1-H1...O_2}(1-2) \rangle$ of about 69%. In [2:2]_{BEN} at 298 K, there exists the probability of the O1–H1...O1 H-bond formation ($\langle t_{O1-H1...O_1}(1-2) \rangle$) of about 29%. The probability of the BA–H₂O 1:1 like complex formation could be inferred from $\langle t_{O1-H1...O_w}(2-4) \rangle$ and $\langle t_{O_w-H_w...O_2}(3-1) \rangle$. They are about 94% and 89%, respectively. The total probability of the cyclic BA–H₂O 1:1 like complex formation, inferred from $\langle t_{O_w-H_w...O_2}(4-2) \rangle$, is about 41%. $\langle E_{BEN}^{sol} \rangle$ derived from MD-4 is –54.06 kJ/mol.

The average H-bond structure in [2:2]_{BEN} at 280 K is similar to [2:1]_{BEN}. However, in this case, the O1–H1...O1 H-bond is responsible for the weak linkage between the two BA molecules. The probability of the O1–H1...O1 H-bond formation ($\langle t_{O1-H1...O_1}(1-2) \rangle$) is only about 50%. On average, only one water molecule

forms cyclic H-bonds with both BA molecules, with a particularly strong preference of the O1–H1...O_w H-bond. The results of MD-4T indicate further that, in [2:2]_{BEN} at 280 K, water molecules form strong cluster among themselves. The presence of the mutual H-bond exchange results in the probability of the O_w–H_w...O_w H-bond formation of about 85%. Since the H-bond between water molecules are quite strong, the existence of $\langle t_{O_w-H_w...O_2}(4-2) \rangle$ reflects the probability of finding the cyclic BA–H₂O 1:2 complex, as in Table 3(e). The total probability in this case is about 31%. $\langle E_{BEN}^{sol} \rangle$ for [2:2]_{BEN} at 280 K is slightly higher than at 298 K. The value of $\langle t_{O_w-H_w...O_2}(3-2) \rangle$ reveals a small probability to detect the cyclic BA–H₂O 1:1 like structure in [2:2]_{BEN} at 280 K.

3.6. Partition of benzoic acid between the benzene and water phases

As mentioned in Section 1 that the partition of BA between the benzene and water phases represents one of the classical problems in the area of molecular association in solutions. At least three important observations in the benzene phase were addressed from experiments [9,11,12,14,15]. They concerned primarily with the structures of the solute clusters, the number of water molecule H-bonding directly at BA and the possibility for water molecules to self-associate in the benzene phase. It was proposed in [14,15] that part of water which dissolves together with BA in the benzene phase is not H-bonded together and water molecules in the benzene phase prefer to H-bond directly with BA. Based on the assumption that the hydrated (BA)₂ can be ignored, it was shown that the concentration of H-bonded water increases along with the increase of the BA monomer. With this experimental information, the authors [14,15] postulated the existence of the BA–H₂O 1:1 complex in dilute benzene solution. Different observations and interpretations were reported in [11,18], in which the authors claimed that the excess of water solubility could be explained in terms of the self-association of water molecules in the benzene phase. They also pointed out that two water molecules hydrate a single BA molecule as well as (BA)₂ in the benzene phase.

Based on the information obtained from MD simulations, we could give some comments on the situations in the benzene phase. Our MD results show that nearly all H-bond complexes proposed in experiment [11] exist in the benzene phase, with different lifetimes. The probabilities of finding these H-bond complexes depend mainly on their size and temperature. The cyclic BA–H₂O 1:1 like complex seems to exist more or less in all benzene solutions considered. This supports the conclusion made in [14,15]. The MD results also suggest self-associations of water in [1:2]_{BEN} at 280 and 298 K, and [2:2]_{BEN} at 280 K. However, due to the strength of the O1–H1–

O_W H-bond, the water clusters tend not to be isolated from BA. From the MD results on $[2:2]_{\text{BEN}}$ at 298 K, water molecules could also stay separate from each other. This agrees well with the experimental observation that part of water molecules dissolving together with BA is not H-bonded together [14,15]. General trends are observed when the temperature is lowered from 298 to 280 K namely, the solute clusters become more associated, accompanied by some structural changes especially for large clusters. The temperature effects on the structures and stability of the BA–H₂O $m:n$ complexes have never been addressed in detail in the previous theoretical and experimental reports [9,11,12,14,15]. In our opinion, different conclusions made from experiments are not completely disagreed. They could be attributed to limitations, conditions and approximations adopted in experiments, as well as the lack of microscopic information. Therefore, modern high-resolution spectroscopic techniques are required to investigate the structures and stability of the BA–H₂O complexes in benzene solutions in details.

4. Conclusion

Attempt was made in the present work to examine structures and stability of the solute clusters formed from BA and water in benzene solution. A series of MD simulations at 280 and 298 K were conducted on $[(\text{BA})_2]_{\text{BEN}}$, as well as $[m:n]_{\text{BEN}}$ with m and $n = 1, 2$. Since the solute–solvent and solvent–solvent interactions are rather moderate in $[m:n]_{\text{BEN}}$ the solvation shells around the solute clusters are expected to be weak and mobile, especially at room temperature. This allows the thermal energy and the structure of the solvation shells to play important roles in determining structures and stability of the BA–H₂O $m:n$ clusters.

The present results revealed that, due to the solvent effects, some microhydrates not particularly associated in the gas phase appeared with quite long lifetime in the course of MD simulations. This reflects the impact of weak but complicated solute–solvent and solvent–solvent interactions, such as C–H··· π , O–H··· π and π – π interactions, on the structures and stability of the H-bond clusters. This seems to agree with the assumption that, if the solute–solvent interaction is much greater than that of the solvent–solvent, then the latter may be ignored. If, however, both the solute–solvent and the solvent–solvent interactions are comparable, then the latter cannot be ignored.

In MD simulations, two types of H-bond exchanges were recognized namely, the mutual and non-mutual H-bond exchanges. The H-bond exchanges were detected since the dynamic behaviors were taken into account in the present theoretical investigations. This allows us to provide insight into the dynamic behaviors

of the interacting molecules in the microscopic scale. The presence of the H-bond exchanges also implies that equilibrium static structures obtained from molecular mechanics (MM) or ab initio energy minimization with continuum model are not complete enough to represent the systems with complicated solute–solvent and solvent–solvent interactions, such as in $[m:n]_{\text{BEN}}$. The approach adopted in the present work is, therefore, appropriate, since the structures of the BA–H₂O complexes were derived in the presence of benzene molecules, and their stability was discussed in terms of probabilities obtained based on the dynamic behaviors of all interacting molecules in the systems.

It should be mentioned that the MD simulations conducted in this work were based on pair-wise additive intermolecular potentials, in which the many-body contributions were not taken into account. Although the solute–solvent and solvent–solvent interactions are very important in the present case, they are not particularly strong. We, therefore, expect that the inclusion of the cooperative effects could lead to slightly stronger H-bond clusters, as well as solvation shells around them. This should not lead to significant change in the structures and stability of the H-bond clusters reported here. The authors wish that the MD results are able to provide additional piece of important information and can attract more attention from theoretician and experimentalist to further investigate this complicated non-aqueous interacting system using more advanced theoretical and spectroscopic techniques.

Acknowledgments

All calculations were performed at Compaq alpha XP1000 and Compaq alpha DS20 at the School of Chemistry and the School of Physics, Suranaree University of Technology (SUT). The authors thank Supaporn Chaiyapongs for reading the manuscript. This work was partially supported by the ASEA-UNINET and the University of Innsbruck, Austria.

References

- [1] Y.K. Park, R.B. Gupta, C.W. Curtis, C.B. Roberts, *J. Phys. Chem. B* 106 (2002) 9696.
- [2] C.S. Claybourne, *J. Phys. Chem.* 76 (1972) 774.
- [3] T. Nakabayashi, H. Sato, F. Hirata, N. Nishi, *J. Phys. Chem. A* 105 (2001) 245.
- [4] J. Chocholousova, J. Vacek, P. Hobza, *J. Phys. Chem. A* 107 (2003) 3086.
- [5] S.D. Christian, H.E. Afsprung, S.A. Taylor, *J. Phys. Chem.* 67 (1963) 187.
- [6] Y. Fujii, H. Yamada, M. Mizuta, *J. Phys. Chem.* 92 (1988) 6768.
- [7] G. Allen, J.G. Watkinson, K.H. Webb, *Spectrochim. Acta* 22 (1966) 807.

- [8] F. Yukio, Y. Hiromichi, M. Masateru, *J. Phys. Chem.* 92 (1988) 6768.
- [9] F.T. Wall, P.E. Rouse Jr., *J. Am. Chem. Soc.* 63 (1941) 3002.
- [10] F.T. Wall, *J. Am. Chem. Soc.* 64 (1942) 472.
- [11] R. Van Duyn, S.A. Taylor, S.D. Christian, H.E. Afsprung, *J. Phys. Chem.* 71 (1967) 3427.
- [12] A.K.M. Shamsul Huq, S.A.K. Lodhi, *J. Phys. Chem.* 70 (1966) 1354.
- [13] N.S. Zaugg, S.P. Steed, E.M. Woolley, *Thermochim. Acta* 3 (1972) 349.
- [14] E. Wieckowska, W. Pawlowski, *Z. Phys. Chem. Neue Folge* 166 (1990) 167.
- [15] W. Pawlowski, E. Wieckowska, *Z. Phys. Chem. Neue Folge* 168 (1990) 205.
- [16] H. Yamada, K. Yajima, H. Wada, G. Nakagawa, *Talanta* 42 (1995) 789.
- [17] W. Nernst, *Z. Phys. Chem. Neue Folge* 8 (1891) 110.
- [18] L. Barcza, A. Buvari, M. Vajda, *Z. Phys. Chem. Neue Folge* 102 (1976) 35.
- [19] Y. Hasegawa, T. Unno, G.R. Choppin, *J. Inorg. Nucl. Chem.* 43 (1981) 2154.
- [20] K. Sagarik, B.M. Rode, *Chem. Phys.* 260 (2000) 159.
- [21] C.J. Gruenloh, F.C. Hagemeister, J.R. Carney, T.S. Zwier, *J. Phys. Chem. A* 103 (1999) 503.
- [22] C.J. Gruenloh, G.M. Florio, J.R. Carney, F.C. Hagemeister, T.S. Zwier, *J. Phys. Chem. A* 103 (1999) 496.
- [23] S. Urahata, K. Coutinho, S. Canuto, *Chem. Phys. Lett.* 274 (1997) 269.
- [24] K.P. Sagarik, R. Ahlrichs, S. Brode, *Mol. Phys.* 57 (1986) 1247.
- [25] K.P. Sagarik, R. Ahlrichs, *J. Chem. Phys.* 86 (1987) 5117.
- [26] K.P. Sagarik, V. Pongpituk, S. Chaiyapongs, P. Siset, *Chem. Phys.* 156 (1991) 439.
- [27] K.P. Sagarik, *J. Mol. Struct. (Theochem.)* 465 (1999) 141.
- [28] K.P. Sagarik, R. Ahlrichs, *Chem. Phys. Lett.* 131 (1986) 74.
- [29] K.P. Sagarik, E. Spohr, *Chem. Phys.* 199 (1995) 73.
- [30] K.P. Sagarik, P. Asawakun, *Chem. Phys.* 219 (1997) 173.
- [31] H.J. Boehm, R. Ahlrichs, *J. Chem. Phys.* 77 (1982) 2028.
- [32] H.J. Boehm, C. Meissner, R. Ahlrichs, *Mol. Phys.* 53 (1984) 651.
- [33] H.J. Boehm, R. Ahlrichs, *Mol. Phys.* 55 (1985) 1159.
- [34] D.E. Williams, R.R. Weller, *J. Am. Chem. Soc.* 105 (1983) 4143.
- [35] C.M. Breneman, K.B. Wiberg, *J. Comput. Chem.* 11 (1990) 361.
- [36] J.H. Dymond, E.B. Smith, *The Virial Coefficients of Pure Gases and Mixtures*, Clarendon Press, Oxford, 1980.
- [37] O. Matsuoka, E. Clementi, M. Yoshimine, *J. Chem. Phys.* 64 (1976) 1351.
- [38] C.J. Wormald, N.M. Lancaster, C.J. Sowden, *J. Chem. Soc., Faraday Trans.* 93 (1997) 1921.
- [39] Selected values of Physical and Thermodynamics Properties of Hydrocarbons and Related Compounds, American Petroleum Institute Research Project 44, Carnegie Press, Pittsburg, 1953.
- [40] K. Refson, *MOLDY*, User's Manual, Department of Earth Science, Oxford University, 1999.

CURRICULUM VATAE

MISS SERMSIRI CHAIWONGWATTANA

Birth : February 19, 1977 in Nakhon Ratchasima, Thailand **Citizenship :** Thailand

Father's name : Tee Chaiwongwattana

Mother's name : Thanyathip Chaiwongwattananukul

Education :

1995 – 1998 B. Sc. in Chemistry, Khon Kaen University, Khon Kaen, Thailand

2002 – 2008 Ph.D. in Chemistry, Suranaree University of Technology,
Nakhon Ratchasima, Thailand

Experiences :

May, 1998 – April, 2002 Chemist, J. V. C. component company,
Nakhon Ratchasima, Thailand

October, 2005 – January, 2006 Scholar Visitor, Department of Chemistry and
Biochemistry, California State University,
Fullerton, Orange, California, United States

February, 2008 – May, 2008 Scholar Visitor, Department of Chemistry,
University of Utah, Utah, United States

Scholarship :

2004-2008 Royal Golden Jubilee (RGJ) Ph. D. research scholarship from Thailand
Research Fund (TRF)